Climate Change Impact Assessment at Watershed Scale

Climate Change Impact Assessment at Watershed Scale

By

Sadik Ahmed, M.A.Sc.

A Thesis

Submitted to the Department of Civil Engineering

and the School of Graduate Studies

of McMaster University

In Partial Fulfilment of the Requirements

For the Degree of

DOCTOR OF PHILOSOPHY

DOCTOR OF PHILOSOPHY (2016)	McMaster University
Civil Engineering	Hamilton, Canada

Title : Climate Change Impact Assessment at Watershed Scale

Author: Sadik Ahmed

M.A.Sc. (McMaster University)

M.Eng. (University of the Ryukyus, Japan)

B.Sc. (Bangladesh University of Engineering and Technology, Bangladesh)

Supervisor: Dr. Ioannis Tsanis

Number of Pages : XIX,148

ABSTRACT

Climate model projections revealed a likelihood of increased frequency and magnitude of hydrological extremes in future climate due to continued emissions of greenhouse gases. Considering that it will significantly affect the planning and designing of flood management systems, for instance stormwater management infrastructures, and designation of flood risk area, it is vital to investigate the climate change impact on the hydrological processes and respective consequences on the flood management systems. The primary objective of this research is to investigate the climate change impact at watershed scale, and the goal was achieved by investigating the climate change impact on hydrological processes, assessing the potential impact of changed hydrological processes on drainage systems and flooding scenarios. The study area in this research includes Spencer Creek watershed, West Central Mountain drainage area and Clearview Creek drainage area located in Southern Ontario, Canada. The climate projections used in this study were the North American Regional Climate Change Assessment Program (NARCCAP) climate simulations based on SRES A2 scenario.

For Spencer Creek watershed, NARCCAP provided eight RCM+GCM pair's climate projections were bias- corrected, and used as input in a calibrated hydrological model HBV to simulate flows at the outlet of the watershed. A significant improvement of bias-corrected precipitation and temperature was revealed by Brier and Rank Probability Skill Score. The results revealed an increase in winter daily average flows and decrease in other seasons, and approximately 13% increase in annual evapotranspiration, and an increase in high flows and decrease in low flows under future climate conditions. Consequences for changed hydrological processes on urban stormwater management systems were investigated for West Central Mountain drainage area. Design storm depths were calculated by using the best fitted distribution among twenty seven distributions and by applying delta change factor. The PCSWMM model was used for flow simulation and hydraulic analysis for the storm-water management system, specifically storm sewer and detention pond. The assessment results indicate that the performance of the detention pond as well as the storm sewer network will deteriorate under future climate condition as design storm depths increase. For Clearview Creek drainage area, a single event hydrologic model Visual OTTHYMO and hydraulic analysis tool HEC-RAS were used to simulate flow and water level. The results revealed an increase of peak flows ranging from about 26 % to 64% for 2yr and 100yr return periods at the outlet of the Creek, and an average increase of water surface elevation and extents by 30 cm and 37.1 m, respectively, for a 100 year return period flood. Finally, non-stationary frequency analyses for design storm calculation were recommended for more robust and accurate investigation of climate change impact.

ACKNOWLEDGMENTS

Firstly, I would like to express my sincerest gratefulness to Dr. Ioannis Tsanis for his guidance, encouragement, enthusiasm and supervision throughout the period of my Ph.D. research work.

I would also like to express my gratitude to the members of the supervisory committee, Dr. Altaf Arain and Dr. Paulin Coulibaly for their significant and invaluable guidance to my research.

The support from the Natural Sciences and Engineering Research Council (NSERC) of Canada, and the Department of Civil Engineering is gratefully acknowledged.

Finally, I am extremely thankful to my parents, wife and brothers for their invaluable support and encouragement throughout this journey.

Contents

List of Tables

List of Figures

List of Abbreviations and Symbols

AOGCM	Atmosphere-Ocean General Circulation Model
BS	Brier Score
BSS	Brier Skill Score
CCSM	Community Climate System Model
CDF	Cumulative Distribution Function
CGCM3	Third Generation Coupled Global Climate Model
CRCM	Canadian Regional Climate Model
CV	Co-efficient of Variation
DTM	Digital Terrain Model
EV	Extreme Value
GCM	General Circulation Model
GEV	Generalized Extreme Value
GFDL	Geophysical Fluid Dynamics Laboratory
GHG	Greenhouse Gas
HADCM3	Hadley Centre Coupled Model 3
HBV	Hydrologiska Byråns Vattenbalan-avdelning
HRM3	Hadley Regional Model 3
IPCC	Intergovernmental Panel on Climate Change
NARCCAP	North American Regional Climate Change Assessment Program
RBG	Royal Botanical Garden
RCM	Regional Climate Model

RCM3	Regional Climate Model 3
RCP	Representative Concentration Pathway
RPS	Rank Probability Skill
RPSS	Rank Probability Skill Score
SDSM	Statistical Downscaling Method
SRES	Special Report on Emissions Scenarios
TLFN	Time-lagged Feedforward Network
WRFG	Weather Research Forecasting Model Grell

Declaration of Academic Achievement

This thesis was prepared in accordance with the guidelines of the McMaster School of Graduate Studies for sandwich thesis consisting of papers published in peer-reviewed journals. Chapter 2, 3 and 4 are three published papers. The three papers included in this thesis are co-authored and the author of this thesis is the main contributor to these journal papers. The thesis author's contribution to each of the papers and the originality of the work as well as the reasons for including the papers to this thesis are outlined below:

Chapter 2: Watershed Response to Bias Corrected Improved skilled Precipitation and Temperature under Future Climate -A Case Study on Spencer Creek Watershed, Ontario, Canada by S. Ahmed and I. Tsanis, Hydrology: Current Research. 7, 246 doi:10.4172/2157-7587.1000246.

The idea of this research work came from S. Ahmed following a discussion with Dr. I. Tsanis. Most of the work was done during 2012-2013, and rest of work was done during 2014-2016. The modeling work, bias-correction, and all the analyses were done by S. Ahmed under the supervision and guidance of I. Tsanis. The manuscript was prepared by S. Ahmed and reviewed and edited by I. Tsanis. This study has been included in the thesis because it is in line with the research plan and objective as well as it triggered the need of further study on climate change impact on flood and stormwater management.

Chapter 3: Climate Change Impact on Design Storm and Performance of Urban Storm-Water Management System - A Case Study on West Central Mountain Drainage Area in Canada by S. Ahmed and I. Tsanis, Hydrology: Current Research, 7, 229, doi: 10.4172/2157-7587.1000229.

The idea of this research work also came from S. Ahmed following a discussion with Dr. I. Tsanis after completing the initial work of previous paper. The analysis of design storm and the modeling work was done by S. Ahmed during 2013-2014 and 2014-2015, respectively in the computer laboratory of I. Tsanis. The manuscript was prepared by S. Ahmed and reviewed and edited by I. Tsanis. This study has been included in the thesis because it is in line with the research plan and objective as well as the method used for design storm calculation was also used for the third paper.

Chapter 4: Hydrologic and Hydraulic Impact of Climate Change on Lake Ontario Tributaryby S.Ahmed and I.Tsanis, American Journal of Water Resources, 4(1), 1-15, doi:10.12691/ajwr-4-1-1.

The idea of this research work also came from S. Ahmed following a discussion with Dr. I. Tsanis after completing the initial work of previous paper. The computation of design storms and the modeling work was done by S. Ahmed during 2014-2015 and 2015-2016, respectively in the computer laboratory of I. Tsanis. The manuscript was prepared by S. Ahmed and reviewed and edited by I. Tsanis. The study results specifically investigated the climate change impact on flood inundation and meet the objective of the research; therefore it should be included in the thesis.

Chapter 1 : Introduction

1.1 Background

A plethora of scientific evidence has established climate change as a fact, leaving no room for doubt. The Earth's climate has changed throughout the history, but the warmth of the second half of the last century is unprecedented in, at least, the past 1300 years (IPCC 2007) and the 30-year period of 1983-2012 was likely the warmest in the last 1400 years in the Northern Hemisphere (IPCC 2014). The Fifth Assessment Report of the Intergovernmental Panel on Climate Change – the most up-to-date scientific assessment of past, present and future climate stated the evidence provided by the climate science community "Warming of the climate system is unequivocal, and since the 1950s, many of the observed changes are unprecedented over decades to millennia. The atmosphere and ocean have warmed, the amounts of snow and ice have diminished, sea level has risen, and the concentrations of greenhouse gases have increased." IPCC in their latest report also indicated that these changes will be continued under future climate as greenhouse gases continued to be released into the atmosphere. The impact of climate change can be referred as consequences of the alteration of statistical properties of the climate system for society and environment. In the context of watershed management, climate change impact on hydrological processes is a vital issue as it is one of the key factors for planning and designing water management systems. Watershed, catchment, and drainage basin are three synonymous terms that refer to the topographic area of land that collects and discharges all surface water from rain, melting snow, or ice to a common outlet at a lower elevation. A watershed may be as small as a parking lot or as large as thousands of square kilometers as represented by the Mississippi River basin (Singh and Woolhiser 2002). Climate change will affect the watershed hydrology in many ways because the hydrological cycle is intimately linked with the atmospheric temperature and radiative fluxes. From the point of sustainable planning and design of water management systems, for instance flood and stormwater management, assessment of watershed responses due to climate change is essential. Study of the impact of climate change at the watershed scale is the focus of this thesis. Three case study areas – Spencer creek watershed, West Central Mountain drainage area and Clearview Creek drainage area located in Southern Ontario, Canada were selected for climate change impact study in this Ph.D. research.

Hydrological model is the key tool for studying the process governing the impacts of climate change. The most widely used approach to predict climate change impact on hydrological processes is done by combining the climate model simulations with hydrological models (Loukas 2002). There are several well-known hydrologic models in current use and those were developed for different purposes and with different theoretical concepts. The hydrologic model can be categorized as conceptual or physically based, lumped or distributed, continuous or event based model and so on, based on different classification criteria. Continuous models are designed for generating outflow hydrographs over a long period of time**,** and the event-based models are designed to simulate a single event such as the hydrograph of a single storm. In this study, a semi-distributed conceptual model, Hydrologiska Byran Vattenbalan-avdelning (HBV) was chosen for continuous simulation, and PCSWMM 2D Professional and Visual OTTHYMO v3.0 (VO3) were chosen to simulate single events. Transformation of runoff simulated by hydrologic model into hydraulic metrics is required to investigate the hydraulic impact of climate change. The Hydrologic Engineer Center's River System Analysis System (HEC-RAS) software and PCSWMM 2D Professional tools were used for this purpose. The HBV model was used to simulate one main water-balance component, actual evapotranspiration, together with other components of the hydrologic cycle. Actual evapotranspiration is calculated by the equations:

$$AE = PE.SM/FC.LPDEL \quad for\ SM < FC.LPDEL \qquad \text{Eq. 1-1}$$

$$AE = PE \qquad for\ SM > FC.LPDEL \qquad \text{Eq. 1-2}$$

Where PE is potential evapotranspiration, SM is actual soil moisture content, FC is the maximum water content of the zone (in mm), and LPDEL a dimensionless parameter (< 1) (Saelthun 1995). Potential evapotranspiration can either be given as parameters to the model or calculated by the model by a simplified variation of Thornthwaite's equation. Integrating the full US EPA SWMM5 engine, PCSWMM accounts for various hydrologic processes and contains a flexible set of hydraulic modeling capabilities used to route runoff and/or external inflows through the drainage system network. EPA SWMM was generally developed for evaluating stormwater runoff hydrology and stormwater drainage and collection systems in an urban setting. PCSWMM model was used for flow simulation and hydraulic analysis for the storm-water management system, specifically storm sewer and detention pond. Visual

OTTHYMO v3.0 (VO3), the third version of the INTERHYMO – OTTHYMO hydrologic model simulation software package designed to simulate runoff from single storm events. Considering the urban hydrological modeling capability, this model was used to simulate flows for storm of different durations and return periods. Peak flows simulated by using Visual OTTHYMO were used as input into the Hydrologic Engineer Center's River System Analysis System (HEC-RAS) software for hydraulic computation. The HEC-RAS model that allows performing one-dimensional steady and unsteady flow river hydraulics calculations was used for flooding scenario analyses. HEC-RAS is likely most suitable for the purpose of flood line delineation because it seems the majority of the floodplain mapping standards have been developed in accordance with HEC-RAS functionality and the model is widely used by conservation authorities in Ontario and other places in the world.

The North American Regional Climate Change Assessment Program (NARCCAP) (NARCCAP 2013, Mearns et al. 2007) is a coordinated multi-model numerical experiment that serves climate projections for several RCM+GCM pairs at similar spatial resolutions of 50 km covering the United States, Canada and Mexico for climate change impact study. It provides the climate data sets for a time span of 33 years for both current (1968-2000) and future (2038-2070) period. Availability of high temporal and spatial resolution climate projections provided by NARCCAP has facilitated the climate change impact study in the present research. NARCCAP simulations for 21st century are carried out by running a set of regional climate models

(RCMs) driven by a set of atmosphere-ocean general circulation models (AOGCMs) that follows greenhouse gas and aerosol concentration based on A2 emission scenario described in the Special Report on Emissions Scenarios (SRES) (Nakicenvoic 2000). The SRES scenarios were used in the IPCC Fourth Assessment Report (AR4) for assessment of projections of future climate change. The SRES scenarios are grouped into four scenario families (A1, A2, B1 and B2) that describe a wide range of demographic, economic and technological driving forces and resulting GHG emissions (IPCC 2007). A2 describes a very heterogeneous world with high population growth, slow economic development and slow technological change. Improvements in climate models since the IPCC Fourth Assessment Report (AR4) are evident in simulations of climate variables such as continental-scale surface temperature, large scale precipitation etc. The climate models in the Fifth Assessment Report (AR5) used a set of scenarios called Representative Concentration Pathways. The projections from climate models in AR4 and AR5 for large-scale patterns of change shows an overall consistency and magnitude of the uncertainty that has not changed significantly. The Representative Concentration Pathways (RCPs) describe four different 21st century pathways of greenhouse gas (GHG) emissions and atmospheric concentrations, air pollutant emissions and land use. The RCPs scenarios include a stringent mitigation scenario (RCP2.6), two intermediate scenarios (RCP4.5 and RCP6.0), and one scenario with very high GHG emissions (RCP8.5). “The RCPs cover a wider range than the scenarios from the Special Report on Emissions Scenarios (SRES) used in previous assessments, as they also represent scenarios with climate policy. In terms of overall forcing, RCP8.5 is broadly comparable to the SRES A2/A1FI scenario, RCP6.0 to B2 and RCP4.5 to B1. For RCP2.6, there is no equivalent scenario in SRES" (IPCC 2014). Therefore, the findings of climate change impact at watershed scale based on SRES A2 scenario would be broadly comparable to the results based on RCP8.5.

1.2 Problem Statement and Motivations

Climate change impact is becoming a critical factor in water resources management and planning. Assessment of climate change at watershed scale is essential for sustainable management of extreme events, for instance flood through structural and non-structural measures as well as optimal design of urban stormwater management infrastructures. IPCC 2014 indicates that our climate is undergoing substantial warming, and further warming will be caused due to continued emissions of greenhouse gases. The extreme precipitation events will become more intense and frequent in the current century over most of the globe (IPCC 2014), consequently the increased risk of floods. Hirabashi et al (2013) revealed that the global exposure to flood would increase depending on the degree of warming. They also stated that "In the past decade, reported annual losses from floods have reached tens of billions of US dollars and thousands of people were killed each year. Losses and the number of casualties could be larger in the future." Anderson 2014 indicated the massive flood event in the summer of 2013 that caused the destruction of several southern Alberta communities was most likely a manifestation of our changing climate. In many cases the nature of storm and resulted flooding in Canada was unprecedented. For example, the Ontario city of Burlington got two months of rain (a highly localized amount of 190 mm recorded by an amateur weather observer) in only four hours on 4 August 2014 (Environment Canada, 2016). Therefore, the structural and non-structural measures designed based on the statistical properties of current climate for flood and stormwater management will not be able to manage extreme events in future climate.

1.3 Objectives of the research

The primary objective of this research is to investigate the climate change impact at watershed scale using NARCCAP ensemble climate simulations. In order to achieve this goal, the following secondary objectives need to be achieved:

- Investigate the climate change impact on hydrological processes in Spencer Creek watershed located in Southern Ontario, Canada
- Assess the potential impact of changed rainfall extreme on drainage systems in the West Central Mountain drainage area located in Southern Ontario, Canada
- Assess the climate change impact on flooding scenario for the Clearview Creek drainage area located in Southern Ontario, Canada

Each of the objective forms the basis of a paper that has been published in peer-reviewed journal.

1.4 Thesis Layout

The first chapter of this Ph.D. thesis presents a primary introduction of the research which includes the background, research motivations, objectives and layout. In chapter 2 a manuscript entitled ‘Watershed Response to Bias-Corrected Improved skilled Precipitation and Temperature under Future Climate -A Case Study on Spencer Creek Watershed, Ontario, Canada’ is presented. Chapter 3 presents a published manuscript entitled ‘Climate Change Impact on Design Storm and Performance of Urban Storm-Water Management System - A Case Study on West Central Mountain Drainage Area in Canada’. The third manuscript entitled ‘Hydrologic and Hydraulic Impact of Climate Change on Lake Ontario Tributary’ is presented in chapter 4. Finally, the chapter 5 includes the conclusions and recommendations for future research.

References

Anderson, S.T. (2014). Hydrological impacts of climate change on the castle river watershed, Alberta, Canada. M.Sc. thesis, Dept. of Geography, University of Lethbridge, Alberta, Canada.

Environment Canada (2016).<https://ec.gc.ca/meteo-weather/default.asp?lang=En&n=C8D88613-1 &offset=15&toc=hide> (May 1, 2016).

Hirabayashi, Y., Mahendran, R., Koirala, S., Konoshima, L., Yamazaki, D., SatoshiWatanabe, S., Hyungjun Kim, H., Kanae, S. (2013). Global flood risk under climate change. Nature Climate Change, 3, 816-821.

IPCC (2014). Climate Change 2014: Synthesis Report. Contribution of Working Groups I, II and III to the Fifth Assessment Report of the Intergovernmental Panel on Climate Change. Core Writing Team, Pachauri, PK, Meyer, LA (eds.) IPCC, Geneva, Switzerland, 151 pp.

IPCC (2007). Summary for Policymakers. In: Climate Change 2007: The Physical Science Basis. Contribution of Working Group I to the Fourth Assessment Report of the Intergovernmental Panel on Climate Change [Solomon, S., D. Qin, M. Manning, Z. Chen, M. Marquis, K.B. Averyt, M.Tignor and H.L. Miller (eds.)]. Cambridge University Press, Cambridge, United Kingdom and New York, NY, USA.

Loukas, A., Vasiliades, L., Dalezios, N.R. (2002). Potential climate change impacts on flood producing mechanisms in southern British Columbia, Canada using the CGCMA1 simulation results. Journal of Hydrology, 259, 163-188

Mearns, L.O., et al. (2007), updated 2012. The North American Regional Climate Change Assessment Program dataset, National Center for Atmospheric Research Earth System Grid data portal, Boulder, CO. Data downloaded 2014-07-07. [DOI:10.5065/D6RN35ST].

Nakicenvoic N, Davidson O, Davis G, Grübler A, Kram T, et al. (2000). Special Report on Emissions Scenarios. A Special Report of Working Group III of the Intergovernmental Panel on Climate Change. Cambridge University Press Cambridge, 599.

NARCCAP (2013) North American Regional Climate Change Assessment Program. <http://www.narccap.ucar.edu/> (January26, 2013).

Saelthun, N. R. (1995). “Nordic” HBV model. Norwegian Water Resources and Energy Administration. Oslo, Norway.

Singh, V.P., and Woolhiser, D.A. (2002). Mathematical modeling of watershed hydrology. Journal of Hydrologic Engineering, 7(4), 270-292.

Chapter 2 : Watershed Response to Bias Corrected Improved skilled Precipitation and Temperature under Future Climate -A Case Study on Spencer Creek Watershed, Ontario, Canada

Summary of Paper I: Ahmed, S., and Tsanis, I. (2016). Watershed Response to Bias Corrected Improved skilled Precipitation and Temperature under Future Climate -A Case Study on Spencer Creek Watershed, Ontario, Canada. Hydrology: Current Research. 7, 246 doi:10.4172/2157-7587.1000246.

The overall objective of this study is to investigate the climate change impact on hydrological processes for Spencer Creek watershed located in Southern Ontario, Canada. The objective was achieved by i) bias correction of raw NARCCAP provided eight RCM+GCM pair's precipitation and temperature time series data, ii) assessment of improvement in bias-corrected NARCCAP projections, iii) performing hydrologic simulation and iv) assessment of flow regime under current and future climate conditions. The bias correction methods demonstrated by Ines and Hansen (2006) and Samuel et al. (2012) were used for bias correction of raw NARCCAP data; the skill scores measures BSS and RPSS were used for assess the improvement of bias-corrected data; and the HBV hydrologic model was used for hydrologic simulation.

The results of this study revealed the followings:

- An overall improvement was achieved for precipitation and temperature when biasicorrection was applied, and higher improvement in the late spring and summer months in the case of precipitation and higher improvement in the summer months in the case of temperature.
- Precipitation will increase in three seasons, fall, winter and spring and decrease in the summer, the temperature will increase in all months, and evapotranspiration will increase in all months except July and August.

- Average of all RCM+GCM pair's data indicated an increase of daily average flow in the winter and decrease in other seasons.
- An increase in annual average temperature, precipitation and evapotranspiration, and a small increase of annual average flow in future are indicated by the average of all RCM+GCM pairs.
- An increase in high flows and decrease in low flows under future climate are indicated. Averages of five RCM+GCM pairs revealed an increase of high flow by 8.8% and a decrease of low flow by 12.9%. The WRFG+CGCM3 and WRFG+CCSM models show the greatest increase in high flow by 13.2% and the highest decrease in low flow by 28.6%, respectively.

References:

Ines AVM, Hansen JW (2006) Bias correction of daily GCM rainfall for crop simulation studies. Agricultural and Forest Meteorology 138: 44–53.

Samuel J, Coulibaly P, Metcalfe R A (2012) Evaluation of future flow variability in ungagged basins: Validation of combined methods. Advances in Water Resources 35: 121-140.

2.1 Abstract

It is widely acknowledged that the statistical properties of precipitation and temperature will change under the future climate condition, and this will cause a significant impact on water resources and its management at watershed scale. This study investigated the hydrological response to climate change for Spencer Creek watershed located in Southern Ontario, Canada. The precipitation and temperature projection used in this study were obtained from the North American Regional Climate Change Assessment Program (NARCCAP) climate simulations. NARCCAP climate projections were bias- corrected for meteorological stations representative of the watershed. The bias-corrected NARCCAP climate projections were used as input in a calibrated hydrological model Hydrologiska Byran Vattenbalan-avdelning (HBV) to simulate flows at the outlet of the watershed. The improvement of bias-corrected NARCCAP precipitation and temperature is revealed by Brier and Rank Probability Skill Score (BSS and RPSS, respectively). The comparison of current and future simulated flow results reveals an increase in winter daily average flows and decrease in other seasons, and approximately 13% increase in annual evapotranspiration under future climate condition. An increase in high flows and decrease in low flows under future climate is revealed by flow-duration analysis.

CE Database subject headings: Climate change; Bias Correction; Hydrology; Watershed; Canada.

2.2 Introduction

The recent Intergovernmental Panel on Climate Change (IPCC) Assessment Report [1] indicates that our climate is undergoing substantial warming, and it is likely that an increasing trend of extreme precipitation will continue. The watershed hydrology will be affected by climate change in many ways because the hydrological cycle is linked with changes in atmospheric temperature and radiative fluxes [2]. The changes in temperature will have a significant effect on the hydrological processes that involve precipitation, snowmelt, evapotranspiration, soil moisture and flow. The prediction of the forthcoming climate change on hydrological processes is vital in water resources management and planning. In this study, climate change impact on hydrological processes has been performed by forcing climate model output to a hydrological model in order to evaluate changes in future flow in the Spencer Creek watershed located in Southern Ontario.

In the last decade, researchers as well as users have shown particular interest in the hydrological impact of climate change. Past research on climate change impact assessment revealed that the hydrological regime of different watersheds could be significantly modified due to the anticipated changes in temperature and precipitation under future climate during the present century [3,4,5]. The assessment results of climate change impact on hydrology at the watershed scale vary significantly with the climate model projections, greenhouse gas emission scenarios, data downscaling/ correction techniques, and hydrologic models. Grillakis et al. [3] examined the climate change impact on future hydrology of Spencer Creek watershed. The study revealed inter-annual trends for precipitation and temperature both in the past data and future simulation. The analysis shows an annual average precipitation increase by approximately 10% to 15% and temperature increase by approximately +2.2°C and +2.3°C at Hamilton Airport and Hamilton RBG. The study also shows that the yearly average flow at Spencer Creek at Dundas increases by about 12% when future projected flows are compared with the observed flow. Sultana and

Coulibaly [4] assessed the climate change impact on hydrological processes of this watershed using a distributed coupled MIKE SHE/MIKE 11 hydrologic model and the projected daily precipitation and temperature from Canadian global climate model (CGCM 3.1). The downscaled GCM predictions show a 14-17% increase in the annual mean precipitation and 2-3°C increase in annual mean maximum temperature. The coupled hydrologic model predicted about 1-5% annual decrease in snow storage, 1-10% increase in annual ET, 0.5-6% decrease in the annual groundwater recharge, 10-25% increase in annual stream flows for all sites for the 2050s when downscaled GCM scenarios were used. Boyer et al. [5] assessed the impact of climate change on the hydrology of St. Lawrence tributaries (Quebec, Canada) located about 650 km northeast of Spencer Creek. The hydrological model HSAMI was used to produce flow in the future by inputting GCM projections for three 30 year horizons (2010-2039, 2040-2069 and 2070-2099, respectively referred to as 2020s, 2050s and 2080s). The future daily climate (precipitation and temperature) for three 30 year horizons were produced by adding anomalies (monthly mean difference between GCMs in the future and the reference period 1961-1990) to the observed temperature and precipitation during the reference period. The study results indicate that the regime will gradually shift from snow to rain. Most of the future flow simulations show an increase in winter discharge and a decrease in spring discharge. The study results also show that the center volume date for the winter/spring period is expected to be in advance 22-34 days depending on the location of the watershed.

The most widely used approach to predict climate change impact on hydrological processes is done by inputting climate model simulations into hydrological models. The climate model (GCM or RCM) provides gridded data, and the climate projected from it is not the same as the climate coming from the observations. Therefore, modelers use different techniques for establishing relationship between climate model outputs and observations for correcting the climate model projections both for current and future period to get more realistic results from the hydrological model. A number of dynamical and statistical downscaling methods are available to downscale climate model gridded data at the target points where the meteorological or rainfall stations are located [6-10]. Sharma et al. [11] examined the necessity of correction of raw RCM data by using a statistical downscaling method (SDSM) and a data-driven technique called a time-lagged feedforward network (TLFN) on raw CRCM4.2 data. They revealed that the downscaling did improve raw RCM precipitation, and consequently, the downscaled CRCM4.2 data improves the HBV hydrologic model ability to simulate streamflow accurately as compared to the use of the raw CRCM4.2 data. Although the statistical downscaling methods have been used in many studies, the application and calibration of this method are complex and highly dependent on expert judgment [12]. The regional climate models (RCMs), generated from dynamical downscaling methods, provide climate projections at much finer scale that is largely used in hydrological impact studies in many watersheds around the world. However, recent studies [11,13] revealed that there are systematic differences between the raw RCMs output and the observations, and the bias-correction methods alternative to statistical and dynamical downscaling method has shown effectiveness in removing the bias between raw RCMs output and the observations [13,14]. The bias correction methods used by Ines and Hansen [15] and Samuel et al. [13] have been used in this study for correcting the NARCCAP climate model output. One of the novelty of this study is that two probabilistic verification measures, namely the Brier skill score (BSS) and the rank probability skill score (RPSS) have been used in this study to assess the improvement of NARCCAP precipitation and temperature data when bias correction method was applied.

The availability of higher spatial and temporal resolution climate data, provided by the NARCCAP created from multiple GCMs and RCMs, has facilitated the climate change impact studies. Using ensemble climate model data will provide multiple possible estimations of flow regime, which assists the water manager towards a sustainable planning and design. Because of the high uncertainty in the climate model projections, Mearns et al. [16] emphasized on the use of ensemble climate model projections for climate change impact study by using climate model simulations. NARCCAP provides both precipitation and temperature time series for both current and future period for eight RCM+GCM pairs at same spatial scale. All the available climate model data have been used in this study. A number of hydrological models have been used by the researchers for climate change impact studies in different countries. In this study, a semi-distributed conceptual model, HBV, was chosen for hydrologic simulation using bias-corrected NARCCAP projections. The motivation of choosing this particular model is that the model was used in previous studies [3,17,18] on Canadian watersheds and showed a good performance.

These recent studies on hydrological impact analysis indicate an overall increasing trend in the mean annual flow in Canadian watersheds. However, further investigation of extreme events such as high and low flow analyses is required. This study focused on the investigation of climate change impact on high and low flows using a number of climate model simulations. The overall objective of this study is to investigate the climate change impact on hydrological processes by using bias-corrected NARCCAP climate model projections for Spencer Creek watershed located in Southern Ontario, Canada. The objective was achieved by correcting the bias of raw NARCCAP precipitation and temperature time series, assessment of improvement in bias-corrected NARCCAP projections, performing hydrologic simulation and assessment of flow regime under current and future climate conditions.

2.3 Study Area and Data

2.3.1 Study Area

The case study area for this study is Spencer Creek watershed located in the Southern Ontario, Canada and is shown in Figure 2-1. The watershed has an area of 160.4 km^2. The surface runoff in the watershed is collected by an extensive network of rivers and stream and discharged into Cootes Paradise at the western end of Lake Ontario. The land-use of the study area can be also characterized by agricultural land use, forest area, wetlands and the urban and paved area in the lower part of the watershed. The watershed is complex because of its extensive river and stream network, heterogeneous soil property and diverse land use [19].

2.3.2 Observed Hydro-meteorological Data

The observed daily precipitation (total precipitation in the form of liquid and snow, measured in mm) and temperature (in °C) data were obtained from meteorological stations; namely the Hamilton Airport, Hamilton RGB, Hamilton RBG CS meteorological station. The meteorological data for 1971-2014 at the stations were collected from Environment Canada. The observed daily flow data for 30 years, from 1985 to 2014, were obtained for a hydrometric station namely Spencer Creek at Dundas (station ID 02HB007) located at latitude and longitude of 43.27°N and 79.96°W, respectively. The daily flow data were collected from Water Survey Canada. The climate of the study area is humid-continental. Based on the meteorological data from 1971 to 2014 at Hamilton Airport, the daily average maximum and minimum temperatures are 13.4°C and 4°C, and extreme maximum 37.4°C and extreme minimum temperature -30 °C were observed on 7 July, 1988 and 16 January, 2004, respectively. The yearly average precipitation is 893.2 mm based on data from 1971 to 2014 at Hamilton Airport, and the maximum daily rainfall and precipitation 107 mm were observed on 26 July, 1989. The yearly average flow is 2.02 m^3/s with highest and lowest monthly average of 4.14 m^3/s and 0.59 m^3/s on March and August, respectively and the maximum daily average flow 32.4 m^3/s was observed on 14 March 2010. These values were obtained based on the available daily time series data from 1985 to 2014 observed at hydrometric station namely Spencer Creek at Dundas.

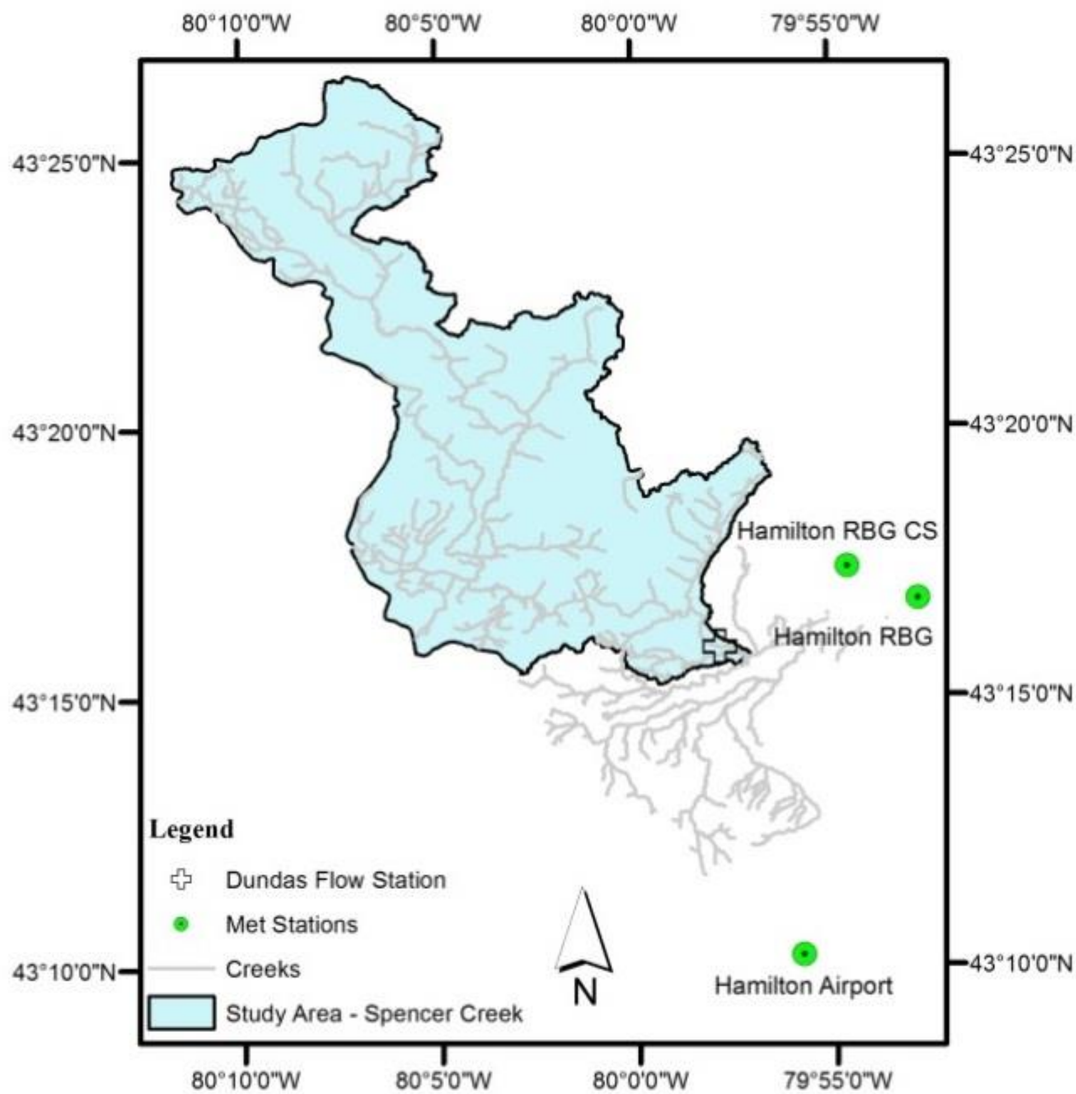

Figure 2-1: Map of the study area

2.3.3 NARCCAP Climate Data

The North American Regional Climate Change Assessment Program (NARCCAP) [20,21] is an international program that serves the high resolution climate scenario for the United States, Canada, and Northern Mexico. It provides the data sets in order to investigate uncertainties in regional scale projections of future climate and generate climate change scenarios for use in impacts research. All the NARCCAP future simulations are driven by a GCM that follows greenhouse gas and aerosol concentration based on A2 emission scenario described in the Special Report on Emissions Scenarios (SRES) [22]. NARCCAP provides data produced by several RCM+GCM pairs, and this study used eight RCM+GCM pairs simulated precipitation and temperature time series. The names of the RCMs and GCMs/drivers produced the data, used in this study, are listed in Table 2-1.

The NARCCAP output data are provided at a gridded horizontal resolution of 50 km, and the precipitation and temperature (maximum and minimum) are provided for three hourly and daily temporal resolutions, respectively. The NARCCAP experimental output spans for two time periods of 33 years – the first time span is for the current/historical period spanning from 1968 to 2000, and the second time span is for the future span from 2038-2070. These two periods permit assessment of mid twenty-first century changes relative to late twentieth century climate. It is notable that the first three years, the spin-up periods [23], of both current and future simulation have been discarded in this study. NARCCAP data are stored in the NetCDF files in 2D arrays. The array dimensions (yc, xc) for the Hamilton Airport, Hamilton RBG/Hamilton RBG CS are found from the grid cell maps for each RCM. The array dimensions (yc, xc) of nearest point of Hamilton Airport for CRCM, HRM3, RCM3 and WRFG are (51,100), (57, 105), (44, 94) and (48, 93), respectively, and array dimensions (yc, xc) of nearest point of Hamilton RBG/Hamilton RBG CS for CRCM, HRM3 and RCM3, WRFG are (51,100), (58, 105), (45, 93) and (48, 93).

Table 2-1: List of RCM+GCM Data Pairs used in this study

RCM+GCM Pairs	RCM	GCM/Drivers
CRCM+CCSM	Canadian Regional Climate Model [24]	Community Climate System Model [29]
CRCM+CGCM3	Canadian Regional Climate Model [24]	Third Generation Coupled Global Climate Model [30]
HRM3+GFDL	Hadley Regional Model 3 [25]	Geophysical Fluid Dynamics Laboratory GCM [31]
HRM3+HADCM3	Hadley Regional Model 3 [25]	Hadley Centre Coupled Model, version 3 [32,33]
RCM3+CGCM3	Regional Climate Model version 3 [26,27]	Third Generation Coupled Global Climate Model [30]
RCM3+GFDL	Regional Climate Model version 3 [26,27]	Geophysical Fluid Dynamics Laboratory GCM [31]
WRFG+CCSM	Weather Research Forecasting Model Grell [28]	Community Climate System Model [29]
WRFG+CGCM3	Weather Research Forecasting Model Grell [28]	Third Generation Coupled Global Climate Model [30]

2.4 Methodology

The procedure followed in this study involves (1) bias correction of NARCCAP precipitation and temperature time series data and analysis of skill score; (2) transforming bias-corrected precipitation and temperature into flows and evapotranspiration using a hydrological model, and (3) comparing hydrologic regime under current and future climate.

2.4.1 Bias Correction

The NARCCAP temperature and precipitation data are gridded areal average, and not point estimates. Bias correction method is used to remove bias between climate model simulated data and observation at a point location to get more accurate results from the hydrological model when NARCCAP data are inputted.

The bias-correction method presented by Ines and Hansen [15] was used to correct the frequency and the intensity of daily precipitation of NARCCAP. This two-step procedure corrects the frequency of daily precipitation at first, and then it corrects the intensity for each of 12 calendar months. The mean precipitation $\bar{X}_m$ (mmd^{-1}) in calendar month m is the product of mean intensity, μ_1 $(mm\,wd^{-1})$ ("wd^{-1}" is wet day, for a threshold 0.1 mm) and relative frequency, π $(wd\,d^{-1})$. Therefore, the correction of any bias of these two components also corrects the monthly total precipitation. In this study, this bias-correction method was applied to remove the bias between the daily precipitation data from NARCCAP and observations at Hamilton Airport and Hamilton RBG meteorological stations.

In the first step in order to correct the frequency of precipitation, the empirical distribution of the raw NARCCAP precipitation was truncated above the $\bar{x}_{NARCCAP}$ threshold value, in such a way that the mean frequency of precipitation above the threshold matches the observed mean precipitation frequency. The threshold value $\bar{x}_{NARCCAP}$ are calculated from the observed and NARCCAP precipitation distributions as show in the following equation,

$$\bar{x}_{NARCCAP} = F^{-1}_{NARCCAP}\left(F_{obs}\left(\bar{x}\right)\right) \qquad \text{Eq. 2-1}$$

where $F(.)$ and $F^{-1}(.)$ denotes the cumulative distribution function (CDF) and its inverse, and subscripts indicate NARCCAP precipitation forecasts or observed daily precipitation. The threshold observed precipitation amount ($\bar{x}$) of a day was set to 0.1 mm to define wet day.

In the second step to correct the intensity of precipitation, a two-parameter gamma distribution as shown in Equation 2-2 was used to fit the truncated daily NARCCAP and observed precipitation data, and then CDF of the truncated daily NARCCAP precipitation data are mapped to the CDF of the observed data as shown in Equation 2-3.

$$F_G(x, \alpha, \beta) = \frac{1}{\beta^{\alpha}\Gamma(\alpha)} x^{\alpha-1}\, exp\left(-\frac{x}{\beta}\right); \quad x \geq \bar{x} \qquad \text{Eq. 2-2}$$

$$F_G(x, \alpha, \beta) = \int_{\bar{x}}^{x} f(t)dt \qquad \text{Eq. 2-3}$$

where the shape parameter (α) and the scale parameter (β) of the gamma distribution are determined by Maximum Likelihood Estimation. The corrected NARCCAP precipitation amount x' on day i is calculated by substituting the fitted gamma CDFs into the following equation:

$$x'_{pi} = \begin{cases} F^{-1}_{I,obs}\left(F_{I,NARCCAP}(x_i)\right) & x_i \geq \bar{x} \\ 0 & x_i < \bar{x} \end{cases} \qquad \text{Eq. 2-4}$$

The bias in the NARCCAP temperature series was corrected using a method presented by Samuel et al. [13]. The distribution of the daily NARCCAP temperature was mapped onto the distribution of observed temperature for each of the 12 calendar months. In the case of temperature , correction of frequency distribution and truncation of the empirical distribution of the raw daily NARCCAP temperature data was not performed by using a normal distribution used in this bias correction method to map the temperature distribution. The CDF of the normal temperature distribution was calculated by using Equation 2-5. The CDF of the daily NARCCAP temperature are mapped to the CDF of the observed data using equation 2-6. The corrected NARCCAP temperature y' on day i is calculated by Equation 2-7:

$$F(y;\ \mu, \alpha,) = \frac{1}{2}\left[1 + erf\left(\frac{y-\mu}{\sqrt{2\alpha^2}}\right)\right]; \quad y \in \Re \qquad \text{Eq. 2-5}$$

$$F_G(y;\ \mu, \alpha) = \int^{\Re} f(t)dt \qquad \text{Eq. 2-6}$$

$$y_i' = F_{T,OBS}^{-1}\left(F_{T,NARCCAP}(y_i)\right) \qquad \text{Eq. 2-7}$$

2.4.2 Description of Skill Scores

Two probabilistic verification measures, namely the Brier skill score (BSS) and the rank probability skill score (RPSS), mostly used in the assessment of meteorological forecasts [34-36], were used in this study to assess the quality of bias-corrected climate model simulated precipitation and temperature time series. The BSS and RPSS are based on the Brier score (BS) and the rank probability score (RPS), respectively.

The Brier score [37], which is essentially the mean-square error of probabilistic forecasts, is the most commonly used scalar measure for probability forecasts. It is widely used for dichotomous predictands [35]. This score is also applied to continuous-valued forecast [38]. The continuous valued forecasts are converted into a binary event using a threshold filter which can either be exceeded or not [38,39]. In this study, for comparison purpose and consistency, 0.1 mm/day (threshold to define wet day) for precipitation, and the means of the daily mean temperature of each month for temperature are used as BS thresholds. The Brier score BS is calculated by the equation 2-8:

$$BS = \frac{1}{n}\sum_{k=1}^{n}(y_k - o_k)^2 \qquad \text{Eq. 2-8}$$

Where n represents the number of days, k is the number of the n simulation/event pair, y_k is the simulation probability and o_k is the observed probability (occurrence and non-occurrence of the event being simulated). y_k is derived by the relative frequency of the ensemble members exceeding the chosen threshold. The observations o_k are translated similar to the simulated values, i.e. the observation o_k = 1 if the event occurs (if the threshold is exceeded) and o_k = 0 if the event does not occur. The Brier score ranges between 0 and 1 because the observation and probability simulations are bounded by 0 and 1, a perfect simulation exhibiting BS=0 and less accurate forecasts receive higher Brier score. The Brier skill score (BSS) is computed using equation 2-9 in order to make comparison between a simulation relative to reference simulation:

$$BSS = \frac{BSS_{ref} - BSS}{BSS_{ref}} \quad \text{Eq. 2-9}$$

The RPS [35] is a score derived from the Brier score to the multi-category [40]. The RPS is calculated by equation 2-10:

$$RPS = \sum_{m=1}^{j} (Y_m - O_m)^2 \quad \text{Eq. 2-10}$$

Where, Y_m is the cumulative probability of the simulation for category m and O_m is the cumulative probability of the observation for category m. For a group of n forecasts, the RPS is the average ($\overline{RPS}$) of the n RPSs:

$$\overline{RPS} = \frac{1}{n} \sum_{k=1}^{n} RPS_k \quad \text{Eq. 2-11}$$

In this study, the procedure presented by Clark and Hay [41] and Gangopadhyay et al.[42] was used to calculate RPS: At first, the observed time series data are used to differentiate 10 (j) possible categories (i.e. the minimum value to the 10th percentile, the 10th percentile to the 20th percentile, the 20th percentile to the 30th percentile up to the 90th percentile to the maximum value). These categories were determined separately for each month. In the next step, the number of ensemble member simulation in each category is determined (out of 8 members), and their cumulative probabilities were computed for each simulation-observation pair. Then, in the same way, the observation’s cumulative probabilities were computed. All categories below the observation's position are assigned '0', and all categories equal to and above the observation's position are assigned '1'. The RPS was determined as the squared difference between cumulative probabilities of the observations and simulation, and the summation of squared differences over 10 categories. RPS is zero for a perfect simulation and positive otherwise. The ranked probability skill score (RPSS) was calculated in order to make comparison between a simulation relative to a reference simulation:

$$RPSS = \frac{\overline{RPS}_{ref} - \overline{RPS}}{\overline{RPS}_{ref}} \qquad \text{Eq. 2-12}$$

In this study, NARCCAP simulated raw data was used as the reference simulation to calculate BSS and RPSS. Here, the calculated BSS and RPSS show the percentage improvement of bias-corrected NARCCAP precipitation and daily mean temperature data over the NARCCAP simulated data.

2.4.3 Hydrologic Modeling

HBV Hydrologic Model

'Although hydrological models have been around for quite some time, there is yet to be one exclusive model that can stand apart from the rest and be declared best at modeling all aspects of the hydrologic system' [43]. A hydrologic model HBV [44] was chosen to simulate flows for current and future period at the outlet of the Spencer Creek Watershed. The model was developed at the Swedish Meteorological and Hydrological Institute (SMHI) and its first application dates back to the early 1970s [45]. The HBV model which includes conceptual numerical descriptions of hydrological processes at the catchment scale is best characterized as a semi-distributed conceptual hydrologic model. The model is usually run on the daily values of precipitation, temperature and estimates of potential evapotranspiration. Flow observations are used for calibration and validation of the model. For most of the applications, the model is run on a daily time step, but it is possible to use shorter time steps. The evapotranspiration values can be used as monthly averaged or daily values. The potential evapotranspiration is calculated using air temperature. The model contains routines for snow accumulation and melt, soil moisture accounting, runoff generation and a routing procedure. The snowmelt routine of the HBV model is a degree-day approach. It is based on air temperature, with a water holding capacity of snow which delays runoff. The soil moisture routine of the model controls runoff formation, accounts for soil field capacity and change in soil moisture storage due to rainfall/snowmelt and evapotranspiration. The excess water from the soil moisture zone transforms to runoff in the response routing. The response function of the model consists of two reservoir – one upper nonlinear, one lower linear, and one transform function. The runoff is computed by adding the contribution from the upper and lower reservoir, and the generated runoff is routed through a transformation function in order to get a proper shape of the hydrograph at the outlet of the watershed.

Model Calibration and Validation

The process of optimization of model parameters to minimize the difference between model output and observed data is referred to as calibration. A calibrated model needs to be verified for ensuring that the optimized parameters are a good representation of the physical behavior of the catchment. The parameters of the HBV model need to be calibrated in order to provide model output that closely resembles observed data as it is a conceptual model. The HBV manual [46] recommends using at least 10 years of data for the calibration period. It is also recommended to use 75% of total data for model calibration and 25% of data for model validation. The first 22 years of data (from 1985 to 2006) were used to calibrate the hydrologic model and the last 8 years of data (2007-2014) were used to validate the model. The calibration and validation of the hydrologic model were carried out using the observed and simulated flow hydrograph of daily time step at the outlet (Spencer Creek at Dundas hydrometric station) of the watershed. Following the recommendation of the HBV manual during calibration, the evaluation of the results was mainly done by comparing the explained variance/ Nash and Sutcliffe coefficient R^2 [47] ,and visually inspecting and comparing the simulated and observed hydrographs. The Nash and Sutcliffe coefficient is the variance around the mean explained by the model. The optimum value of the Nash and Sutcliffe coefficient is one (1), and a value less than 0.7 represent poor performance [48]. The model calibration and validation results of the Spencer Creek watershed model show a good performance according to the Nash and Sutcliffe coefficient of 0.76 for the calibration period and 0.75 for the validation period. The equation used to calculate the Nash and Sutcliffe coefficient (R^2) is as follows:

$$NASH(R^2) = 1 - \frac{\sum_{i}^{N}(y_i - y_i')^2}{\sum_{i=1}^{N}(y_i - y_{mean})^2} \qquad \text{Eq. 2-13}$$

where, y_i is the observed streamflow at time step i, y_i' is simulated streamflow at time step i, y_{mean} is the mean of observed streamflow, and N is the number of data points. Figures 2-2 and 2-3 demonstrate observed flow and simulated flow from the hydrologic model for two years of both calibration and validation period.

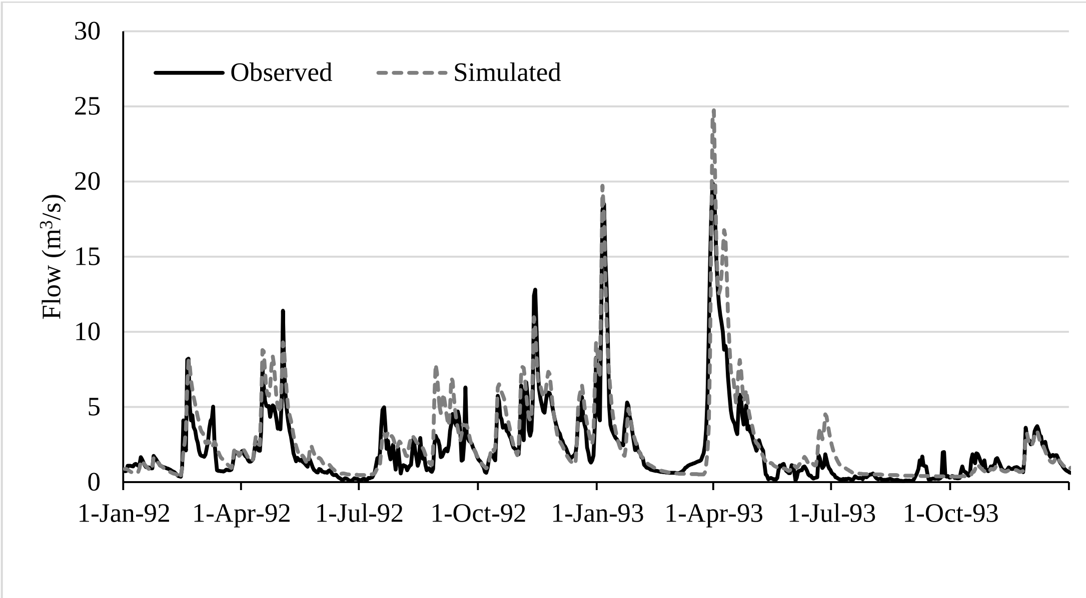

Figure 2-2: Observed and simulated flows at Dundas station in the calibration period of 1992-1993

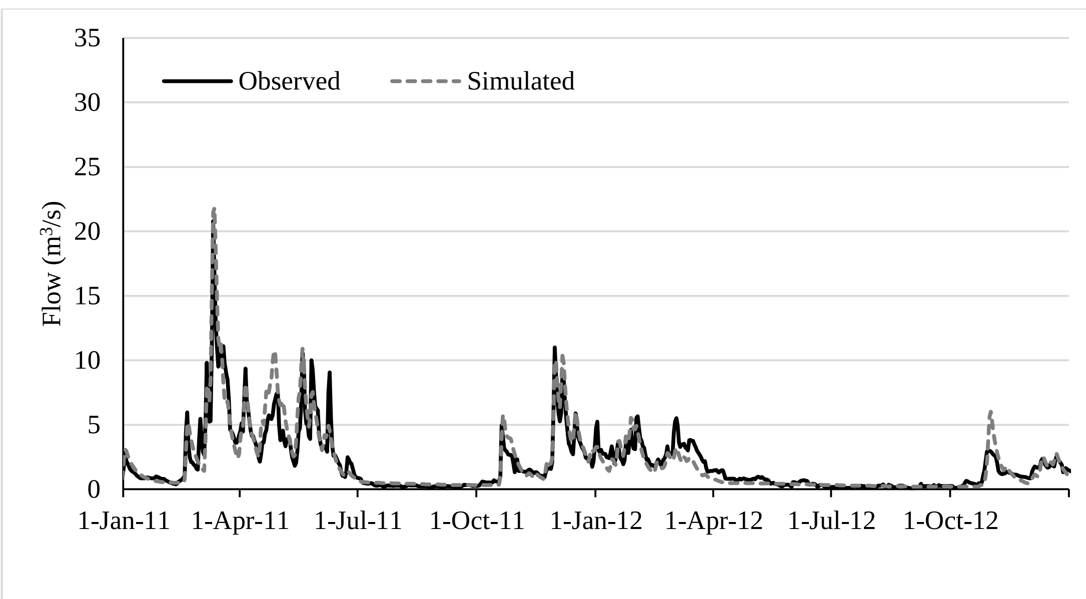

Figure 2-3: Observed and simulated flows at Dundas station in the validation period of 2011-2012

Hydrologic Simulation

The calibrated HBV model was used to simulate flows at the outlet and evapotranspiration from the watershed at a daily time step for both current (1971-2000) and future (2041-2070) period. The bias-corrected daily total precipitation and daily mean temperature from eight RCM+GCM pairs for current (1971-2000) and future (2041-2070) period were used as input in the watershed model for hydrologic simulation.

2.5 Results and Discussion

2.5.1 Evaluation of Bias-Corrected data

Bias correction was applied to raw NARCCAP daily precipitation and mean temperature (calculated from NARCCAP daily maximum and minimum temperature) both for current (1971-2000) and future (2041-2070) period using the method described in section 2.4.1. The improvement in bias-corrected NARCCAP projections was assessed using skill score BSS and RPSS described in section 2.4.2, and the BSS and RPSS show the percentage improvement in this study. The BS and RPS were calculated for raw and bias-corrected NARCCAP eight RCM+GCM pair's data for the current period. The scores and skill scores calculated for two meteorological stations namely Hamilton Airport and Hamilton RBG are presented in Tables 2-2 to 2-5. The skill scores represent the improvement of bias-corrected NARCCAP data over raw NARCCAP data produced by eight RCM+GCM pairs. The calculated skill scores revealed an overall improvement in both precipitation and temperature at both stations when bias correction is made. In the case of precipitation, the BS values do not show a seasonal pattern in skill, but the RPS values show that overall skill in other seasons is better than the skill in winter months. Both BSS and RPSS results shown in Table 2-2 indicate that improvement is higher in the late spring and summer months than others months, and the highest improvement is shown in the month of July with BSS and RPSS values of 18.8% and 8.6%, respectively. A similar seasonal pattern in the improvement of bias-corrected precipitation at Hamilton RBG is shown in Table 2-3, and it also shows that the highest improvement is in the month of June with BSS and RPSS values of 21.2% and 7.1%, respectively. Results in Table 2-2 and 2-3 show that the improvement presented by RPSS is higher when the RPS of raw NARCCAP precipitation is lower in general. For example, RPS values for raw NARCCAP precipitation at Hamilton Airport are 0.57 and 1.15 in the month of June and December, respectively, and the corresponding RPSS values are 7% and 1.7%. Both BSS and RPSS values shown in Tables 2-4 and 2-5 indicate that there is a significant improvement in quality in bias-corrected daily mean temperature for both meteorological stations, and the improvement is slightly better for Hamilton RBG station than Hamilton Airport station. Both BSS and RPSS values also show that the improvement in the quality of bias-corrected daily mean temperature is highest in the month of June for both stations. The BSS and RPSS values are 10.7% and 9.1% in the month of June for Hamilton Airport, and these values are 16.1% and 16.5% for Hamilton RBG station. The RPSS values show that the overall improvement in the quality of bias-corrected temperature is better in the summer months than other seasons.

Table 2-2: Skill score of bias-corrected precipitation at Hamilton Airport

Month	BS	BS	BSS (%)	RPS	RPS	RPSS (%)
	Raw	Bias-Cor		Raw	Bias-Cor	
Jan	0.29	0.28	3.4	1.10	1.09	0.9
Feb	0.32	0.29	9.4	1.14	1.12	1.8
Mar	0.32	0.29	9.4	0.81	0.8	1.2
Apr	0.31	0.28	9.7	0.87	0.82	5.7
May	0.34	0.28	17.6	0.57	0.54	5.3
Jun	0.33	0.27	18.2	0.57	0.53	7.0
Jul	0.32	0.26	18.8	0.58	0.53	8.6
Aug	0.30	0.26	13.3	0.55	0.53	3.6
Sep	0.29	0.27	6.9	0.54	0.54	0.0
Oct	0.31	0.28	9.7	0.86	0.84	2.3
Nov	0.32	0.29	9.4	0.83	0.81	2.4
Dec	0.33	0.29	12.1	1.15	1.13	1.7

Table 2-3: Skill score of bias-corrected precipitation at Hamilton RBG

Month	BS	BS	BSS (%)	RPS	RPS	RPSS (%)
	Raw	Bias-Cor		Raw	Bias-Cor	
Jan	0.32	0.29	9.4	0.84	0.83	1.2
Feb	0.33	0.29	12.1	0.85	0.82	3.5
Mar	0.34	0.28	17.6	0.55	0.55	0.0
Apr	0.32	0.28	12.5	0.89	0.83	6.7
May	0.34	0.27	20.6	0.55	0.53	3.6
Jun	0.33	0.26	21.2	0.56	0.52	7.1
Jul	0.32	0.26	18.8	0.56	0.53	5.4
Aug	0.30	0.27	10.0	0.54	0.53	1.9
Sep	0.30	0.28	6.7	0.55	0.55	0.0
Oct	0.31	0.27	12.9	0.57	0.55	3.5
Nov	0.33	0.29	12.1	0.84	0.83	1.2
Dec	0.34	0.29	14.7	0.85	0.84	1.2

Table 2-4: Skill score of bias-corrected temperature at Hamilton Airport

Month	BS	BS	BSS (%)	RPS	RPS	RPSS (%)
	Raw	Bias-Cor		Raw	Bias-Cor	
Jan	0.31	0.30	3.2	1.97	1.96	0.5
Feb	0.29	0.28	3.4	1.91	1.89	1.0
Mar	0.26	0.25	3.8	1.76	1.73	1.7
Apr	0.26	0.25	3.8	1.75	1.73	1.1
May	0.25	0.24	4.0	1.68	1.62	3.6
Jun	0.28	0.25	10.7	1.87	1.70	9.1
Jul	0.29	0.28	3.4	2.03	1.93	4.9
Aug	0.29	0.28	3.4	2.03	1.92	5.4
Sep	0.27	0.26	3.7	1.85	1.76	4.9
Oct	0.27	0.27	0.0	1.86	1.81	2.7
Nov	0.27	0.27	0.0	1.84	1.80	2.2
Dec	0.30	0.30	0.0	1.91	1.90	0.5

Table 2-5: Skill score of bias-corrected temperature at Hamilton RBG

Month	BS	BS	BSS (%)	RPS	RPS	RPSS (%)
	Raw	Bias-Cor		Raw	Bias-Cor	
Jan	0.33	0.3	9.1	2.11	1.96	7.1
Feb	0.30	0.28	6.7	2.09	1.88	10.0
Mar	0.28	0.26	7.1	1.84	1.76	4.3
Apr	0.26	0.25	3.8	1.80	1.74	3.3
May	0.25	0.25	0.0	1.81	1.65	8.8
Jun	0.31	0.26	16.1	2.06	1.72	16.5
Jul	0.32	0.30	6.3	2.29	1.96	14.4
Aug	0.30	0.28	6.7	2.12	1.90	10.4
Sep	0.29	0.26	10.3	2.03	1.77	12.8
Oct	0.27	0.26	3.7	1.95	1.78	8.7
Nov	0.30	0.27	10.0	2.07	1.81	12.6
Dec	0.33	0.29	12.1	2.12	1.92	9.4

2.5.2 Monthly Average Changes in Climate Variables and Flows

The bias-corrected NARCCAP precipitation and daily mean temperature time series over thirty years for both current (1971-2000) and future (2041-2070) periods were analyzed to show the changes under future climate condition. The hydrologic model simulated actual evapotranspiration for the same periods was also analyzed to show any changes. The monthly average values for these variables were calculated to get insight about how the changes are distributed seasonally. Here, the monthly average values were calculated from the average of eight RCM+GCM pairs. The calculated monthly average precipitation and daily mean temperature for Hamilton Airport and Hamilton RBG stations are presented in Figures 2-4 to 2-7. Figure 2-4 and 2-5 show that precipitation increases significantly for the most part of the year except the summer months including September. The increase in precipitation under future climate at Hamilton Airport station varies between 3% and 17%, and the lowest and highest increase are in a fall month, October and a winter month, January, respectively. A similar increase in future precipitation is shown at Hamilton RBG as the lowest increase of 6% in a fall month – November and the higher increase of 16-17% in two winter months, December and January. The increase in precipitation during March, April and May are similar as shown in Figures 2-4 and 2-5. The decrease in precipitation will be highest (10-11%) in the summer month of July for both Hamilton and Hamilton RBG station, and the decrease of precipitation in June is insignificant for both meteorological stations. Figures 2-4 and 2-5 also show that the higher amounts of monthly average precipitation in the future are in April and December at Hamilton Airport, and in May and December at Hamilton RBG station. The precipitation projection of average RCMs shows a clear signal of seasonal distribution of change in the precipitation regime. From Figures 2-6 and 2-7, it appears that the daily mean temperature will increase in all months at both meteorological stations. Figures 2-6 and 2-7 show that the highest and lowest daily mean temperatures are in July and January, respectively at both stations. The increase in temperature under future climate varies between 1.91°C and 3.44°C at Hamilton Airport station and 1.9°C and 3.37°C at Hamilton RBG. The lowest and highest increases are in October and January, respectively. These increases of temperature are close to the increases revealed by Sultana and Coulibaly [4]. A higher increase in the summer month of June than other months in spring, summer and fall are also shown in the figures. Overall, the increase in daily mean temperature in all winter months is higher than other seasons. The temperature projection of average RCMs shows a clear signal of seasonal distribution of change in the temperature. The actual evapotranspiration on daily time step was simulated by the hydrologic model for current and future periods, and the monthly average values of the average of eight RCM+GCM pairs are presented in Figure 2-8. It can be seen from Figure 2-8 that the actual evapotranspiration in the future is higher than the current period in all months except in July and August. Increase in evapotranspiration in July is insignificant because of an insignificant decrease in monthly average precipitation, although there is a significant increase in temperature (2.97°C and 3.16°C at Hamilton Airport and Hamilton RBG) in future. The higher decrease in precipitation and lower increase in temperature in other summer months, July and August than in June resulted in about 10% decrease in evapotranspiration. Figure 2-8 also shows a small amount of evapotranspiration in the winter. Although the actual evapotranspiration is very low in the winter months, the percentage increase is higher in the winter than in other seasons because of a higher increase in temperature and increase in precipitation. In can be seen from Figure 2-8 that the total increase in evapotranspiration in each month (21mm, 24mm and 18 mm in March, April and May, respectively) of spring is much higher than in other seasons.

Figure 2-9 presents the monthly average flows of the average of eight RCM+GCM pairs for both current and future periods. It can be seen from Figure 2-9 that the monthly flows increase in the winter and decrease in other seasons except an insignificant increase (0.03 m^3/s) in October.

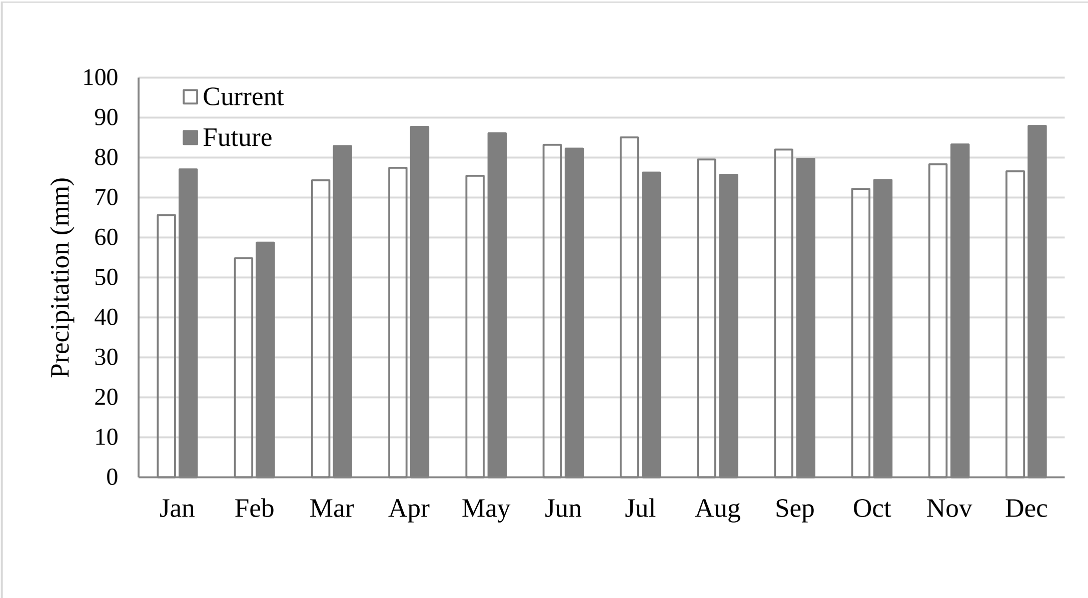

Figure 2-4: Bias-corrected current and future climate model simulated precipitation at Hamilton Airport

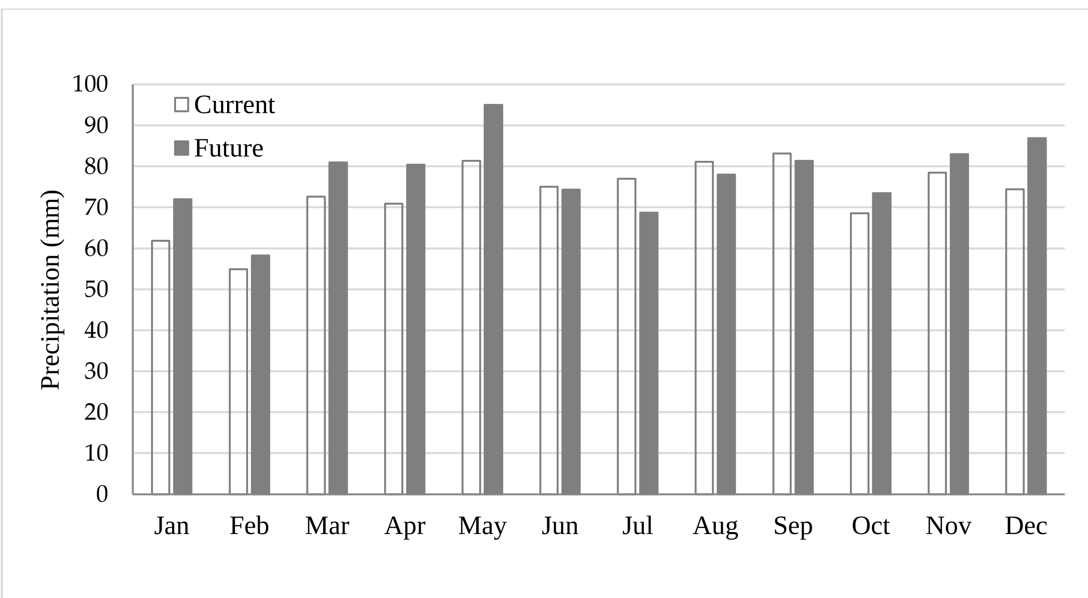

Figure 2-5: Bias-corrected current and future climate model simulated precipitation at Hamilton RBG

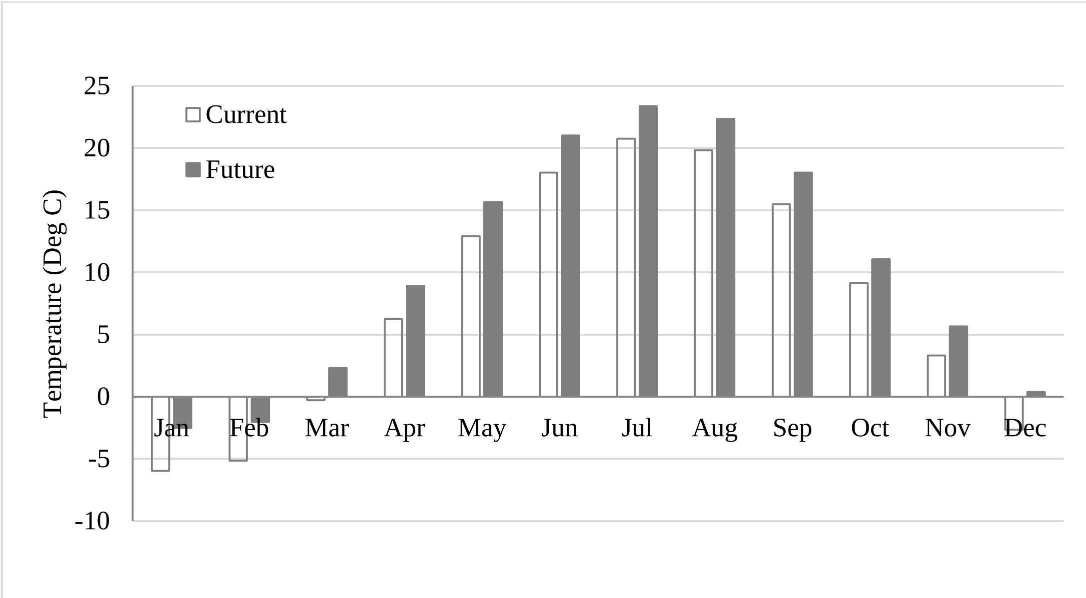

Figure 2-6: Bias-corrected current and future climate model simulated mean temperature at Hamilton Airport

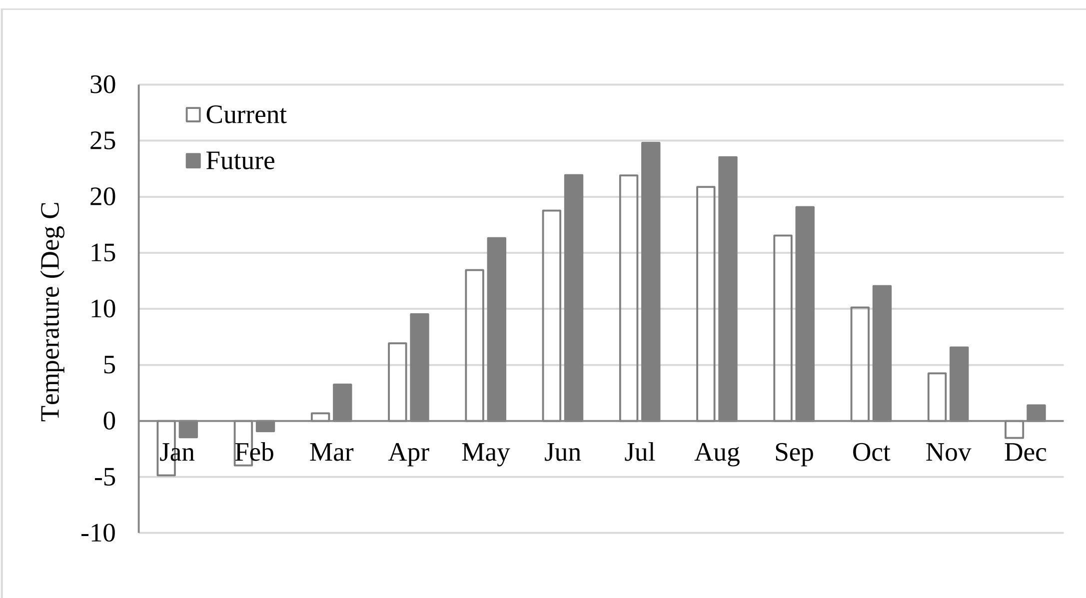

Figure 2-7: Bias-corrected current and future climate model simulated mean temperature at Hamilton RBG

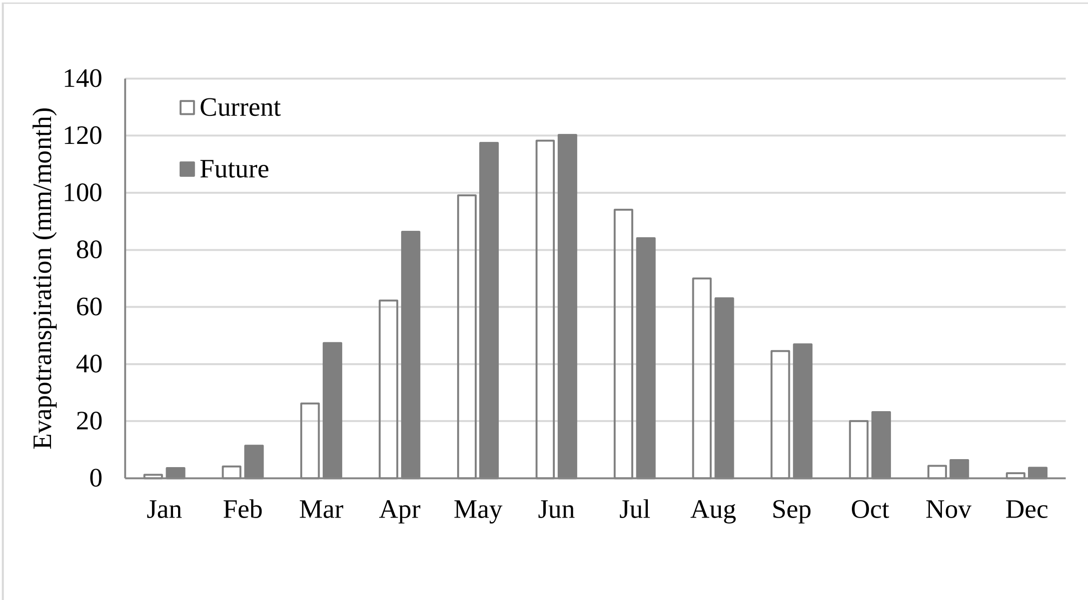

Figure 2-8: Model simulated monthly evapotranspiration at the watershed

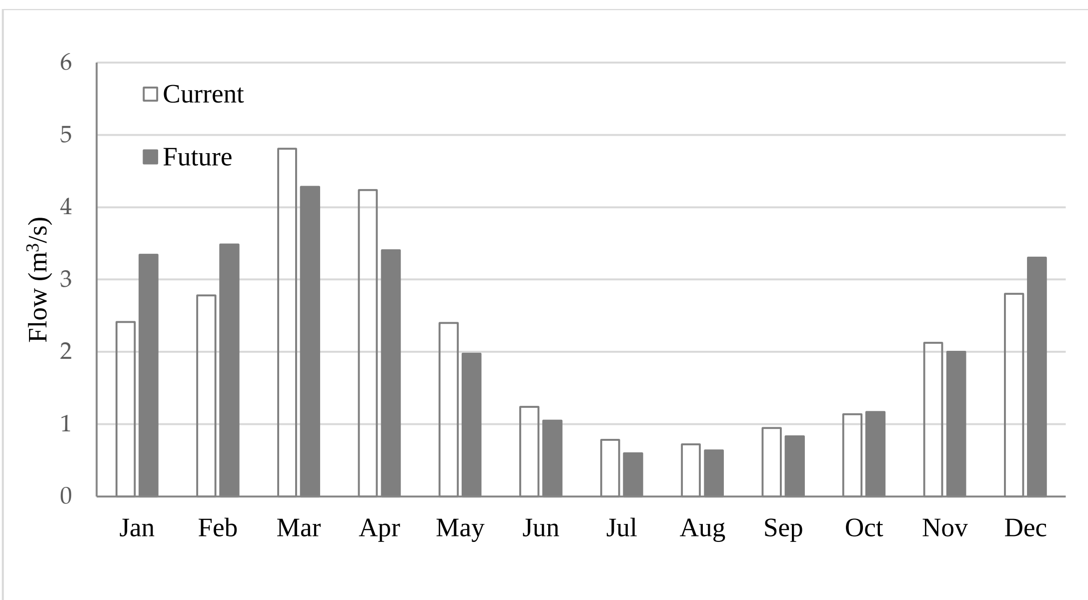

Figure 2-9: Model simulated average monthly flow at the Spencer Creek at Dundas station

The seasonal distribution of future flow is similar to the findings presented by Grillakis et al. [3]. The increase in flow in December, January and February are 17.9% (or 0.50 m^3/s), 38.5% (or 0.93 m^3/s) and 25.3% (0.70 m^3/s), respectively. The decrease in flows in future varies between 6% (or 0.13 m^3/s) and 24.1% (or 0.19 m^3/s), and the lowest and the highest decrease are in November and in July, however the highest decrease in terms of flow magnitude is in April, where the change is 0.83 m^3/s (or 19.7%). The effect of a change in precipitation, temperature, and evapotranspiration for the resultant change in future flow is complex. The effect of a change in evapotranspiration on flow in the winter months is small as the monthly average evapotranspiration is very small in these months. The higher increase in flows in winter months could be attributed to the increase in both winter month's precipitation and temperature in future. The warmer winter temperature in future will increase the winter snowmelt, and will result in the decrease of snowpack for annual basis and termination of snowmelt in the earlier in the spring. Despite the increase in the future precipitation in the spring, the flow will be decreased in the spring because thinner snowpack left to be melted and high evapotranspiration increase in this season. The decrease in flows in the summer is caused by the decrease in precipitation in future, and a comparatively small decrease in the fall could be attributed to the increase of evapotranspiration.

2.5.3 Yearly Average Changes in Climate variables and Flows

The difference between the current and future climate variables and flows were analysed, and the annual average of precipitation, daily mean temperature, and the hydrologic model simulated actual evapotranspiration and flows are presented in Table 2-6. It can be seen from Table 2-6 that six RCM+GCM pairs out of eight pairs projected an increase in precipitation with the highest increase projected by WRFG+CGCM3 model at 13% and 14% for Hamilton Airport and Hamilton RBG, respectively. It is worth mentioning that all the RCM+GCM pairs show an increase in the annual average of daily mean temperature. The increase in temperature in future varies between 2.27°C and 3.4°C at Hamilton Airport and between 2.26°C and 3.59°C at Hamilton RBG. The greatest change in terms of temperature increase is projected by HRM3+GFDL models and the most conservative change is projected by WRFG+CCSM and WRFG+CGCM3 models for Hamilton Airport and Hamilton RBG, respectively. The CRCM model projected temperature change is higher than other models except the HRM3+GFDL, and the WRFG model projected temperature increase is lower than the other models. It is notable that the annual average evapotranspiration under future climate compared to current climate will increase for all the RCM+GCM pairs. Table 2-6 shows that the annual average flows at the Spencer Creek at Dundas hydrometric station will be increased in the case of five RCM+GCM pairs out of eight pairs, and the higher increase (10%) is exhibited by RCM3+GFDL and WRFG+CGCM3 model while the highest decrease (14.7%) is exhibited by HRM3+GFDL model. Overall, the decrease in flows is also shown by one GCM (CCSM) with two RCMs. Averages of eight RCM+GCM pairs show an increase for all climate variables and a small increase of annual average flow in future. In the case of annual average flows, a difference from the study done by Grillakis et al. [3] is noticed, and the difference resulted due to the use of a different period of data for bias correction and flow comparison for current and future period, and the use of a different number of RCM+GCM pairs. Taking into account the future increase in annual average flow, analysis of flow duration were performed to get insight into how the flow regime will be changed under future climate condition.

Table 2-6: Changes in annual average precipitation, daily mean temperature, evapotranspiration and flow

			Crcm Ccsm	Crcm Cgcm3	Hrm3 Gfdl	Hrm3 Hadcm3	Rcm3 Cgcm3	Rcm3 Gfdl	Wrfg Ccsm	Wrfg Cgcm3	Average
Hamilton	P (mm/day)	Current	2.44	2.46	2.48	2.48	2.46	2.45	2.52	2.51	2.47
Airport	P (mm/day)	Future	2.47	2.67	2.35	2.74	2.64	2.69	2.45	2.84	2.57
	%	Change	**1.0**	**8.7**	**-5.2**	**10.6**	**7.3**	**9.6**	**-2.8**	**13.0**	**4.1**
	T (°C)	Current	7.70	7.70	7.70	7.70	7.70	7.70	7.70	7.70	7.70
	T (°C)	Future	10.61	10.81	11.11	10.31	10.28	10.25	9.98	9.99	10.48
	°C	Change	**2.90**	**3.11**	**3.40**	**2.61**	**2.58**	**2.54**	**2.27**	**2.28**	**2.77**
Hamilton	P (mm/day)	Current	2.37	2.38	2.43	2.46	2.37	2.37	2.45	2.43	2.40
RBG	P (mm/day)	Future	2.39	2.60	2.34	2.62	2.62	2.68	2.40	2.77	2.52
	%	Change	**0.8**	**9.2**	**-3.7**	**6.7**	**10.3**	**13.0**	**-1.8**	**14.0**	**4.9**
	T (°C)	Current	8.65	8.65	8.65	8.65	8.65	8.65	8.65	8.65	8.65
	T (°C)	Future	11.53	11.73	12.25	11.36	11.21	11.21	10.92	10.92	11.46
	°C	Change	**2.87**	**3.08**	**3.59**	**2.71**	**2.56**	**2.56**	**2.27**	**2.26**	**2.80**
Spencer	E (mm/day)	Current	1.60	1.74	1.59	1.74	1.71	1.73	1.63	1.71	1.68
	E (mm/day)	Future	1.47	1.48	1.52	1.51	1.50	1.51	1.49	1.47	1.49
	%	Change	**8.7**	**17.6**	**4.8**	**14.7**	**14.4**	**14.2**	**9.6**	**16.3**	**12.51**
Dundas	Q (m^3/s)	Current	2.00	2.19	1.87	2.28	2.20	2.32	1.96	2.51	1.92
	Q (m^3/s)	Future	2.16	2.18	2.19	2.23	2.13	2.11	2.28	2.28	1.91
	%	Change	**-7.3**	**0.1**	**-14.7**	**1.9**	**3.3**	**10.0**	**-13.8**	**10.0**	**0.5**

2.5.4 High and Low Flows

Figures 2-10 and 2-11 present the flow duration curves created using simulated flows at the Spencer Creek at Dundas hydrometric station for the current (1971-2000) and future period (2041-2070). The simulated current and future flows were obtained by inputting the bias-corrected NARCCAP's eight RCM+GCM pair's precipitation and temperatures into a calibrated hydrologic model. Figure 2-10 presents the flow duration curves for four RCM+GCM pairs, and Figure 2-11 presents the flow duration curve for the other four RCM+GCM pairs. For better visualization of the difference between flow duration curves, the maximum value on the ordinates is set to 6 m^3/s, and the eight RCM+GCM results are presented in two Figures. For every time series of daily flow data, the exceedance probability of each flow was calculated, and flow duration curves were produced by plotting discharge on the ordinate and exceedance probability on the abscissa. The large difference between the highest and the lowest flow values as shown in the flow duration curves in Figures 2-10 and 2-11 reveals that the watershed has a relatively low flow during the dry periods, but responds to extreme precipitation event with a relatively high flow. Two flow statistics, Q_{95} and Q_{10}, were used to compare the flow duration curves for current and future periods. Q_{95} and Q_{10} are the flow values that are equaled or exceeded 95% and 10% of the time, respectively. Q_{95} and Q_{10} are used for analysis of low flow and high flow, respectively [49]. As illustrated in Figures 2-10 and 2-11, the low flow decreased for all RCM+GCM pairs with the highest decrease (28.6%) exhibited by WRFG+CCSM model and lowest decrease (3.4%) exhibited by RCM3+CGCM3, and the calculated average low flow value for eight models indicates a decrease by 16.7% under future climate condition. It can be seen from Figures 2-10 and 2-11 that the high flow will increase for five RCM+GCM pairs (8.2%, 7.3%, 6.9%, 8.1% and 13.2% for CRCM+CGCM3, HRM3+HADCM3, RCM3+CGCM3, RCM3+GFDL and WRFG+CGCM3, respectively), and decrease for other three RCM+GCM pairs (0.4%, 16.1% and 7.1% for CRCM+CCSM, HRM3+GFDL and WRFG+CCSM, respectively), and the calculated average high flow value for eight models indicates an increase by 2.4 % under future climate condition. The maximum increase in high flow is obtained for WRFG+CGCM3 model, for which the increase of annual average precipitation is the highest, and a maximum decrease of high flow is obtained for HRM3+GFDL model, for which the decrease of annual average precipitation and increase of mean temperature is the highest. Taking into account that the increase in precipitation is consistent, and the high flow is mainly attributed to the precipitation amount, flow duration curves were constructed for the average of five RCM+GCM pairs (CRCM+CGCM3, HRM3+HADCM3, RCM3+CGCM3, RCM3+GFDL and WRFG+CGCM3), and shown in Figure 2-12. It is shown in the figure that the high flow will increase, and low flow will decrease significantly. The Q_{95} is obtained as 0.31 m^3/s and 0.27 m^3/s for current and future climate that resulted in 12.9% decrease in low flow, and Q_{10} is obtained as 5.11 m^3/s and 5.56 m^3/s for current and future climate that resulted in 8.8 % increase in high flow.

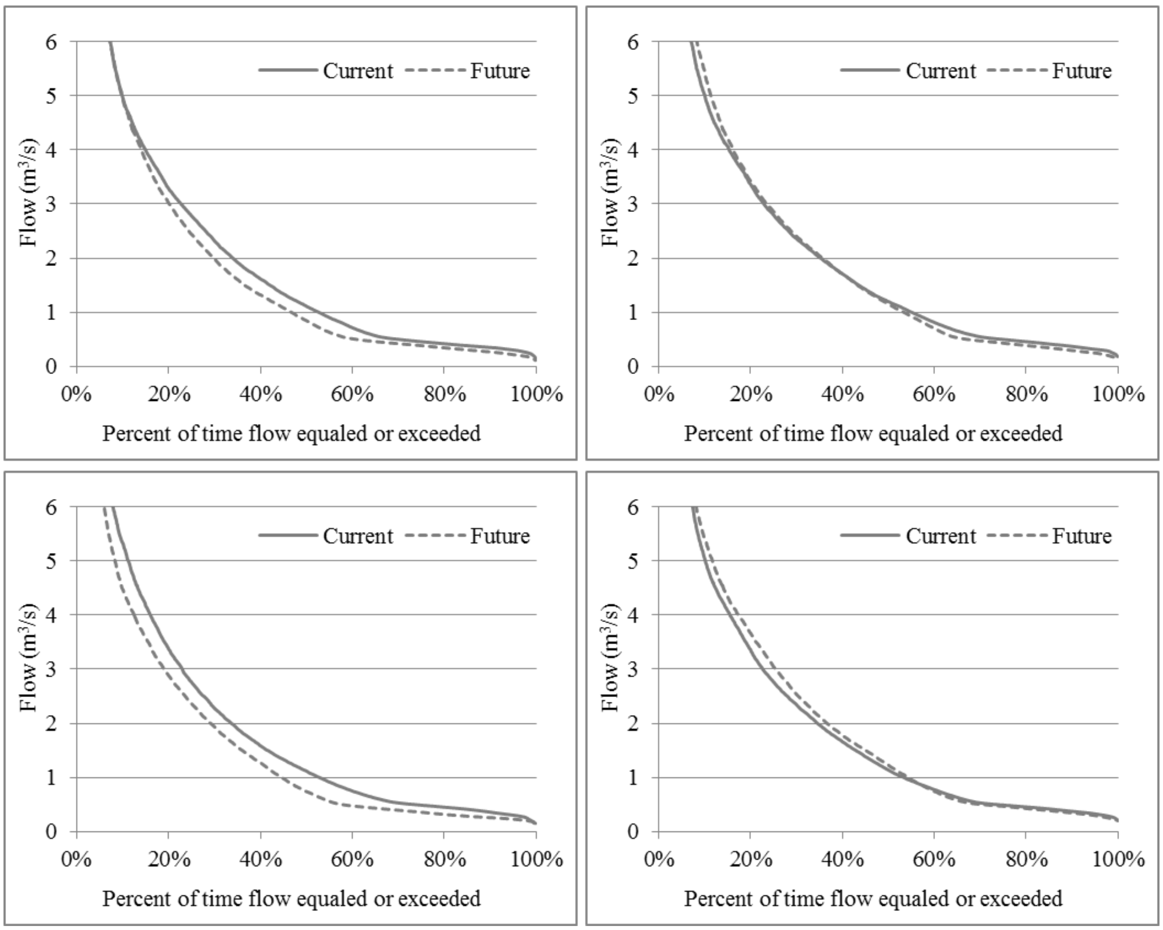

Figure 2-10: Flow duration curve for the Spencer Creek watershed (top left, top right, bottom left and bottom right represent CrcmCcsm, CrcmCgcm3, Hrm3Gfdl and Hrm3Hadcm3, respectively)

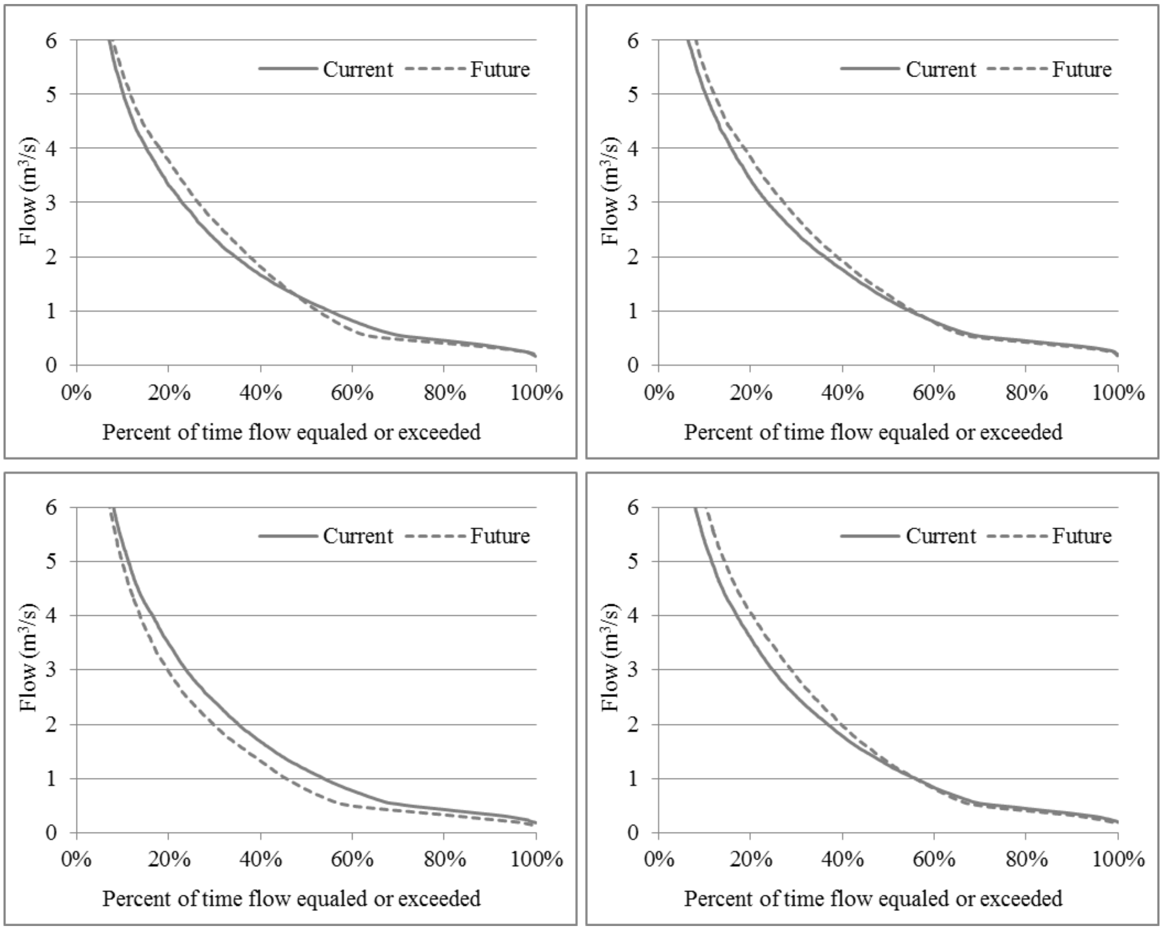

Figure 2-11: Flow duration curve for the Spencer Creek watershed (top left, top right, bottom left and bottom right represent Rcm3Cgcm3, Rcm3Gfdl, WrfgCcsm and WrfgCgcm3, respectively)

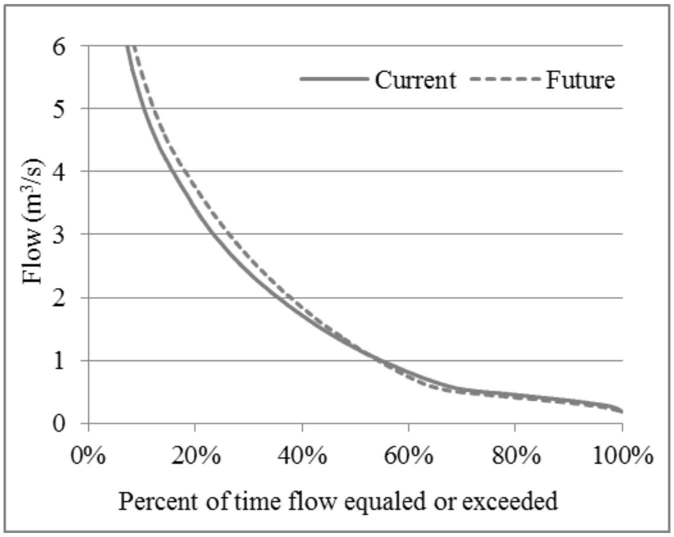

Figure 2-12: Flow duration curve of average of 5 RCM+GCM pairs for the Spencer Creek watershed

2.6 Conclusions

The potential impact of climate change on the hydrology of Spencer Creek watershed was analyzed based on the NARCCAP provided eight RCM+GCM pair's precipitation and temperature projections and simulations by using HBV hydrologic model for the current (1971-2000) and future (2041-2070) period.

The NARCCAP meteorological projections were bias corrected to get more realistic simulations from the hydrologic model. An overall improvement for the quality of NARCCAP precipitation and temperature simulations at both Hamilton Airport and Hamilton RBG meteorological stations was achieved when bias correction was applied. Both BSS and RPSS indicate that improvement is high in the late spring and summer months in the case of precipitation. The overall improvement in the quality of bias-corrected temperature is the best for summer months as revealed by RPSS with the highest improvement obtained in June as revealed by both BSS and RPSS.

The climate variables and flow were analyzed on monthly and annually to get insight into the seasonal and overall change under future climate compared to the current climate. Finally, high and low flow were analyzed by using the flow duration curves for eight RCM+GCM pair's data and average of the RCM+GCM pair's data. The RCM+GCM average shows that the precipitation will increase in the fall, winter and spring and decrease in the summer, the temperature will increase in all months, actual evapotranspiration will increase in all months except July and August, and the flow will increase in the winter and decrease in the other seasons. The RCM+GCM averages also show a significant increase in all climate variables and a small increase in annual average flow. The small increase in annual average flow could be attributed to the very high decrease in low flow despite an increase in high flow. The WRFG+CGCM3 model projected the greatest increase in high flow by 13.2% and the WRFG+CCSM model projected the highest decrease in low flow by 28.6%. The averages of eight RCM+GCM pairs show an increase of high flow by 2.4% and a decrease of low flow by 16.7% and the average of five RCM+GCM pairs (precipitation projected by this model are consistent) revealed an increase of high flow by 8.8% and a decrease of low flow by 12.9%. The changes in winter and spring flow will influence the water management at watershed scale. The authorities have to adopt new strategies to manage higher winter and lower spring flow and higher uncertainty in flows for the watershed management infrastructures.

Acknowledgement

We wish to thank the North American Regional Climate Change Assessment Program (NARCCAP) for providing the data used in this paper. The authors gratefully acknowledged Hamilton Region Conservation Authority, Water Survey Canada and Environment Canada for providing data for the study area. This study was supported by the Natural Sciences and Engineering Research Council (NSERC) of Canada in the form of discovery grant (RGPIN04808-14).

References

1. IPCC (2014) Climate Change 2014: Synthesis Report. Contribution of Working Groups I, II and III to the Fifth Assessment Report of the Intergovernmental Panel on Climate Change. Core Writing Team, Pachauri, PK, Meyer, LA (eds.) IPCC, Geneva, Switzerland, 151 pp.
2. Islam Z, Gan TY (2014) Effect of climate change on the surface-water management of South Saskatchewan river basin. Journal of Water Resources Planning and Management 140:332-342.
3. Grillakis MG, Koutroulis AG, Tsanis IK (2011) Climate change impact on the hydrology of Spencer creek watershed in Southern Ontario, Canada. Journal of Hydrology 409: 1-19.
4. Sultana Z, Coulibaly P (2011) Distributed modeling of future changes in hydrological processes of Spencer Creek watershed. Hydrological Processes 25 (8): 1254–1270. DOI:10.1002/hyp.7891.
5. Boyer C, Chaumont D, Chartier I, Roy AG (2010) Impact of climate change on the hydrology of St. Lawrence tributaries. Journal of Hydrology 384: 65–83.
6. Dibike YB, Coulibaly P (2005) Hydrologic impact of climate change in the Saguenay watershed: comparison of downscaling methods and hydrologic models. Journal of Hydrology 307 (1–4): 145–163.

7. Fowler HJ, Blenkinsop S, Tebaldi C (2007) Linking climate change modeling to impacts studies: Recent advances in downscaling techniques for hydrological modeling. Int J Climatol 27(12): 1547–1578.
8. Praskievicz S, Chang HJ (2009) A review of hydrological modeling of basin-scale climate change and urban development impacts. Progress in Physical Geography 33 (5): 650-671.
9. Prudhomme C, Reynard N, Crooks S (2002) Downscaling of global climate models for flood frequency analysis: Where are we now? Hydrol. Processes 16 (6): 1137-1150.
10. Kalra A, Ahmad S (2011) Evaluating changes and estimating seasonal precipitation for Colorado River Basin using stochastic nonparametric disaggregation technique. Water Resour Res 47: W05555.
11. Sharma M, Coulibaly P, Dibike Y (2011) Assessing the need for downscaling RCM data for hydrologic impact study. Journal of Hydrologic Engineering 16 (6): 534–539. DOI:10.1061/(ASCE)HE.1943-5584.0000349.
12. Mpelasoka FS, Chiew FHS (2009) Influence of rainfall scenario construction methods on runoff projections. J Hydrometeor 10:1168-83, doi:10.1175/2009JHM1045.
13. Samuel J, Coulibaly P, Metcalfe R A (2012) Evaluation of future flow variability in ungagged basins: Validation of combined methods. Advances in Water Resources 35: 121-140.
14. Payne JT, Wood AW, Hamlet AF, Palmer RN, Lettenmaier DP(2004) Mittigating the effect of climate change on the water resources of the Coumbia river basin, Clim Change 62:233-56.
15. Ines AVM, Hansen JW (2006) Bias correction of daily GCM rainfall for crop simulation studies. Agricultural and Forest Meteorology 138: 44–53.
16. Mearns LO, Gutowski WJ, Jones R, Leung LY, McGinnis S, et al. (2009) A regional climate change assessment program for North America. EOS, 90: 311-312.

17. Ahmed S, Coulibaly P, Tsanis I (2015) Improved spring peak-flow forecasting using ensemble meteorological predictions. Journal of Hydrologic Engineering 20(2): 04014044(14), DOI:10.1061/(ASCE)HE.1943-5584.0001014.
18. Liu X, Coulibaly P (2011) Downscaling ensemble weather predictions for improved week-2 hydrologic forecasts. Journal of Hydrometeorology 12(6): 1564-1580.
19. HRCA (1990) Hamilton Region Conservation Authority-MacLaren Plansearch Lavalin, Volume 1-Technical Report: Canada/Ontario Flood Damage Reduction Program.
20. NARCCAP (2013) North Americal Regional Climate Change Assessment Program. <http://www.narccap.ucar.edu/> (January26, 2013)
21. Mearns, L.O., et al. (2007), updated 2012. The North American Regional Climate Change Assessment Program dataset, National Center for Atmospheric Research Earth System Grid data portal, Boulder, CO. Data downloaded 2014-07-07. [DOI:10.5065/D6RN35ST].
22. Nakicenvoic N, Davidson O, Davis G, Grübler A, Kram T, et al. (2000) Special Report on Emissions Scenarios. A Special Report of Working Group III of the Intergovernmental Panel on Climate Change. Cambridge University Press Cambridge, 599.
23. Mailhot A, Beauregard I, Talbot G, Caya D, Biner S (2012) Future changes in intense precipitation over Canada assessed from multi-model NARCCAP ensemble simulations. Int J Climato 32: 1151-1163.
24. Music B, Caya D (2007) Evaluation of the hydrological cycle over the Mississippi River Basin as simulated by the Canadian regional climate model (CRCM). J Hydrometeor 8: 969-988.
25. Jones R, Noguer M, Hassell D, Hudson D, Wilson S, et al. (2004) Generating high resolution climate change scenarios using PRECIS. Met Office Hadley Center. Exter p 40.

26. Elguindi N, Bi X, Giorgi F, Nagarajan B, Pal J, et al. (2007) RegCM Version 3.1 User's Guide, Trieste, Italy. <https://users.ictp.it/RegCNET/regcm.pdf) (July 9, 2015)
27. Giorgi F, Marinucci MR, Bates GT (1993) Development of second generation regional climate model (RegCM2) I: boundary layer and radiative transfer processes. Mon Weather Rev 121: 2794-2813.
28. Skamarock WC, Klemp JB, Dudhia J, Gill DO, Barjer DM, Wang W, Powers JG (2005) A description of the advanced research WRF Version 2, NCAR Tech Notes-468+STR http://www.mmm.ucar.edu/wrf/users/docs/arw_v2.pdf (January 25, 2016)
29. Collins WD, Bitz CM, Blackmon ML, Bonan GB, Bretherton CS, et al. (2006) The community climate system model version 3 (CCSM3). J Climate 19: 2122-2143.
30. Flato GM (2005) The Third Generation Coupled Global Climate Model (CGCM3). <http://www.ec.gc.ca/ccmac-cccma/default.asp?n=1299529F-1> (August 9, 2015).
31. GFDL GAMDT (2004) The new GFDL global atmospheric and land model AM2-LM2: Evaluation with prescribed SST simulations. J Climate 17: 4641-4673.
32. Gordon C, Cooper C, Senior CA, Banks H, Gregory JM, et al. (2000) The simulation of SST, sea ice extents and ocean heat transports in a version of the Hadley Centre coupled model without fluxadjustments. Climate Dynamics 16: 147-168.
33. Pope VD, Gallani ML, Rowntree PR, Stratton RA (2000) The impact of new physical parameterizations in the Hadley Centre climate model-HadAM3. Climate Dynamics 16: 123-146.
34. Murphy AH, Brown BG, Chen Y (1989) Diagnostic verification of temperature forecasts." Weather Forecasting 4(4): 485-501.
35. Wilks DS (2000) Diagnostic verification of the Climate Prediction Center long-lead outlooks, 1995-1998. Journal of Climate 13(13): 2389-2403.

36. Hartmann HC, Pagano TC, Bales R, Sorooshian S (2002) Confidence builders: Evaluating seasonal climate forecasts from user perspectives. Bull. American Meteorological Society 83: 683-698.

37. Brier GW (1950) Verification of forecasts expressed in terms of probabilities. Monthly Weather Review 78: 1-3.

38. Renner M, Werner MG, Rademacher S, Sprokkereef E (2009) Verification of ensemble flow forecasts for the river Rhine. Journal of Hydrology 376(3-4): 463-475.

39. Roulin E (2007) Skill and relative economic value of medium-range hydrological ensemble predictions. Hydrology and Earth System Sciences 11(2): 725-737.

40. Mullen SL, Buizza R (2011) Quantitative precipitation forecasts over the United States by the ECMWF ensemble prediction system. Mon Weather Rev 129(4): 638-663.

41. Clark MP, Hay LE (2004) Use of medium-range numerical weather prediction model output to produce forecasts of streamflow. Journal of Hydrometeorology 5(1):15-32.

42. Gangopadhyay S, Clark M, Brandon D,Wener K, Rajagopalan B (2004) Effects of spatial and temporal aggregation on the accuracy of statistically downscaled precipitation estimates in the upper Colorado river basin. Journal of Hydrometeorology 5 (6):1192-1206.

43. Sharma M (2009) Comparison of downscaled RCM and GCM data for hydrologic impact assessment. M.A.Sc Thesis, Dept. of Civil Engineering, McMaster University, Hamilton, Ontario, Canada.

44. Bergstrom S (1991) Principles and confidence in hydrological modelling. Nordic Hydrology 22: 123-136.

45. Lindstrom G, Johansson B, Magnus P, Gardelin M, Bergstrom S (1997) Development and test of the distributed HBV-96 hydrological model. Journal of Hydrology 201: 272-288.

46. Swedish Meteorological and Hydrological Institute (SMHI) (2012) Integrated hydrological modelling system manual, version 6.3. Norrköping, Sweden.
47. Nash JE, Sutcliffe JV(1970) River flow forecasting through conceptual models. Part I – a discussion of Principals. Journal of Hydrology 10: 282-290.
48. Coulibaly P, Anctil F, Bobee B (2001) Multivariate reservoir inflow forecasting using temporal neural networks. Journal of Hydrologic Engineering 6: 367-376.
49. Zahmatkesh Z, Karamouz M, Goharian E, Burian SJ (2015) Analysis of the effect of climate change on urban storm water runoff using statistical downscaled precipitation data and a change factor approach. Journal of Hydrologic Engineering 20: 05014022(11). DOI: 10.1061/(ASCE)HE.1943-5584.0001064.

Chapter 3 : Climate Change Impact on Design Storm and Performance of Urban Storm-Water Management System - A Case Study on West Central Mountain Drainage Area in Canada

Summary of Paper II : Ahmed, S., and Tsanis, I. (2016). Climate Change Impact on Design Storm and Performance of Urban Storm-Water Management System - A Case Study on West Central Mountain Drainage Area in Canada. Hydrology: Current Research, 7, 229. doi: 10.4172/2157-7587.1000229.

The objective of this study was to investigate the potential impact of changed rainfall extreme under future climate on urban drainage systems in the West Central Mountain drainage area located in Southern Ontario, Canada. The objective was achieved by exploring the potential impact of climate change on the design storm depths and its effect on the performance of detention pond and storm sewer network under future climate condition**.** NARCCAP six RCM+GCM pair's data sets were used for design storm calculation by applying the best fitted distribution among twenty seven distributions tested by Pearson chi-square test and Kolmogorov-Smirnov test, and by applying delta change factor to transpose design storm depth calculated from gridded NARCCAP projection. The PCSWMM modeling tool was used for hydrologic simulation and hydraulic analysis of the storm-water management system.

The results of this study revealed the followings:

- Among the twenty seven distributions, the L-moment Pareto was selected the most often for annual maximum time series data for different duration calculated from six RCM+GCM pairs.
- Design storm depth will increase significantly for all duration (3h to 24hr) and return period (2yr to 100yr). Generally, the difference (increase) of design storm depths increases with the increase of return period. The increase of storm depth is higher for

shorter duration with higher return period and also higher for longer duration with lower return period. The increase of design storm depth under future climate is higher for higher values overall.

- The performance of detention pond will deteriorate under future climate condition. This was revealed by visual inspection of time series plot of inflow, outflow, storage volume and depth, and the performance ratio calculated for eight metrics for all ponds.
- For both the detention ponds and storm sewer network, the worst performance was observed under the RCM3+GFDL future scenario.

3.1 Abstract

A number of future climate projections indicate a likelihood of increased magnitude and frequency of hydrological extremes for many regions around the world. The urban storm-water management infrastructures are designed to mitigate the effect of extreme hydrological events. Changes in extreme rainfall events will have a significant implication on the design of storm-water management infrastructures. This study assessed the potential impact of changed rainfall extreme on drainage systems in the West Central Mountain drainage area located in Southern Ontario, Canada. First, the design storms for the study area were calculated from observed rainfall data and the North American Regional Climate Change Assessment Program (NARCCAP) climate simulations based on SRES A2 Scenario. Frequency analysis was performed on the annual maximum time series data by using the best fitted distribution among twenty seven distributions. The Pearson chi-square test and Kolmogorov-Smirnov were used to test the goodness of fit of each distribution. The results show that L-moment Pareto distribution was selected the most often for data from six RCM+GCM pairs. Overall increase of storm depth in the future is highest when the distributions were identified by the Kolmogorov-Smirnov test. The design storm depths calculated from the observed and climate model simulated data were used as input into an existing PCSWMM model of the study area for flow simulation and hydraulic analysis for the storm-water management system, specifically storm sewer and detention pond. The results show an increase in design storm depths under projected climatic change scenarios that suggest an update of current standard for designing both the minor system and detention pond in the study

area. The assessment results of storm water management infrastructures indicate that performance of the detention pond as well as the storm sewer network will deteriorate under future climate condition.

Keywords: Climate change; Storm-water management; Frequency analysis; Detention pond; Storm sewers; Canada

3.2 Introduction

The release of greenhouse gases and aerosols due to anthropogenic activities are changing the amount of radiation coming into and leaving the atmosphere. These are, in turn, changing the composition of atmosphere that may influence temperature, precipitation, storms and sea level. Observed increases in global average air and ocean temperatures, melting of polar ice and significant increases in net anthropogenic radiative forcing revealed that our global climate system is undergoing substantial warming [1]. An increased intense of ‘dry and hot’ extremes for many regions around the world was revealed by a number of studies on different climate model projections [2-6]. It is well known that increasing temperatures tend to increase evaporation which leads to more precipitation; so the changes in global temperature will have a significant effect on increasing magnitude and frequency of extreme precipitation events. These changes in temperature and precipitation will significantly affect frequency and severity of floods. Therefore, the design standards of storm-water management infrastructure, such as storm-water detention pond, and storm sewer have to adapt to the changing hydrologic process under future climate.

The storm-water infrastructures in an urban area are usually designed based on the rainfall depth calculated employing statistical analyses of observed precipitation data. The rainfall depths are calculated from the historic rainfall time series without considering climate change impact i.e., based on the assumption of a stationary climate. But, the climate is now non-stationary [7,8] because of the anthropogenic force. So, the designing of storm-water management infrastructure based on design storm considering the assumption of non-stationary climate will not be able to manage extreme events in future climate. The importance of developing design standard for addressing the climate change was indicated by many researchers [9-11]. Forsee and Ahmed [12] explored the projected changes in design-storm depths for Pittman watershed in Las Vegas using five NARCCAP data sets, and they showed a significant increase in case of three GCM+RCM pairs. Zhu et al. [13] investigated the potential changes in IDF curve due to climate change impact for six regions in the United States. They found strong regional patterns and increase in the intensity of extreme events under future climate for most of the study sites. Mailhot et al. [14] investigated the climate change impact in IDF curves for Southern Quebec using the Canadian Regional Model projections. The study results show that return period of 2 hour and 6 hour storm events will be approximately halved and return period of 12 hour and 24 hour storm events will decrease by one third. Coulibaly et al. [15] found significant increases in storm depth in 2050s and 2080s in Grand River, Kenora and Rainy River region in Canada by analyzing the storm depth calculated from climate simulations. In most of the studies, frequency analysis was performed on the annual maximum precipitation time series by fitting only one to three distributions for design storm depth calculations. For example, the Log-Pearson Type III for NARCCAP future precipitation time series was used by Moglen and Vidal [11], generalized extreme value was used by some studies [12,14], Extreme value type I (EV I) was used by Zhu et al. [13], Gumbel and generalized extreme value were used by Zhu [16]. This study explored the climate change impact on design storm depth calculated by employing frequency analyses of NARCCAP precipitation data sets. In this study, twenty seven distributions were tested for the observed, NARCCAP current and future dataset, and the best among the fitted distribution was used for frequency analysis to calculate design storm depths. Two statistical tests were used to test the goodness of fit at a 95% confidence level. The source of uncertainty involved in climate change impact studies are resulted from climate model projections, the hydrologic model and data downscaling techniques. The main sources of uncertainty, climate model projections, are derived from three main sources: forcing, model response and internal variability [17]. The climate change impact assessment using climate model data should consider multiple scenarios due to uncertainty in climate model projections. NARCCAP data provide several RCM+GCM pairs, and in this study six pairs of climate projection datasets were used for design storm depth calculation. All the NARCCAP dataset are provided at grid scale. One of the main challenges in climate change impact assessment is bridging the gridded climate change projections with the historic observation at meteorological station. A number of dynamical and statistical downscaling methods are available to downscale climate model gridded data at the target point locations [18-22]. A simple method for transposing gridded climate projections to station scale is the use of delta change factor [13]. In some studies delta change factors have been applied to precipitation time series [22-25], and in other studies it has been applied to design storm depth [12,13]. The delta change method was applied to transpose design storm depth calculated from gridded NARCCAP data to Hamilton Airport meteorological station.

The design and operation of urban drainage system is associated with local rainfall characteristics, i.e., design storm depth [23]. The design criteria of the urban drainage management infrastructure must be revised with the consideration of possible impact of climate change [10]. Moglen and Vidal [11] examined the changes in detention basin performance under several climate change scenario at a study location north of Washington, DC, and indicated that in most cases, the performance of detention basin would be inadequate under future climate condition. Forsee and Ahmad [12] also revealed the inadequate performance of detention basin under future climate condition in a watershed in Las Vegas Valley, Nevada. There are other studies showing inadequate performance of storm sewer and combined sewer under future climate condition [23,25,26]. This study investigated the performance of storm water management system at a study location in the City of Hamilton, Canada using several different climate projections. The following section details the study location.

3.3 Study Area and Data

3.3.1 Study Area

The study area (Figure 3-1), West Central Mountain drainage area, is a part of Red Hill Creek watershed located in the City of Hamilton, Southern Ontario, Canada. The modeling area is about 525 ha. The climate of Hamilton is humid-continental and characterized by changeable weather patterns. However, its climate is moderate compared with most of Canada. The daily average temperature in this area is 7.9 °C based on the data from 1981 to 2010 at Hamilton Airport, and extreme maximum 37.4 °C and extreme minimum temperature -30 °C were observed on 7 July, 1988 and 16 January, 2004 respectively. The yearly average rainfall and precipitation (rain and snow) are 791.7 mm and 929.8 mm based on data from 1981 to 2010 at Hamilton Airport, and the maximum daily rainfall and precipitation 107 mm were observed on 26 July, 1989. Grillakis et al. [27] analysed observed meteorological data over a twenty year period (1989-2008) from Hamilton Airport to show the interannual trend of precipitation and temperature, and revealed an increase of precipitation 3.5 mm/year and average temperature 0.041°C/year.

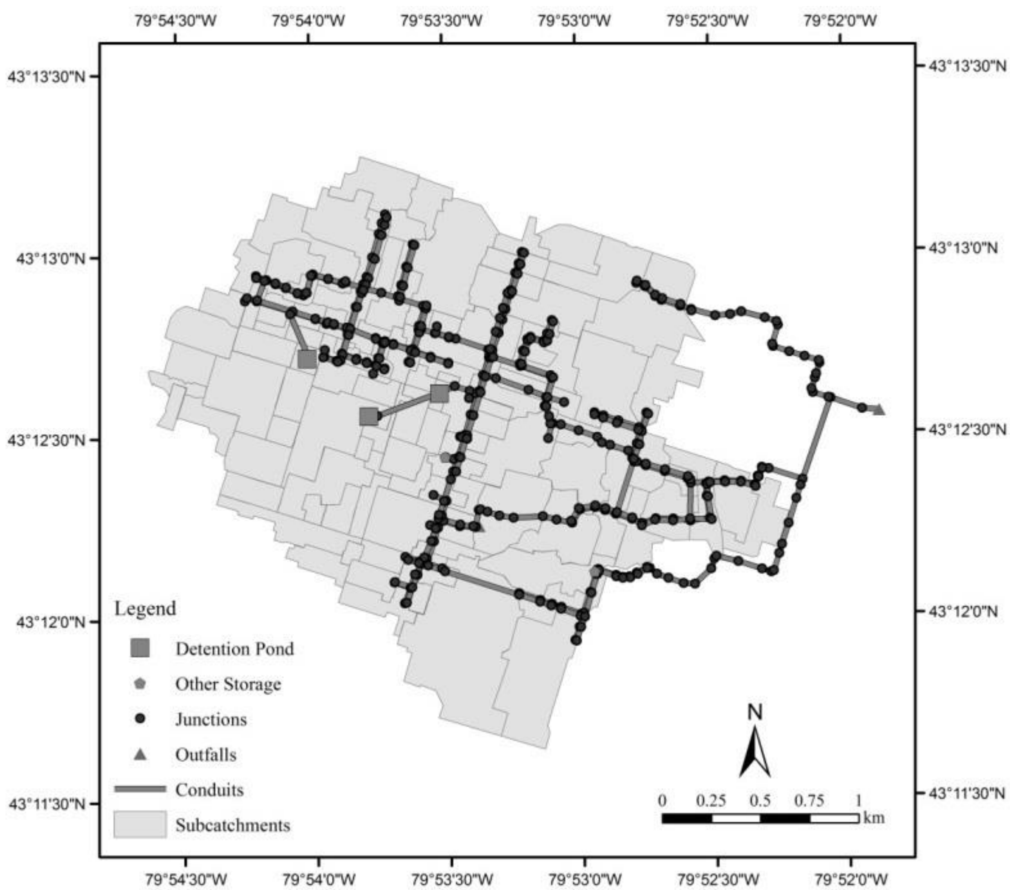

Figure 3-1: Map of the study area showing the stormwater management infrastructures

3.3.2 Observed Meteorological Data

The observed hourly rainfall data for 30 years, from 1971 to 2000, were obtained from meteorological station, namely Hamilton Airport meteorological station with latitude and longitude 43 10 25.00 N and 79 56 06.00 W. The hourly rainfall time series of this station was used to calculate the design storm because City of Hamilton uses the design storm calculated from this meteorological station for the study area. This hourly observed precipitation time series was provided by Ontario Climate Center, Environment Canada.

3.3.3 NARCCAP Climate Data

The climate data sets used in this research were obtained from The North American Regional Climate Change Assessment Program [28-30]. NARCCAP is an international program to produce high resolution climate change simulations covering the conterminous United States and most of Canada. It provides the data sets in order to investigate uncertainties in regional scale projections of future climate and generate climate change scenarios for use in impacts research. The climate data sets are generated by running a set of regional climate models (RCMs) driven by a set of atmosphere-ocean general circulation models (AOGCMs). The AOGCM involves coupling comprehensive three-dimensional atmospheric general circulation models, with ocean general circulation models, with sea-ice models, and with models of land-surface processes. RCM enhance the simulation of atmospheric circulations and climatic variables at fine spatial scales. This study uses the precipitation time series provided by six different RCM+GCM pairs. NARCCAP provides complete data for current and future for these six RCM+GCM pairs, and these six pairs include two pairs of each three RCMs. Table 3-1 provides the names of the RCMs and GCMs/ drivers used in this study.

The spatial resolution of all NARCCAP data sets is 50 km and the temporal resolution of precipitation time series is 3 hour [30]. NARCCAP provides precipitation time series data of time span 33 years for both current (1968-2000) and future (2038-2070) period. First three years of each simulation are spin-up periods [31] and the data of the spin-up period has been discarded. Therefore, the precipitation time series data of time span 30 years for both current (1971-2000) and future (2041-2070) period are actually considered in this study. All the NARCCAP future simulations are driven by a GCM with greenhouse gas and aerosol concentration based on A2 emission scenario described in the Special Report on Emissions Scenarios (SRES) [32]. The A2 scenario was preferred from an impacts and adaptation point of view. Data are stored in the NetCDF files in 2D arrays. The array dimensions are named "xc" and "yc" within the file. The array dimensions (yc, xc) are found from the grid cell maps for each RCMs. The array dimensions (yc, xc) of nearest point of Hamilton Airport for CRCM, HRM3 and RCM3 are (51,100), (57, 105) and (44, 94) respectively.

3.4 Methodology

The method used in this study can be described as a two-step procedure. At first an extensive frequency analysis was performed on the observed, NARCCAP current and future period data sets for design storm calculation. Then, the storm information was transformed into runoff and hydraulic information by employing a fully featured urban drainage system modeling tool.

Table 3-1: List of RCM+GCM Data Pairs used in this study

RCM+GCM Pairs	**RCM**	**GCM/Drivers**
CRCM+CCSM	Canadian Regional Climate Model [34]	Community Climate System Model [38]
CRCM+CGCM3	Canadian Regional Climate Model [34]	Third Generation Coupled Global Climate Model [39]
HRM3+GFDL	Hadley Regional Model 3 [35]	Geophysical Fluid Dynamics Laboratory GCM [40]
HRM3+HADCM3	Hadley Regional Model 3 [35]	Hadley Centre Coupled Model, version 3 [41,42]
RCM3+CGCM3	Regional Climate Model version 3 [36, 37]	Third Generation Coupled Global Climate Model [39]
RCM3+GFDL	Regional Climate Model version 3 [36, 37]	Geophysical Fluid Dynamics Laboratory GCM [40]

3.4.1 Design storm

Frequency analysis

A design storm can be represented by a value of rainfall depths or intensity (presented by IDF curves) or by a design hyetograph specifying the time distribution of rainfall during a storm. Design storm depths associated with different duration (3 h, 6 h, 12 h and 24 h) and return period (2 yr, 5 yr, 10 yr, 25 yr, 50 yr and 100 yr) were calculated for historic observations at station scale and climate model simulations at grid-scale. Data of the each time series were aggregated into 3-, 6-, 12- and 24 h duration on an annual basis, and the yearly maximum value for each duration was determined from the aggregated time series to generate time series of annual maximum rainfall depth. Frequency analysis was performed on these annual maximum time series data by using the best fitted distribution among twenty seven distribution as shown in Table 3-2 as well as Extreme Value type 1 (EV1) which is Gumbel distribution. Environment Canada provides the design storm information in the form of IDF curves and uses Gumbel Extreme Value distribution to fit the annual extremes of rainfall for the study area. Therefore, Extreme Value type 1 (EV1) was used for frequency analyses together with the best fitted distribution. Pearson chi-square test and Kolmogorov-Smirnov were used to test the goodness of fit of each distribution. The best fitted distribution is the distribution that attained the highest percentage of a. The percentage value of ‘a’ for Chi-square test (equation 3-1) and Kolmogorov-Smirnov (equation 3-2) are defined by the following two equations:

$$a_{attained} = 1 - x^2(m = k - r - 1, q) \qquad \text{Eq. 3-1}$$

$$a_{attained} = 1 - x^2(m, q) \qquad \text{Eq. 3-2}$$

where m are the degrees of freedom of chi square test, k is the number of bins used in chi square test, r is numbers of parameters of the distribution and q is the Pearson parameter. Kozanis et al. [33] described the theoretical background of all the tested distributions. The statistical analysis software, Hydrognomon [33], was used to find the best fitted distribution among 27 statistical distributions based on the criteria given in equation 1 and 2 for both observed and climate data.

Table 3-2: Best fitted distribution for NARCCAP data for different duration [Case 1 (current x, future √), case 2 (current *, future +)]

	CrcmCcsm				CrcmCgcm3				Hrm3Gfdl				Hrm3Hadcm3				Rcm3Cgcm3				Rcm3Gfdl			
Distribution	3	6	12	24	3	6	12	24	3	6	12	24	3	6	12	24	3	6	12	24	3	6	12	24
Normal						√																		
LogNormal											+, √	+, √												
Galton																								
Exponential										*											√x			
Gamma				+								* x		*										
Pearson III											x		√							x		x		
LogPearson III								*																
Gumbel EV 1 Max		*	x		+	*							+			x	*	+				*		
EV2-Max	+	+							+	+											*			+
Gumbel EV 1 Min							+																	*
Weibull							*																	
GEV Max				√																				
GEV Min	x																							
Pareto								√					* x		+									
L-Moments Normal	√					x		x																
L-Moments Exponential			+											+	*	+			+		+		*	
L-Moments EV1 Max	*	√ x				+																		
L-Moments EV2 Max			*						√*x								+					+		
L-Moments EV1 Min																								
L-Moments EV3 Min																								x
L-Moments GEV Max					√					x										*				√
L-Moments GEV Min			√											√	√	√	x	x				√	x	
L-Moments Pareto				x	*, x		√, x							x	x		√	√	√x	+,√			√	
GEV-Max (k spec.)										√														
GEV-Min (k spec.)								+											*				+	
L-Moments GEV-Max (k spec.)				*							*					*		*						
L-Moments GEV-Min (k spec.)																								

Three sets of storm depths were calculated: (1) Case 1: storm depth with best fitted distribution tested by Chi-square test (2) Case 2: storm depth with best fitted distribution tested by Kolmogorov-Smirnov, and (3) storm depth with Extreme Value type 1 (EV1) distribution.

Delta change factor

The climate models (RCMs) provide gridded data; those are areal average and not point estimates [43]. The systematic difference between climate model simulated and observed precipitation is a problem for using RCMs for hydrological purposes [44]. The storm depth values calculated from the NARCCAP datasets are for grid scale. Delta change factor can be applied to discrete totals i.e., design storm depths [12] to transpose projected future change in climate onto point observation. The assumption in this conversion is that areal-to-point relationships of precipitation remain constant in future climates [14]. The delta change factor application procedure (presented by equations 3-3, 3-4 and 3-5) described by Zhu et al. [13] to adjust the historic station scale intensities/depths to produce future station-scale values for the same duration and return period will be used in this study:

$$I_F^{(g)} = I_H^{(s)} \left[1 + \Delta_{F-H}{}^{(g)}(T,d)\right] \quad \text{Eq. 3-3}$$

$$\Delta_{F-H}{}^{(g)}(T,d) = \frac{I_F^{(g)}(T,d) - I_H^{(g)}(T,d)}{I_H^{(g)}(T,d)} \quad \text{Eq. 3-4}$$

$$\mathrm{I}_F^{(s)}(T,d) = I_H^{(s)}(T,d)\,\frac{I_F^{(g)}(T,d)}{I_H^{(g)}(T,d)} \quad \text{Eq. 3-5}$$

Table 3-3: Design storm depths (in mm) calculated from observed data and NARCCAP future datasets

Return Period	Duration (h)	Observed			CrcmCcsm			CrcmCgcm3			Hrm3Gfdl			Hrm3Hadcm3			Rcm3Cgcm3			Rcm3Gfdl		
		Case 1	Case2	Case3	Case 1	Case2	Case3	Case 1	Case2	Case3	Case 1	Case2	Case3	Case 1	Case2	Case3	Case 1	Case2	Case3	Case 1	Case2	Case3
2yr	3	31.1	31.0	32.5	33.1	34.0	34.6	35.0	34.7	37.2	31.9	31.2	33.3	36.8	34.7	38.7	30.8	31.7	35.0	37.4	38.6	41.2
	6	38.3	37.1	39.5	40.0	39.3	41.9	43.3	42.4	44.9	41.3	39.7	41.5	37.8	40.2	42.7	42.9	39.1	42.6	42.9	43.1	47.3
	12	43.5	43.8	45.1	44.8	45.8	47.3	52.0	52.4	52.6	51.1	51.0	51.2	47.7	47.2	48.4	42.1	46.6	50.7	60.8	52.2	55.7
	24	53.3	50.6	52.4	61.9	58.4	57.9	65.8	57.3	60.9	62.9	59.7	62.4	55.0	53.2	55.7	62.1	58.4	63.1	62.0	60.0	66.5
5yr	3	42.0	42.1	46.7	42.9	43.8	48.9	47.2	47.1	55.0	41.8	42.4	44.7	50.0	49.2	59.7	44.1	46.5	54.4	60.6	58.3	65.3
	6	52.6	53.7	55.3	53.9	55.9	58.3	60.7	61.8	63.3	52.9	57.4	56.5	55.3	56.7	60.7	58.4	57.6	59.4	65.0	70.8	72.5
	12	56.9	59.2	61.9	60.1	62.4	64.0	65.1	69.2	71.4	66.6	68.0	70.2	64.8	64.5	68.8	61.2	63.4	70.0	79.0	80.2	82.7
	24	72.0	68.7	70.6	80.9	73.7	76.1	85.3	82.5	81.8	86.3	82.3	85.2	78.5	75.4	76.2	83.5	79.8	80.8	93.5	91.8	98.4
10yr	3	51.1	51.5	56.2	51.7	51.8	58.3	60.1	60.6	67.8	49.9	52.0	52.4	64.1	65.1	73.9	58.0	60.4	67.3	79.9	74.9	81.6
	6	63.5	65.9	65.8	65.2	67.9	69.0	74.1	76.0	75.8	61.9	69.0	66.4	71.2	70.1	72.6	68.4	71.6	70.6	85.5	92.2	89.9
	12	68.0	71.0	73.0	72.2	74.4	75.0	75.9	80.5	83.8	77.7	80.2	82.7	76.7	78.7	82.5	81.0	80.4	82.7	89.6	101.3	101.3
	24	83.3	82.4	82.7	89.1	85.0	88.0	94.2	99.1	95.9	101.1	100.0	100.4	93.2	91.6	89.9	95.5	95.5	92.5	120.0	121.1	120.6
25yr	3	65.6	66.5	68.1	66.3	64.6	69.6	83.6	86.3	83.4	62.3	67.1	61.9	90.6	94.6	91.7	85.3	83.8	83.8	107.8	100.8	102.7
	6	79.2	82.0	79.1	82.6	83.9	82.5	93.3	94.8	91.5	76.0	82.1	78.9	95.5	88.2	89.6	81.3	89.9	84.9	121.1	121.1	112.2
	12	85.2	88.0	87.1	89.4	90.8	88.9	92.8	96.4	99.2	92.5	97.3	98.6	92.8	100.6	99.8	115.4	108.6	98.8	103.5	130.0	125.3
	24	96.5	102.2	97.9	95.3	103.0	103.0	102.8	120.3	113.2	119.1	126.1	119.5	109.0	113.8	107.0	107.2	115.9	107.2	161.1	170.7	149.5
50yr	3	79.0	80.3	76.9	81.0	76.5	78.1	107.6	113.1	95.4	73.7	81.0	68.9	118.4	125.5	104.8	115.3	106.5	95.9	131.0	124.4	118.1
	6	92.3	94.1	89.0	98.3	95.5	92.6	109.0	108.9	103.1	89.3	90.1	88.1	116.7	104.8	100.9	90.6	103.2	95.4	156.6	143.2	129.1
	12	100.7	102.2	97.6	103.4	104.1	99.4	108.2	109.6	110.9	104.5	111.3	110.6	106.0	120.5	112.8	148.6	134.5	110.9	115.1	152.6	143.4
	24	105.7	118.8	109.2	97.8	119.0	114.2	108.1	136.3	126.4	132.0	148.4	133.7	118.7	131.7	119.8	113.9	131.7	118.1	198.1	217.9	171.2
100yr	3	94.9	99.0	85.6	99.0	92.1	86.8	137.5	150.8	107.0	86.8	100.0	75.8	154.2	169.3	117.9	157.1	137.4	107.9	156.0	156.3	133.8
	6	106.7	106.2	98.7	116.8	107.4	102.4	127.0	123.0	114.6	105.2	96.5	97.2	140.8	124.7	110.3	99.9	116.3	105.8	202.4	165.3	145.7
	12	118.9	117.9	107.9	118.1	117.9	109.5	126.2	124.5	122.3	117.3	126.7	122.2	120.4	143.7	125.6	190.1	164.9	122.7	128.2	176.1	161.5
	24	114.5	137.1	120.4	98.8	137.6	125.3	112.6	152.7	139.1	144.8	173.4	147.9	126.4	150.8	132.4	119.2	147.7	128.8	241.7	276.1	193.2

Where, T and d denote return period and duration respectively, H and F denote historic and future, and s and g denote station and grid respectively.

The point estimates of storm depth for all six RCM+GCM pairs for all three cases are presented in Table 3-3.

3.4.2 Hydrologic and hydraulic modeling

A large number of hydrological models are used in different countries for different purposes. 'Although hydrological models have been around for quite some time, there is yet to be one exclusive model that can stand apart from the rest and be declared best at modeling in all aspects of the hydrologic system [45]. Considering the urban hydrological and hydraulic modeling capabilities, this study aimed to use PCSWMM 2D Professional, a leading decision support system for US EPA SWMM. PCSWMM also contains a flexible set of hydraulic modeling capabilities used to route runoff and/or external inflows through the drainage system network of natural channels, pipes, storage/treatment units, diversion structures [46]. This study used an existing model, developed using PCSWMM, of the study area. The existing model of the study area was provided by the City of Hamilton. The models that contain proposed detention pond/ storm water management facilities considering the future development are used for minor system/ storm sewer and detention basin performance assessment. The model contains 126 sub-catchments with 172.2 ha impervious area out of 525.06 ha total area. The models used curve number infiltration method and dynamic wave routing method. Three detention pond (pond 1, pond 2 and pond 3) elements were selected for analyses of detention pond performance. The contributing area of pond 1, pond 2 and pond 3 are

44.77 ha (11 sub-catchments, 13.06 ha impervious area), 15.36 ha (8 sub-catchments, 7.7 ha impervious area), 37.63 ha (8 sub-catchments, 13.77 ha impervious area) respectively.

The City of Hamilton used 6hour Chicago and 24 hour SCS storm distribution for this study area and found 24 hour SCS distribution to be the governing condition [47]. This study used 24 hour SCS storm distribution for both storm sewer and detention pond performance analysis. The 24 hr -25 yr and 24 hr -5 yr design storm depths (only for case 2, shown in Table 3-4) were used for detention ponds and storm sewer performance analysis respectively. The last column of the Table 3-4 provides the average of design storm calculated from six RCM+GCM pairs. A number of hydrologic and hydraulic parameters used by Moglen and Vidal [11] and Berggren et al. [23] as well as other parameter as described in result and discussion section were used for detention ponds and storm sewer performance analysis.

Table 3-4: Design storm depths (in mm) used for detention pond and storm sewer performance analysis

Design Storm	Observed	CrcmCcsm	CrcmCgcm3	Hrm3Gfdl	Hrm3Hadcm3	Rcm3Cgcm3	Rcm3Gfdl	Average
24 hr 25 yr for detention pond	102.2	103.0	120.3	126.1	113.8	115.9	170.7	125
24 hr 5 yr for storm sewer	68.7	73.7	82.5	82.3	75.4	79.8	91.8	80.9

3.5 Results and Discussion

3.5.1 Design Storm

Design storm depths were calculated for four different duration (3 hr, 6 hr, 12 hr and 24 hr) and six different return periods (2 yr, 5 yr, 10 yr, 25 yr, 50 yr and 100 yr) for observed time series and NARCCAP current and future simulations of six different RCM+GCM pairs. Therefore, a total of 52 (4 observed, 24 NARCCAP current and 24 NARCCAP future) annual maximum time series were used for frequency analysis. The best fitted distribution among twenty seven distributions for NARCCAP current and future datasets are listed in the Table 3-2. For example, the best fitted distribution for NARCCAP current data in Case 1 was identified by ‘x’ mark in Table 3-2 and is GEV Min for CrcmCcsm 3h storm. As two tests were used to test the goodness of fit of each distribution, Table 3-2 provides 96 selections for 48 NARCCAP datasets. Table 3-2 shows that L-moment Pareto distribution was selected 14 times (the highest), that is 14.6% of the total selections. Gumbel EV1 Max was selected for 9 times that is 9.4% of the total selection. Therefore, only Gumbel EV1 Max used by different stakeholders for design storm calculation for this study area is not appropriate for climate change impact study. Four distributions namely Galton, L-Momnet EV1 Min, L-Moments EV3 min and L-Moments GEV-Min (k spec.) were not selected as best fitted distribution for any climate data sets. L-moment Pareto distribution was selected 7 times (the highest), for both current and future climate datasets. L-moment Pareto was also selected 12 times (the highest), when Chi-square test was used to test the goodness of fit. Both L-Moment Exponential and Gumbel EV1 Max were selected 7 times (the highest), when Kolmogorov- Smirnov was used to test the goodness of fit. This study identified the best fitted distribution for observed and NARCCAP datasets, and used them for design storm calculation to minimize the uncertainty related to appropriate distribution selections. The design storm depths calculated from observed data and NARCCAP future datasets are presented in Table 3-3. It is mentionable that the delta change factor was applied on the datasets to get the design storm values for NARCCAP datasets presented in the Table 3-3.

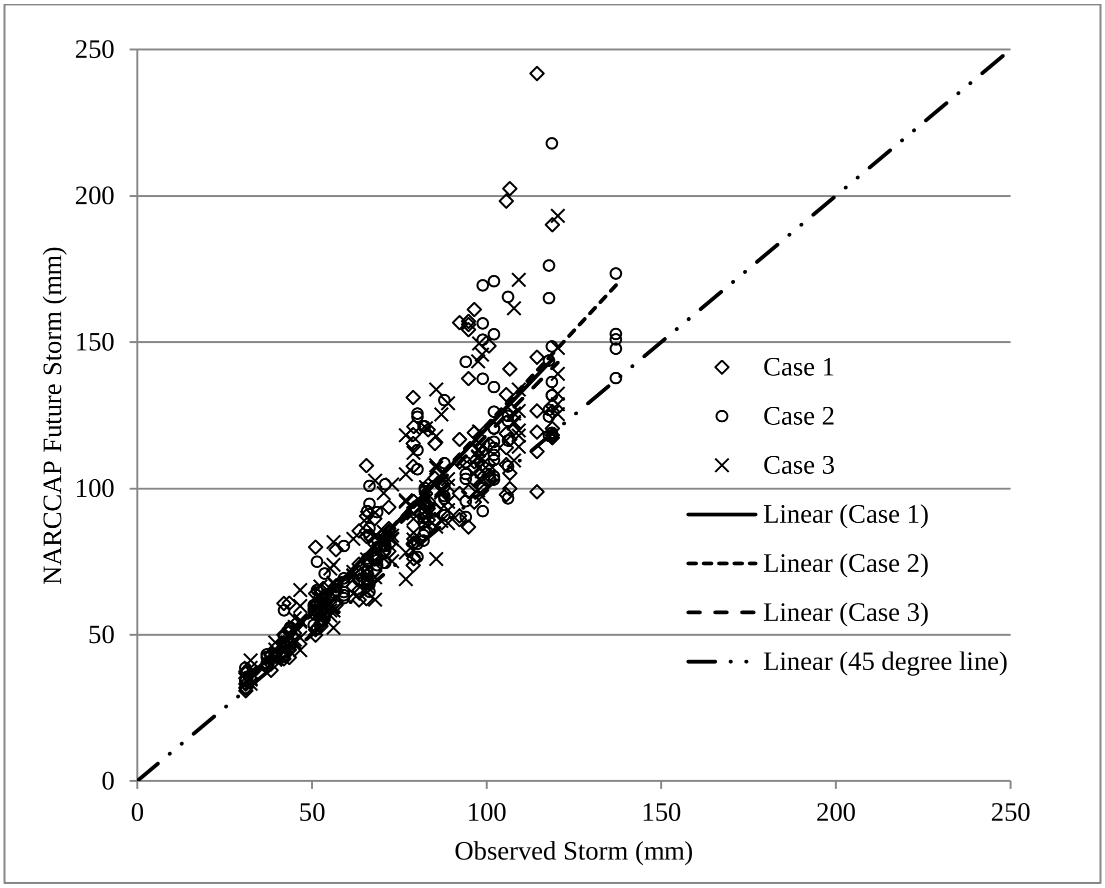

Figure 3-2: Scatterplot of design storm depths calculated from observed data and NARCCAP future datasets

Table 3-3 shows that there is a significant increase in design storm depths for all six RCM+GCM pairs. Results in the Table 3-3 also show the overall variability of the design storm depths calculated from the climate data. For example, 3 hr-2 yr storm depths calculated from six RCM+GCM pairs in case 2 are 34, 34.7, 31.2, 34.7, 31.7 and 38.6 mm with mean 34.2 mm and coefficient of variation 7.1%; 3 hr- 100 yr storm depths are 92.1, 150.8, 100. 169.3, 137.4 and 156.3 mm with mean 134.3 mm and coefficient of variation 21.4%. The calculated coefficient of variations also show that the variability increases with the increase of return period. The increase in design storm depths under future climate conditions are also shown in the Figure 3-2. Figure 3-2 shows the scatterplot of all design storm depths (in Table 3-3) calculated from observed data and NARCCAP future datasets. The scatterplots in Figure 3-2 shows that the data are more dispersed from the 45-degree line for higher values. It revealed that the increase of design storm depth under future climate is higher for higher values. It is notable that the higher values may represent storm depths for higher return period or higher duration. The linear trendlines in Figure 3-2 also shows overall increase of storm depth is higher for case 2 (when distribution were identified by Kolmogorov-Smirnov test) than other two cases, lowest for case 3 (when frequency analysis was performed using Gumbel EV1 Max). Figures 3-3, 3-4 and 3-5 show the difference between design storm depths calculated from observed data and NARCCAP future datasets for different return period and different duration. Here, the positive values refer to an increase of storm depths in future. Visual inspection of these figures revealed that the difference (increase) of design storm depths increase with the increase of return period overall. For example, design storm depths increased by 15.6%, 20%, 22.8% for 24 hr storm of return period 2 yr, 25 yr and 100 yr respectively for case 1, these increase are 14%, 22.3% and 26.2% for case 2, and 16.6%, 19.1% and 20% for case 3. The increasing trend in case 3 is not as significant as other cases; the reason might be that the Gumbel EV1 Max is not the best fitted distribution for most of the datasets for case 3. Considering only the 3 hr and 24 hr duration storm, Figures 3-3 and 3-4 shows that the increase is higher for shorter duration with higher return period and also higher for longer duration with lower return period. For example, the increase of storm depths is 38.8% and 22% for 3 hr and 24 hr storm of

100 year return period respectively, 9.9% and 15% for 3 hr and 24 hr storm of 2 year return period respectively for case 1; 35.7% and 26.2% for 3 hr and 24 hr storm of 100 year return period respectively, 10.2% and 14% for 3 hr and 24 hr storm of 2 year return period respectively for case 2. Figures 3-3 and 3-4 also show that overall increase of storm depths under future condition is higher in case 2 than that in case 1. Considering this issue and sustainable storm water infrastructure design, the design storm depths calculated in case 2 will be used for investigation of detention pond and storm sewer performance study.

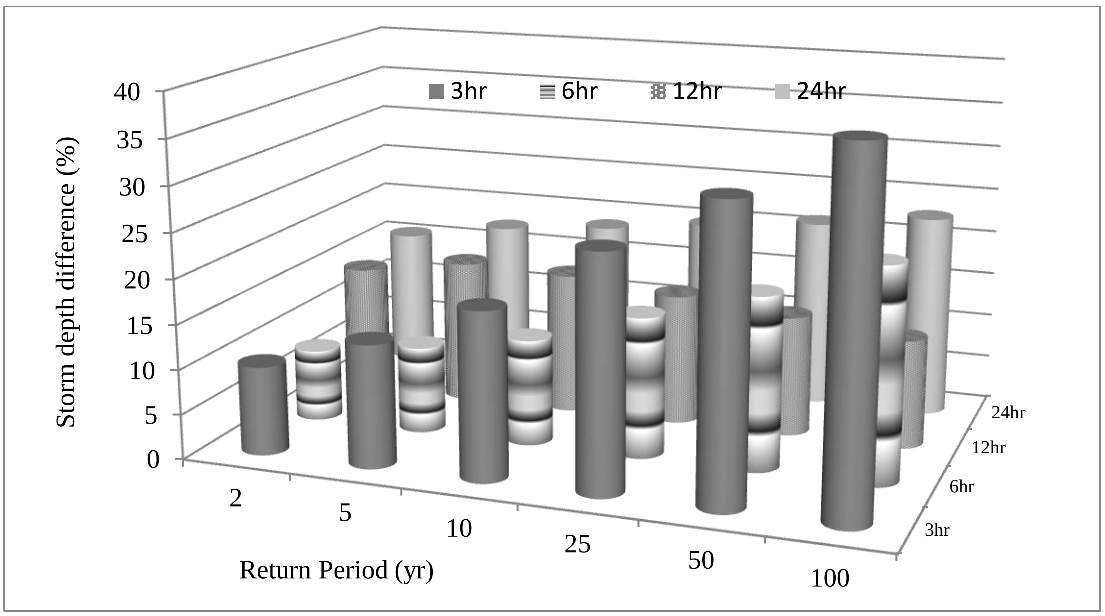

Figure 3-3: Difference between design storm depths calculated from observed and NARCCAP future datasets for case 1

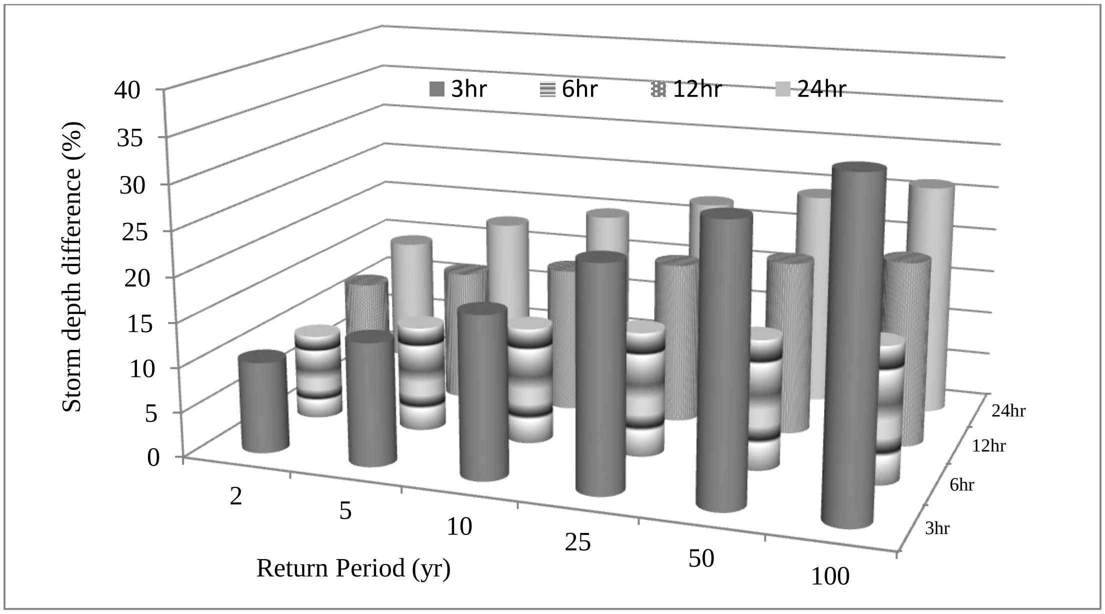

Figure 3-4: Difference between design storm depths calculated from observed and NARCCAP future dataset for case 2

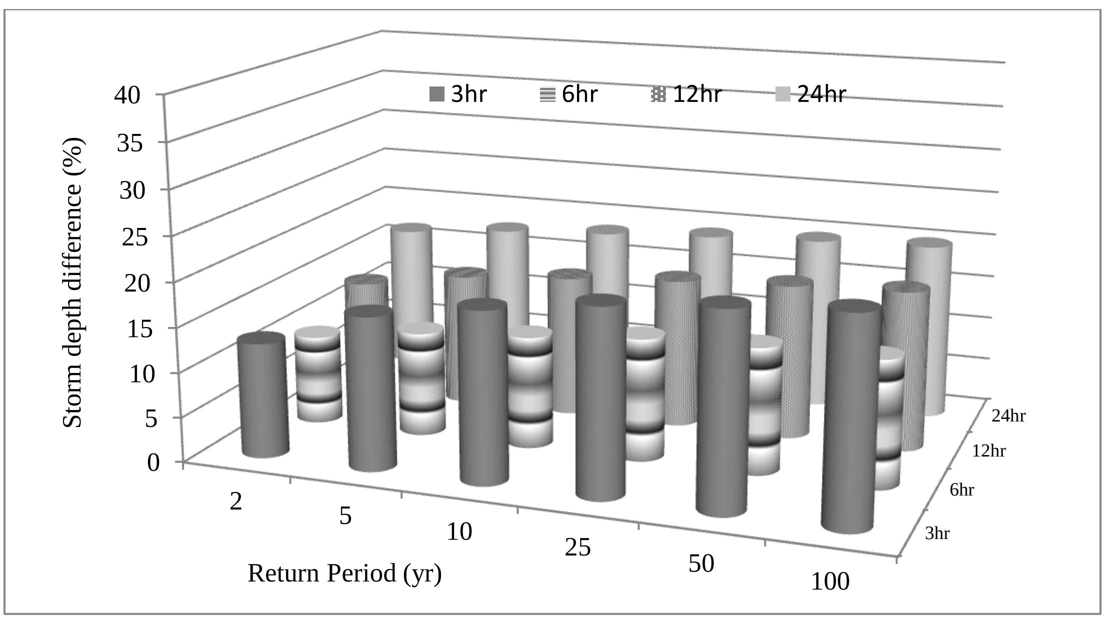

Figure 3-5: Difference between design storm depths calculated from observed and NARCCAP future datasets for case 3

3.5.2 Detention Pond

The 24 hr 25 yr storm depths listed in the Table 3-4 were used as input in the PCSWMM model, simulation were performed and the following metrics were collected: Average depth (m), maximum depth (m), maximum total inflow (m^3/s), average volume (1000 m^3), average percent full (%), max volume (1000 m^3), max percent full (%) and max outflow (m^3/s). These metrics for three detention ponds are reported in Table 3-5. The third column in the Table 3-5 shows performance values using the design storm calculated from observed data. All other values in the Table 3-5 are detention pond performance values for NARCCAP future storm normalized by the values in the column 3. Almost all the performance ratios greater than 1 for all six RCM+GCM pairs and average value indicate that the detention ponds will not perform as expected under future climate. The performance ratios of all eight metrics for RCM3+GFDL are highest among the ratios for all six RCM+GCM pairs, that indicates the worst performance of all detention ponds under RCM3+GFDL future scenario. The performance ratios for RCM3+GFDL models varies from 1.2 for average depth to 2.44 for maximum outflow for pond 1, i.e., average depth increase by 20% and maximum outflow increase by 144% under future climate presented by RCM3+GFDL models. The very high increase in the uncontrolled peak discharge indicates the vulnerability of flooding in the downstream of the detention pond. One model, CRCM+CCSM, among the six pairs shows no change for some metrics and insignificant (only 3% for maximum outflow) change for some metrics for all three ponds. Using the future to present performance ratio greater than 1 (i.e., future condition are greater than present conditions), the increases are observed in 93% of all the metrics for all 3 ponds. Results in the Table 3-5 show that the performance ratios varies from 1.08 for average depth for pond1 to 2.11 for maximum outflow for pond 3 for average design storm, i.e., average depth increase by 8% and maximum outflow increase by 111% under average future climate condition. The performance ratios varies 1.08-1.95, 1.10-1.66 and 1.10-2.11 for average future climate condition for pond 1, pond 2 and pond 3 respectively, the performance ratio varies 1.2-2.44, 1.38-2.23 and 1.27-2.41 for highest increased 24 hr 25 yr design storm by RCM3+GFDL models.

Table 3-5: Detention Pond Performance Ratios (Future values normalized by observed performance values) for 24 hr 25 yr design storm

Features	Metric	Observed	Crcm Ccsm	Crcm Cgcm3	Hrm3 Gfdl	Hrm3 Hadcm3	Rcm3 Cgcm3	Rcm3 Gfdl	Average
Pond 1	Avg Depth (m)	0.64	1.00	1.06	1.08	1.05	1.05	1.20	1.08
	Max Depth (m)	1.45	1.01	1.11	1.14	1.08	1.08	1.20	1.14
	Max Total Inflow (m^3/s)	9.28	1.01	1.25	1.33	1.16	1.19	1.97	1.32
	Avg Volume ($1000m^3$)	6.06	1.00	1.08	1.11	1.05	1.06	1.24	1.10
	Avg Percent Full (%)	31	1.00	1.10	1.10	1.06	1.06	1.23	1.10
	Max Volume ($1000m^3$)	15.35	1.01	1.15	1.19	1.09	1.11	1.27	1.18
	Max Percent Full (%)	79	1.00	1.14	1.19	1.09	1.10	1.27	1.18
	Max Outflow (m^3/s)	1.20	1.03	1.74	1.99	1.47	1.56	2.44	1.95
Pond 2	Avg Depth (m)	0.34	1.03	1.12	1.15	1.09	1.09	1.38	1.15
	Max Depth (m)	1.59	1.00	1.11	1.15	1.07	1.08	1.54	1.14
	Max Total Inflow (m^3/s)	4.10	1.01	1.21	1.28	1.13	1.16	1.89	1.27
	Avg Volume($1000m^3$)	0.88	1.01	1.11	1.14	1.07	1.09	1.42	1.14
	Avg Percent Full (%)	10	1.00	1.10	1.10	1.00	1.10	1.40	1.10
	Max Volume ($1000m^3$)	4.84	1.01	1.15	1.21	1.10	1.11	1.81	1.20
	Max Percent Full (%)	53	1.02	1.15	1.23	1.11	1.13	1.83	1.21
	Max Outflow (m^3/s)	1.59	1.03	1.56	1.66	1.37	1.43	2.23	1.66
Pond 3	Avg Depth (m)	0.59	1.00	1.08	1.12	1.05	1.07	1.27	1.10
	Max Depth (m)	1.62	1.00	1.14	1.20	1.08	1.10	1.23	1.19
	Max Total Inflow(m^3/s)	8.53	1.01	1.25	1.33	1.16	1.19	1.96	1.31
	Avg Volume ($1000m^3$)	4.31	1.00	1.09	1.12	1.06	1.07	1.30	1.12
	Avg Percent Full (%)	26	1.00	1.12	1.12	1.08	1.08	1.31	1.12
	Max Volume ($1000m^3$)	12.70	1.01	1.17	1.25	1.10	1.12	1.29	1.24
	Max Percent Full (%)	77	1.01	1.18	1.26	1.10	1.13	1.30	1.25
	Max Outflow (m^3/s)	1.50	1.03	1.87	2.17	1.53	1.64	2.41	2.11

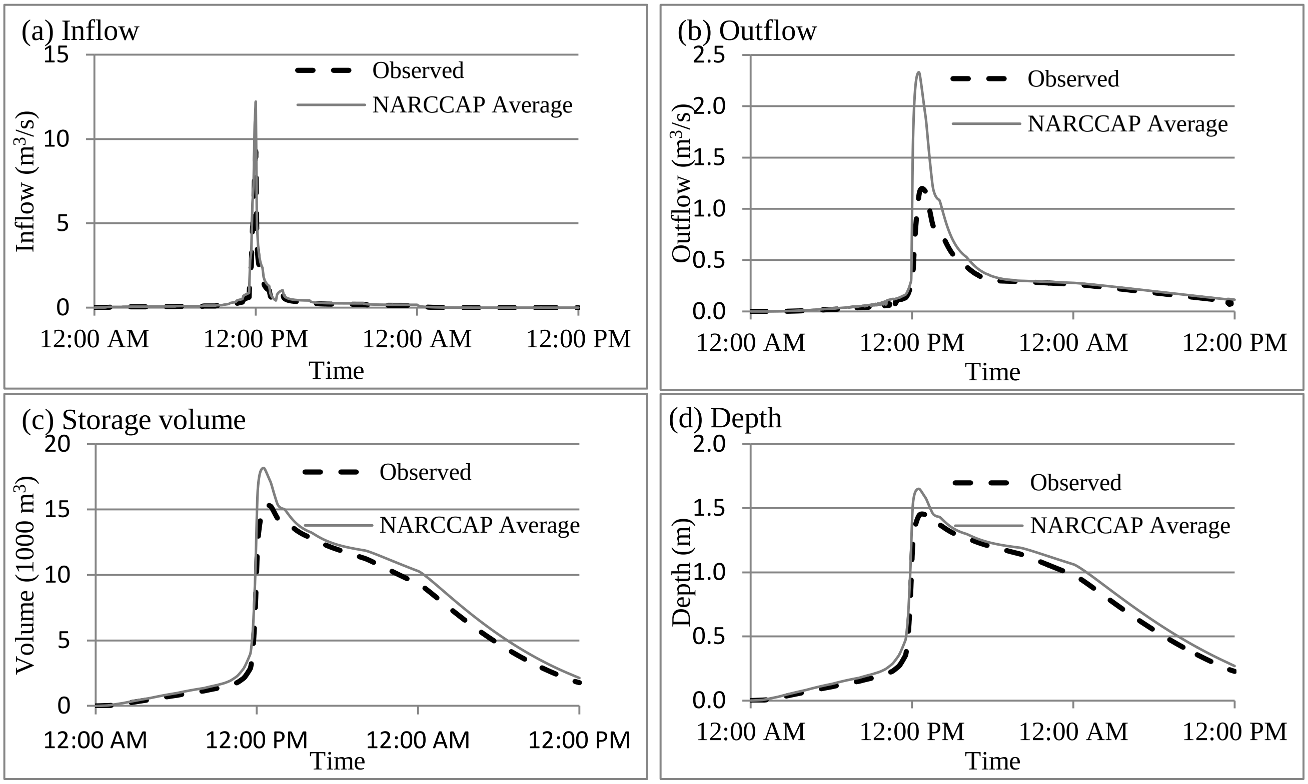

Figure 3-6: Plots showing time series of inflow, outflow, storage volume and depth from 25 year return period storm for detention pond 1 (observed/baseline values obtained using storm depths calculated from observed data)

Figure 3-6 presents the time series plot of inflow, outflow, storage volume and depth for detention pond 1. These time series data were produced by inputting design storm depth from observed data and average (listed in Table 3-4) of design storm from 6 RCM+GCM pairs. Figure 3-6 shows that maximum inflow increased from 9.28 m^3/s for observed to 12.21 m^3/s for NARCCAP average that is an increase of 32%. The outflow from the pond increased from 1.198 m^3/s for observed to 2.331 m^3/s for NARCCAP average, i.e., the controlled peak flow will be increased by 95% under future average climate condition. Figure 3-6 shows that the maximum storage volume and maximum depth will increase by 18% and 14% respectively. The maximum values obtained from the simulated time series, the maximum storage volumes are 15347 m^3 and 18175 m^3, and the maximum depths are 1.45 m and 1.65 m for observed and NARCCAP average respectively.

3.5.3 Storm Sewer

The 24 hr - 5 yr storm depths listed in the Table 3-4 were used for storm sewer performance analysis. These design storm depths with SCS storm distribution was inputted in the PCSWMM model. Then, a number of hydraulic parameters were obtained from the PCSWMM generated status files. The parameters, maximum water level and pipe flow ratio, used by Berggren et al. [23] for measuring hydraulic impact were calculated. Pipe flow ratio is the ratio of the actual maximum flow rate and the flow rate when the pipes were running full in the system.

At the outset, the number of nodes flooded and surcharged observed/baseline scenario and future climate were compared. The number of node flooded and surcharged for 24 hr - 5 yr SCS storm are presented in Table 3-6. Flooding refers to all water that overflows a node, and surcharge occurs when water rises above the crown of highest conduit. There was only one node flooded under present climate condition. The number of flooded node increased under future climate condition ranging from 4 for CRCM+CCSM models to 72 for RCM3+GFDL models, and 17 for average design storm calculated from 24 hr 5 yr design storm of 6 RCM+GCM pairs. There were 58 nodes surcharged for observed/baseline condition, these numbers increased under future climate with the smallest for CRCM+CCSM models which are 92, the largest for RCM3+GFDL models which is 189, and 131 nodes will be surcharged for average future climate condition.

Table 3-6: Number of node flooded and surcharged

Features	Observed	CrcmCcsm	CrcmCgcm3	Hrm3Gfdl	Hrm3Hadcm3	Rcm3Cgcm3	Rcm3Gfdl	Average
Node Flooded	1	4	22	18	15	15	72	17
Node Surcharged	58	92	146	143	98	125	189	131

Then, the difference between the observed/baseline scenario and future climate for maximum water level and pipe flow ratio are presented in Table 3-7. The mean difference between the observed/baseline scenario and future climate for maximum water level at all the nodes varies from 0.42 m for CRCM+CCSM models and 2.62 m for RCM3+GFDL, and the difference between observed and climate average is 1.07, i.e., the maximum water level increase on an average of 26% for CRCM+CCSM models, 162% for RCM3+GFDL models and 66% for average design storms under future climate. Similarly, The mean difference between the observed/baseline scenario and future climate for pipe flow ratios varies from 0.08 m for CRCM+CCSM models and 0.31 m for RCM3+GFDL, and the difference between observed and climate average is 0.18, i.e., the pipe flow ratios increase on an average of 10% for CRCM+CCSM models, 39% for RCM3+GFDL models and 23% for average design storms under future climate.

Table 3-7: Difference between the observed/baseline scenario and future climate for maximum water level and pipe flow ratio

Features		CrcmCcsm	CrcmCgcm3	Hrm3Gfdl	Hrm3Hadcm3	Rcm3Cgcm3	Rcm3Gfdl	Average
Max Water Level	mean difference (m)	0.42	1.28	1.27	.57	.97	2.60	1.07
	mean difference (%)	26	79	79	36	60	162	66
Pipe Flow Ratio	mean difference	.08	.20	.20	.10	.16	.31	.18
	mean difference (%)	10	25	25	13	20	39	23

Figure 3-7 presents the number of conduits above full normal flow and Figure 3-8 presents the number of conduits for capacity limited. These numbers for the observed/baseline period and future period are categorized for three durations: 0=<hr<0.15, 0.15=<hr<0.25 and 0.25=<hr. The numbers are always higher for all categories for all six RCM+GCM models. The number of conduits above full normal flow and for capacity limited for RCM3+GFDL are the highest among the six RCM+GCM pairs for durations 0=<hr<0.15 and 0.25=<hr.

The higher numbers are observed for CRCM+CGCM and HRM3+GFDL models for second category. The numbers of conduits above full normal flow are 62, 8 and 5 for observed and 96, 40 and 12 for future average climate for three categories, i.e., the numbers increase by 55%, 400% and 140%. The numbers of conduits for capacity limited are 62, 9 and 4 for observed and 82, 52 and 14 for future average climate for three categories, i.e., the numbers increase by 32%, 477% and 250%.

Figure 3-9 shows the spatial distribution of number of nodes flooded, number of nodes surcharged and pipe flow ratio, and it contributes to the understanding of most vulnerable locations in the study area under future climate condition.

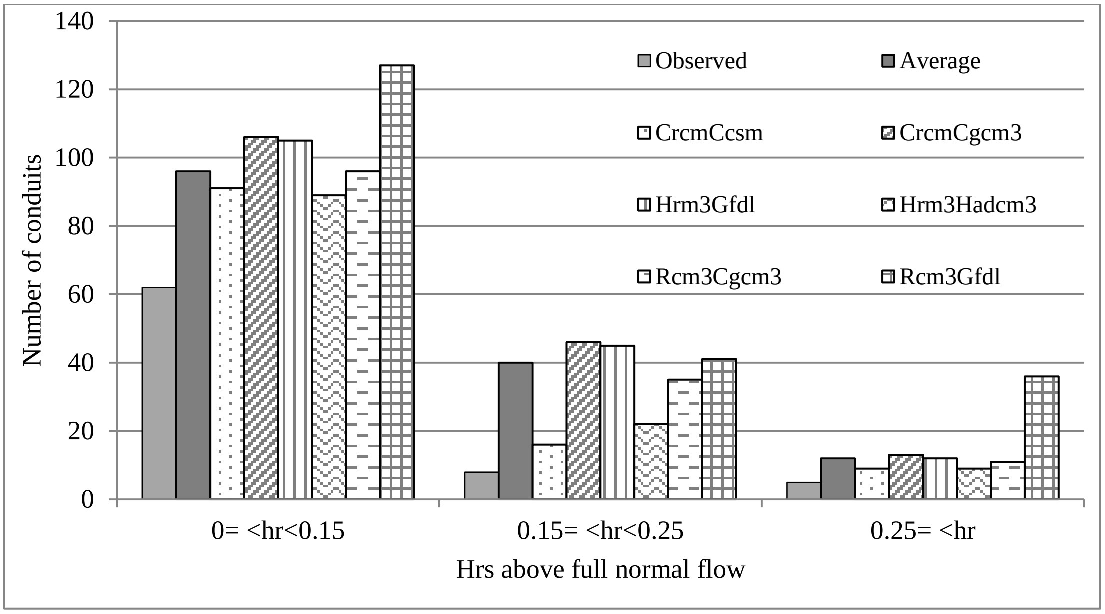

Figure 3-7: Number of conduits above full normal flow for 5 year return period storm

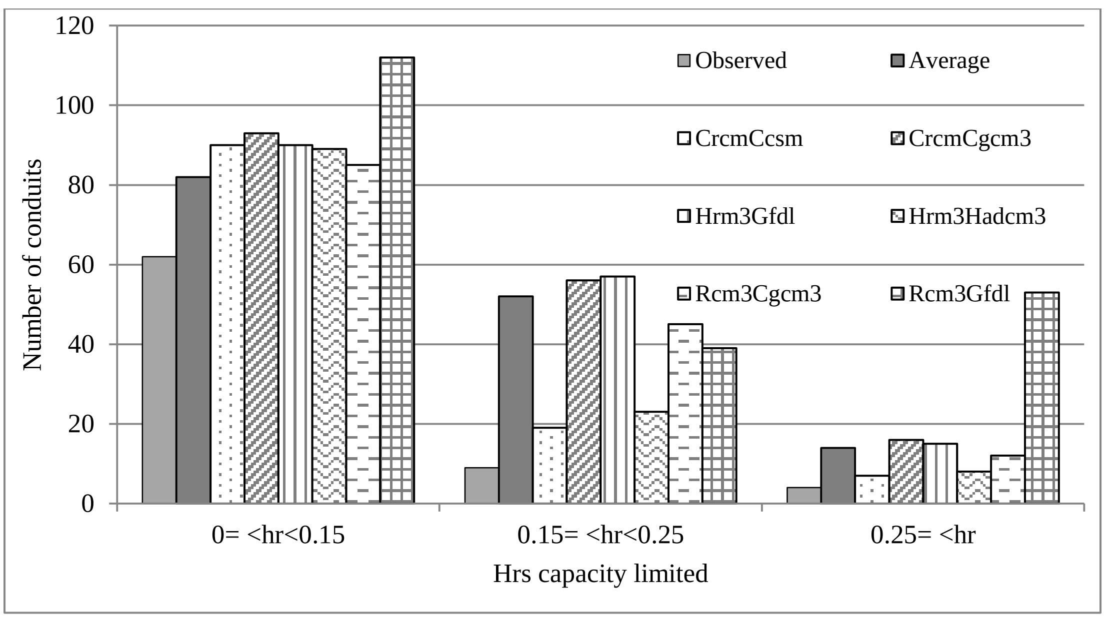

Figure 3-8: Number of conduits for capacity limited for 5 year return period storm

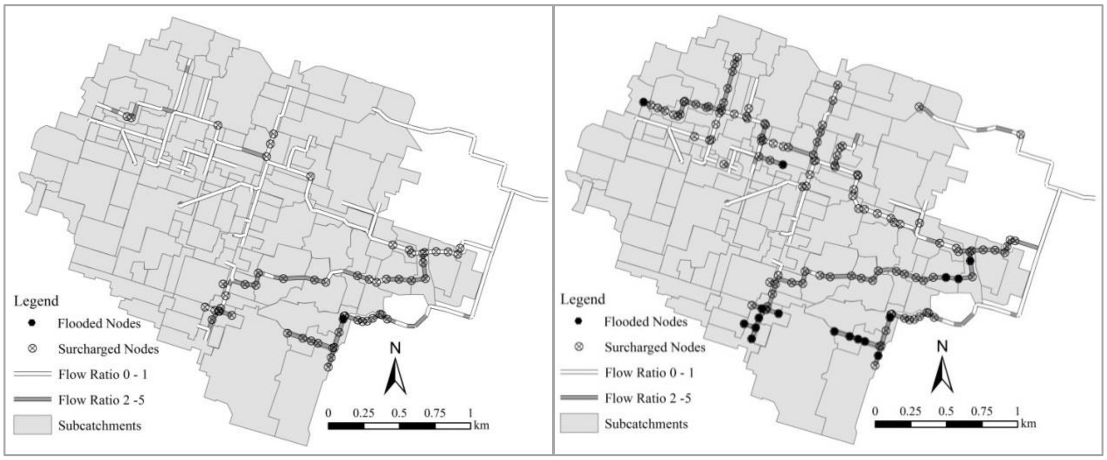

Figure 3-9: Flooded and surcharged nodes, and pipe flow ratio for observed/baseline (to the left) and future NARCCAP average (to the right) for 5 year return period storm

3.6 Conclusions

This study explored the potential impact of climate change on the design storm depths and consequent effect on the performance of detention pond and storm sewer network under future climate condition at a study area located in the City of Hamilton, Ontario, Canada.

The best fitted distribution among twenty seven distributions for observed and NARCCAP datasets for design storm calculation were identified in this study. The precipitation time series provided by six different RCM+GCM pairs were used in frequency analysis; two statistical tests were used to test the goodness of fit of each distribution. The delta change factor was used to convert the storm depths calculated from gridded data to station scale values. The results show that there is an overall significant increase of design storm depths for all six RCM+GCM pairs. The visual inspection of scatter plots revealed that the increase of design storm depths under future climate condition is higher for higher values. Visual inspections also revealed that increase of design storm depths also increase with the increase of return period overall. The results also show overall increase of storm depths in future is higher in the case when distributions were identified by Kolmogorov- Smirnov test. The design storm depths calculated using the distribution identified by Kolmogorov-Smirnov test are suggested to use for investigation of stormwater management infrastructure performance study for sustainable infrastructure design.

The 24 hr - 25 yr and 24 hr - 5 yr design storm depths were inputted in the PCSWMM model for analyses of detention pond and storm sewer network performance respectively under future climate condition. The deteriorated performance of three detention ponds were indicated by the performance ratio calculated from eight metrics. The time series plot of inflow, outflow, storage volume and depth also shows increase of the metrics. Results also indicate the worst performance of all detention ponds under RCM3+GFDL future scenario. A number of hydraulic parameters were used to assess the system capacity, and all the parameters show deteriorated performance under future climate condition. Similar to detention pond, the worst performance of the storm sewer network were observed under RCM3+GFDL future scenario. Overall, the urban drainage management infrastructures designed based on current climate condition will not be able to cope with the increased design storm depth under future climate condition. The findings of this study would encourage municipalities and other stakeholders for considering climate change impact in planning and designing of drainage management infrastructures to ensure that they will work effectively in future.

Acknowledgement

We wish to thank the North American Regional Climate Change Assessment Program (NARCCAP) for providing the data used in this paper. The authors gratefully acknowledged City of Hamilton, Environment Canada and Computational Hydraulics International (CHI) for providing data and models for the study area. Finally, support from the Natural Sciences and Engineering Research Council (NSERC) of Canada in the form of Discovery Grant (RGPIN04808-14) is greatly acknowledged.

References

1. IPCC (2014) Climate Change 2014: Synthesis Report. Contribution of Working Groups I, II and III to the Fifth Assessment Report of the Intergovernmental Panel on Climate Change. In: Pachauri PK, Meyer LA (eds.) IPCC, Geneva, Switzerland, pp: 151-175.
2. Beniston M, Stephenson DB, Christensen OB, Ferro CAT, Frei C, et al. (2007) Future extreme events in European climate: an exploration of regional climate model projections. Climatic Change 81: 71-95.
3. Christensen JH, Christensen OB (2003) Climate modelling: severe summertime flooding in Europe. Nature 421: 805-806.
4. Kundzewicz ZW, Radziejewski M, Pinskwar I (2006) Precipitation extremes in the changing climate of Europe. Climate Research 31: 51-58.
5. Semmler T, Jacob D (2004) Modeling extreme precipitation events-a climate change simulation for Europe. Global and Planetary Change 44: 119-127.

6. Tsanis IK, Koutroulis AG, Daliakopoulos NI, Jacob D (2011) Severe climate-induced water shortage and extremes in Crete: A letter. Climatic Change 106 (4): 667-677.
7. Brown C (2010) The end of reliability. J Water Resour Plann Manage 136: 143- 145.
8. Karla A, Ahmad S (2009) Using Oceanic-atmospheric oscillations for long lead time streamflow forecasting. Water Resour Res 45(3): DOI:10.1029/2008WR006855.
9. Guo YP (2006) Updating rainfall IDF relationships to maintain urban drainage design standard. J Hydrol Eng 11 (5): 506-509.
10. Mailhot A, Duchesne S (2010) Design criteria of urban drainage infrastructures under climate change. J Water Resour Plann Manage 136 (2): 201-208.
11. Moglen GE, Vidal GER (2014) Climate change impact and storm water infrastructure in the Mid-Atlantic region: design mismatch coming. J Hydrol Eng 19 (11): DOI:10.1061/(ASCE)HE.1943-5584.0000967.
12. Forsee WJ, Ahmad S (2011) Evaluating urban storm-water infrastructure design in response to projected climate change. J Hydrol Eng 16 (11): 865-873.
13. Zhu J, Stone MC, Forsee W (2012) Analysis of potential impact of climate change on intensity-duration-frequency (IDF) relationships for six regions in the United States. J Water and Climate Change 3 (3): 185-196.
14. Mailhot A, Duchesne S, Caya D, Talbot G (2007) Assessment of future change in intensity-duration-frequency (IDF) curves for Southern Quebec using the Canadian Regional Climate Model (CRCM). J Hydrol 347: 197-210.
15. Coulibaly P, Shi X (2005) Identification of the effect of climate change on future design standards of drainage infrastructure in Ontario. Highway Infrastructure Innovation Funding Program, Ministry of Transportation of Ontario, Canada.

16. Zhu J (2013) Impact of climate change on extreme rainfall across the United States. J Hydrol Eng 18 (10): 1301-1309.

17. Deser C, Phillips A, Bourdette V (2012) Uncertainty in climate change projections: the role of internal variability. Climate Dyn 38: 527-546.

18. Dibike YB, Coulibaly P (2005) Hydrologic impact of climate change in the Saguenay watershed: comparison of downscaling methods and hydrologic models. J Hydrol 307 (1-4): 145-163.

19. Fowler HJ, Blenkinsop S, Tebaldi C (2007) Linking climate change modeling to impacts studies: Recent advances in downscaling techniques for hydrological modeling. Int J Climatol 27 (12): 1547-1578.

20. Kalra A, Ahmad S (2011) Evaluating changes and estimating seasonal precipitation for Colorado River Basin using stochastic nonparametric disaggregation technique. Water Resour Res 47: W05555.

21. Praskievicz S, Chang HJ (2009) A review of hydrological modeling of basin-scale climate change and urban development impacts. Progress in Physical Geography 33 (5): 650-671.

22. Prudhomme C, Reynard N, Crooks S (2002) Downscaling of global climate models for flood frequency analysis: Where are we now? Hydrol. Processes 16 (6): 1137-1150.

23. Berggren K, Olofsson M, Viklander M, Svensson G, Gustafsson A (2012) Hydraulic Impacts on Urban Drainage Systems due to Changes in Rainfall Caused by Climatic Change. J Hydrol Eng 17 (1): 92-98.

24. Olsson J, Berggren K, Olofsson M, Viklander M (2009) Applying precipitation model climate scenarios for urban hydrological assessment: A case study in Kalmar City, Sweden. Atmos Res 92 (3): 364-375

25. Semadeni-Davies A, Hernebring C, Svensson G, Gustafsson L (2008) The impacts of climate change and urbanisation on drainage in Helsingborg, Sweden: Combined sewer system. J Hydrol 350: 100-113.

26. Fortier C, Mailhot A (2015) Climate change impact on combined sewer outflows. J Water Resour Plann Manage 141(5), DOI:10.1061/(ASCE)WR.1943- 5452.0000468.

27. Grillakis MG, Koutroulis AG, Tsanis IK (2011) Climate change impact on the hydrology of Spencer creek watershed in Southern Ontario, Canada. Journal of Hydrology 409: 1-19.

28. Mearns, L.O., et al. (2007), updated 2012. The North American Regional Climate Change Assessment Program dataset, National Center for Atmospheric Research Earth System Grid data portal, Boulder, CO. Data downloaded 2014- 07-07. [DOI:10.5065/D6RN35ST].

29. Mearns LO, Gutowski WJ, Jones R, Leung LY, McGinnis S, et al. (2009) A regional climate change assessment program for North America. EOS, 90: 311- 312.

30. NARCCAP (2013) North Americal Regional Climate Change Assessment Program. <http://www.narccap.ucar.edu/> (January 26, 2013).

31. Mailhot A, Beauregard I, Talbot G, Caya D, Biner S (2012) Future changes in intense precipitation over Canada assessed from multi-model NARCCAP ensemble simulations. Int J Climato 32: 1151-1163.

32. Nakicenvoic N, Davidson O, Davis G, Grübler A, Kram T, et al. (2000) Special Report on Emissions Scenarios. A Special Report of Working Group III of the Intergovernmental Panel on Climate Change. Cambridge University Press Cambridge, 599.
33. Kozanis S, Christofides A, Efstratiadis A (2010) Scientific documentation of the hydrogram software version 4, Athens, pp 173.
34. Music B, Caya D (2007) Evaluation of the hydrological cycle over the Mississippi River Basin as simulated by the Canadian regional climate model (CRCM). J Hydrometeor 8: 969-988
35. Jones R, Noguer M, Hassell D, Hudson D, Wilson S, et al. (2004) Generating high resolution climate change scenarios using PRECIS. Met Office Hadley Center. Exter p 40.
36. Elguindi N, Bi X, Giorgi F, Nagarajan B, Pal J, et al. (2007) RegCM Version 3.1 User's Guide, Trieste, Italy. <https://users.ictp.it/RegCNET/regcm.pdf) (July 9, 2015)
37. Giorgi F, Marinucci MR, Bates GT (1993) Development of second generation regional climate model (RegCM2) I: boundary layer and radiative transfer processes. Mon Weather Rev 121: 2794-2813.
38. Collins WD, Bitz CM, Blackmon ML, Bonan GB, Bretherton CS, et al. (2006) The community climate system model version 3 (CCSM3). J Climate 19: 2122- 2143.
39. Flato GM (2005) The Third Generation Coupled Global Climate Model (CGCM3). <http://www.ec.gc.ca/ccmac-cccma/default.asp?n=1299529F-1> (August 9, 2015).
40. GFDL GAMDT (2004) The new GFDL global atmospheric and land model AM2-LM2: Evaluation with prescribed SST simulations. J Climate 17: 4641-4673.

41. Gordon C, Cooper C, Senior CA, Banks H, Gregory JM, et al. (2000) The simulation of SST, sea ice extents and ocean heat transports in a version of the Hadley Centre coupled model without flux adjustments. Climate Dynamics 16: 147-168

42. Pope VD, Gallani ML, Rowntree PR, Stratton RA (2000) The impact of new physical parameterizations in the Hadley Centre climate model-HadAM3. Climate Dynamics 16: 123-146.

43. Chen C, Knutson T (2008) On the verification and comparison of extreme rainfall indices from climate models. J Clim 21 (7): 1605-1621.

44. Leander R, Buishand TA (2007) Resampling of regional climate model output for the simulation of extreme river flows. J Hydrol 332: 487- 496.

45. Sharma M (2009) Comparison of downscaled RCM and GCM data for hydrologic impact assessment M.A.Sc. Thesis, Dept. of Civil Engineering, McMaster University, Hamilton, Ontario, Canada.

46. James W, Rossman LA, James WRC (2010) User's guide to SWMM 5, 13th edition. CHI, Guelph, Ontario, Canada.

47. City of Hamilton (2011) West central mountain drainage assessment supplemental capacity analysis and SWM sizing Mewburn and Sheldon neighbourhoods." AMEC Environment and Infrastructure, Burlington, Ontario, Canada.

Chapter 4 : Hydrologic and Hydraulic Impact of Climate Change on Lake Ontario Tributary

Summary of Paper III: Ahmed, S., and Tsanis, I. (2016). Hydrologic and Hydraulic Impact of Climate Change on Lake Ontario Tributary. American Journal of Water Resources, 4(1), 1-15. doi:10.12691/ajwr-4-1-1.

The objective of this study was to investigate the potential climate change on flooding scenarios in a Lake Ontario Tributary, namely the Clearview Creek, drainage area located in Southern Ontario, Canada. The objective was achieved by exploring the potential impact of climate change on the design storm depths and storm peak flows, and the consequent effect on flood depth and extents under future climate condition**.** The design storm depths for the study area were calculated for NARCCAP six RCM+GCM pair's data sets by applying the best fitted distribution among twenty seven distributions tested by Pearson chi-square test and Kolmogorov-Smirnov test, and by applying delta change factor for convert gridded values to station scale values. The Visual OTTHYMO and HEC-RAS models were used for hydrologic and hydraulic simulation, respectively. The results of this study revealed the followings:

- The L-Moment GEV Min was selected 15.6% (the highest) of the total selection among the twenty seven distributions for all NARCCAP datasets. Overall, the increase of storm depths is higher when the distribution was identified by the Chi-square test.
- The storm depths will increase significantly for all duration (3hr to 24hr) and all return period, and the increase is higher for longer duration and higher return period.

- The peak flow will increase with a range of 26% to 64% for 2yr and 100yr return period for 24hr duration storm at the outlet of the Creek. Percentage increase of peak flows will be higher than storm depths. Notably, the percentage increase of peak flows is higher in a catchment with a less impervious area.
- The variability of relative change of storm depths increases with the increase of return period and decrease of duration. The variability of flow and flow area are much higher than the variability of the storm depths under future climate condition overall.
- The comparison of flooding scenario under current and future climate conditions revealed an average increase in water surface elevation and extents by 30cm and 37.1m, respectively, for a 100 year return period flood in case of the average of six RCM+GCM model data.

4.1 Abstract

Climate model projections indicate that the frequency and magnitude of hydrological extremes will increase in a future climate due to increasing concentration of greenhouse gases. Increase in precipitation depth will lead to higher peak flows, and will bring floods with higher inundation depths and larger extends. This study involves the climate change impact analysis of design storms, peak flows and flooding scenario for the Clearview Creek drainage area located in Southern Ontario, Canada. First, the storm depths for different return periods and durations were calculated from the observed rainfall data and the North American Regional Climate Change Assessment Program (NARCCAP) climate simulations. The storm depths were calculated by using the best fitted distribution among twenty seven distributions. The design storm depths calculated from the observed and climate model simulated data are used as input into an existing Visual OTTHYMO model of the study area for flow simulation. The simulated peak flows for 24hr Storm of different return periods are used as input in the HEC-RAS model for hydraulic analyses. Frequency analysis results show that the storm depths are predicted to increase significantly under future climate. Simulated flow results show an increase of peak flows ranging from about 26 % to 64% for 2yr and 100yr return periods at the outlet of the Creek. Finally, the analyses of flooding scenario revealed an average increase of water surface elevation and extents by 30 cm and 37.1 m, respectively, for a 100 year return period flood. It is also revealed that the variability of flow simulated by hydrologic model and flow area simulated by the hydraulic analyses tool are much higher than the variability of the storm depths under future climate condition.

Key words: climate change, frequency analysis, design storm, hydrology, flood, Canada

4.2 Introduction

The anthropogenic gas emissions is now higher than ever, and more than half of the observed increase in global average surface temperature from 1951 to 2010 was caused by the anthropogenic increase in GHG concentration and other anthropogenic forcing together [25]. Climate change studies revealed that warming trends are linked to global hydrological cycle [1], such as increase in extreme precipitation [10,32]. The potential increase of rainfall events can lead to an increase in rain generated flood [1,31,45,50,51]. Flood is one of the greatest natural disasters to human society and it severely affects the social and economic development of a country. Its adverse impact includes loss of life and property, environmental degradation and shortage of food, energy, water and other basic needs. Flood management strategy continuously evolved in many flood prone countries over time. The flood management strategy has gradually shifted from narrow focus on structural flood control measures to a combination of structural and non-structural flood control measures and further to Integrated Flood Management (IFM). Flood risk map is one of the effective non-structural measures widely used by many countries around the world. In Canada, the federal government in conjunction with provinces invested millions of dollars to control flood by building structural measures in 1950s, 1960s and 1970s. But after the extensive flood damage across Canada in the early 1970s, it was realized that prevention of flood and non-structural measures are needed to reduce flood damage. This realization made the federal government to initiate the Flood Damage Reduction Program [16]. The main activities under this program are identifying, mapping and designating flood risk area and then applying policies to discourage development in the flood risk area. After designation of flood risk area, both federal and provincial governments do not build or support any flood vulnerable development in such areas. The flood standards used to define flood limit in Ontario are (i) flood resulted from a rainfall actually experienced during a major storm such as the Hurricane Hazel storm that struck Southern Ontario on October 15, 1954 (ii) 100 year return period flood and (iii) an observed flood event, and 100 year flood is the minimum acceptable regulatory flood standard [46]. The regulatory flood limit for Clearview Creek, the study area for this study, is the water level produced by a 100 year return period flood. In absence of adequate streamflow records, rainfall data is used to simulate stream flows. When flow is simulated from a specific return period storm, the commonly made assumption is that storm of a specific frequency produces streamflows of the same frequency. Credit Valley Conservation uses a 24 hour 100 year return period storm depth for flood mapping study for this study area. The storm depths are calculated from the historic rainfall time series without consideration of climate change impact. This study aims to investigate the climate change impact on hydrological processes by analyzing storm depths and storm flows, and impact on hydraulics by analyzing water level and flooding scenario addressing the climate change impact.

The design storm depths are calculated employing statistical analyses on observed rainfall time series based on the assumption of a stationary climate, but the Earth is now in a nonstationary climate [3,27,38]. Owing to this nonstationary, sustainability of non-structural flood management measures such as flood mapping would benefit from calculating storm depth addressing the climate change impact. A number of studies have been conducted recently to calculate storm depths of different duration and return period addressing the impact of climate change, but maximum three probability distributions were used to fit the annual maximum precipitation time series for calculating storm depths by employing frequency analysis. As example, [39] used the Log-Pearson Type III, some studies [17,35] used generalized extreme value, [56] used Extreme value type I (EV I), [55] used Gumbel and generalized extreme value for storm depth calculation. Considering the importance of selection of probability distribution, twenty seven distributions were tested using two statistical tests for observed, NARCCAP current and future datasets, and the best fitted distribution was used for frequency analysis to calculate design storm depths.

The North American Regional Climate Change Assessment Program (NARCCAP) provides high resolution climate scenarios created from multiple GCMs and RCMs to facilitate climate change impact assessment. Climate change impact study using climate model simulations should consider multiple projections to address the inherent uncertainty in climate projections [37]. In this study, six RCM+GCM pairs provided by NARCCAP were used for storm depth calculation to address the uncertainty in the climate projections. The precipitation dataset from NARCCAP are available as gridded data, and are areal average not point estimates [4]. Some studies applied delta change factors to precipitation time series [e.g., [2,45,48,49]], and others applied it to design storm depth [17,56]. The delta change method was applied to transpose design storm depth calculated from gridded NARCCAP data to Toronto Pearson Airport meteorological station to remove the systematically difference between climate model simulated and observed precipitation.

Climate change impact on river/stream flow has been investigated by a number of researches using different climate model simulations in the last decades, most of the study focused on continuous simulation of river flow for comparatively big and rural catchments [52,53]. There are very few studies which investigated the impact of climate change on storm flow in urban areas using design storm as input in an event-based hydrologic modeling tools. However, studies investigated the effect of climate change on urban-catchment scale storm water runoff using long-term simulation revealed significant increase of peak flows in different areas. [54], for example, found a significant increase up to 80% for the average peak flows under climate change scenarios of 2030-2059 in the Bronx River watershed in New York City. The increase of peak flow will heighten the flood risk under future climate condition. [14] reported that, under future climate, the extent of flood will be larger and will increase the level of risk to public infrastructure in the Upper Thames River basin in Canada. They also indicated insignificant differences of flood lines between current and future scenario for 100 yr return period flood due to steep slope in some areas, despite the difference in water surface elevation of approximately 40cm. This study used a single event hydrologic model simulation software Visual OTTHYMO for flow simulation and a hydraulic modeling tool - the Hydrologic Engineer Center's River System Analysis System (HEC-RAS) software for flooding scenario analyses. To achieve the objectives, the following main activities were carried out in this research: performing frequency analyses to compute storm depths for observed, NARCCAP current and future datasets; transposing design storm depth calculated from gridded NARCCAP data to Toronto Pearson Airport meteorological station using delta change factor; simulation of peak flows for different return period using the Visual OTTHYMO rainfall runoff model; simulation of hydraulic metrics using HEC-RAS hydraulic model; and analyses of storm depths, flows and flooding scenarios under current and future climate conditions.

4.3 Study Area and Data

4.3.1 Study Area

The study area, Clearview Creek drainage area which is under the jurisdiction of Credit Valley conservation, is located mostly in the City of Mississauga and also in the Town of Oakville, Southern Ontario, Canada. The study area has undergone significant urban growth in recent years, and the climate of this area can be characterised by humid-continental. The climate of the study area is represented by the meteorological data of Pearson International Airport station. Based on the meteorological data from 1981 to 2010 observed at Toronto Lester B. Pearson International Airport, the daily average temperature over the year is 8.2°C. The extreme maximum temperature 38.3°C and minimum temperatures - 31.3 °C were observed on 25 August 1948 and 4 January 1981, respectively. The total yearly precipitation, rainfall and snowfall at this area are 785.9 mm, 681.6 mm and 108.5 cm respectively based on the data from 1981-2010 [13]. The total area draining from the Clearview Creek drainage area to the Lake Ontario is about 478.66 ha.

4.3.2 Observed Meteorological Data

This study used the rainfall time series for 30 years, from 1971 to 2000, observed at Toronto Lester B. Pearson International Airport meteorological station with a latitude and longitude of 43°40'38.000" N and 79°37'50.000" W respectively. The hourly observed rainfall time series were obtained from Ontario Climate Center, Environment Canada. The Intensity-Duration-Frequency curves used by city of Mississauga and Credit Valley Conservation for development studies for the study area were originally derived from the observed rainfall data taken from the Pearson International Airport. Therefore, the observed rainfall data at this meteorological station were used to calculate the design storm depths for observed/baseline scenario in this study.

4.3.3 NARCCAP Climate Data

This study used the climate data sets collected from the North American Regional Climate Change Assessment Program [36,37,44]. NARCCAP is a coordinated multi-model numerical experiment [37] that provides climate projections for several RCM+GCM pairs at similar spatial resolutions over identical periods covering the conterminous United States and most of Canada. It provides all the data at a gridded horizontal resolution of 50km and time span 33 years for both current (1968-2000) and future (2038-2070) period. The first three years of data, spin-up periods [34] has been discarded in this study. NARCCAP data permits assessment of climate change impact by comparing the climate of mid twenty-first century with that of twentieth century. Every future simulation in NARCCAP follows greenhouse gas and aerosol concentration based on A2 emission scenario described in the Special Report on Emissions Scenarios (SRES) [43]. The data are stored in the NetCDF files in 2D arrays and array dimensions are named "xc" and "yc" within the file. The array dimensions (yc, xc) of nearest point of Toronto Lester B. Pearson International Airport found from the grid cell maps for CRCM, HRM3 and RCM3 are (52,100), (59, 105) and (45, 94) respectively.

The precipitation time series of temporal resolution 3 hour provided by six different RCM+GCM pairs were used in this study. These six pairs includes three RCMs and four GCMs, the RCMs are Canadian Regional Climate Model (CRCM) [42], Hadley Regional Model 3 (HRM3) [26] and Regional Climate Model version 3 (RCM3) [12,20], and the GCMs are Community Climate System Model (CCSM) [8], Third Generation Coupled Global Climate Model (CGCM3) [15], Geophysical Fluid Dynamics Laboratory GCM (GFDL) [19] and Hadley Centre Coupled Model, version 3 (HADCM3) [21,47]. The six RCM+GCM pairs' data used in this study are CRCM+CCSM, CRCM+CGCM3, HRM3+GFDL, HRM3+HADCM3, RCM3+CGCM3 and RCM3+GFDL.

4.4 Methodology

The procedure used in this study involves (1) storm depths calculation under current and future climate condition; (2) transforming storm depths into runoff using a hydrological model, and (3) transforming runoff into water surface elevation required to develop flooding scenario under current and future climate condition using a river system analyses tool.

4.4.1 Design Storm

Design storm depths were calculated for different duration (3h, 6h, 12h and 24h) and six different return periods (2yr, 5yr, 10yr, 25yr, 50yr and 100yr) for historic observations and climate model simulations for current and future period. NARCCAP provided precipitation time series of 3h resolution were aggregated into 3-, 6-, 12- and 24 h duration on an annual basis. Then time series of annual maximum rainfall depth were generated by determining the yearly maximum value for each duration from the aggregated time series. Frequency analysis was performed on these annual maximum time series data of each duration to calculate storm depths. Two tests, Pearson chi-square test and Kolmogorov-Smirnov, were used to test the goodness of fit of each distribution among twenty seven distributions as shown in Table 4-1. Environment Canada uses Gumbel Extreme Value distribution to fit the annual extremes of rainfall for the study area for developing IDF curves. Therefore, Extreme Value type 1 (EV1) was used for frequency analyses together with the best fitted distribution. Each distribution was tested for its goodness of fit following the attained percentage of the parameter "a", and the distribution that attained the highest percentage of 'a' for a particular time was selected for frequency analyses for that time series. The percentage value of 'a' for Chi-square test (equation 4-1) and Kolmogorov-Smirnov (equation 4-2) are defined by the following two equations:

$$a_{attained} = 1 - x^2(m = k - r - 1, q) \qquad \text{Eq. 4-1}$$

$$a_{attained} = 1 - x^2(m, q) \qquad \text{Eq. 4-2}$$

where m are the degrees of freedom of chi square test, k is the number of bins used in chi square test, r is numbers of parameters of the distribution and q is the Pearson parameter. The theoretical background of the tested distributions is presented in [30]. A statistical analysis software, Hydrognomon [30], was used to find the best fitted distribution among 27 statistical distributions.

Three sets of storm depth were calculated for historical observation, NARCCAP current and future simulations. The three sets are: (1) Case 1: storm depth with best fitted distribution tested by Chi-square test (2) Case 2: storm depth with best fitted distribution tested by Kolmogorov-Smirnov, and (3) Case 3: storm depth with Extreme Value type 1 (EV1).

Table 4-1: Best fitted distribution for NARCCAP data for different duration [Case 1 (current x, future √), case 2 (current *, future +)]

	CrcmCcsm				CrcmCgcm3				Hrm3Gfdl				Hrm3Hadcm3				Rcm3Cgcm3				Rcm3Gfdl			
Distribution	3	6	12	24	3	6	12	24	3	6	12	24	3	6	12	24	3	6	12	24	3	6	12	24
Normal	x	x											√		√	x						x		
LogNormal						+	√		x			x												
Galton																*								
Exponential				x					√	x														x
Gamma						x	x							√	*				+					
Pearson III													+											
LogPearson III																		+		+		+		
Gumbel EV 1 Max	*√		x√		√	√		√						x					x√				x	
EV2-Max		√+						x									x√	*		x√	√			√
Gumbel EV 1 Min																								
Weibull										√			*											
GEV Max																								
GEV Min		*					+															*		
Pareto			+							*	+					+								
L-Moments Normal											x		x		x				*	*				
L-Moments Exponential				√												√								
L-Moments EV1 Max					x			+						*									*	
L-Moments EV2 Max	+											√					*	√						+
L-Moments EV1 Min																								
L-Moments EV3 Min																								
L-Moments GEV Max												+									+			*
L-Moments GEV Min			*	*+	+	*	*		*+	+	*√	*		+			+				*			
L-Moments Pareto					*										+						x			
GEV-Max (k spec.)								*										x				√	+	
GEV-Min (k spec.)																								
L-Moments GEV-Max (k spec.)																							√	
L-Moments GEV-Min (k spec.)																								

All the NARCCAP dataset are provided at grid scale, therefore storm depth values calculated from the NARCCAP datasets are for grid scale. The bridging of the gridded climate change projections with the historic observation at meteorological station is essential for climate change impact study at watershed scale. Delta change factor can be applied to discrete totals i.e. design storm depths [17] to estimate future rainfall intensities at the station scale from the estimated values at the model grid-scale (both current/historic and future) and at the observed station scale (current/historic). The assumption in transposing projected future change in climate onto point observation is that the areal-to-point relationships of precipitation remain constant in future climates [35]. The delta change factor application procedure (presented by equations 4-3, 4-4 and 4-5) described by [56] was used to produce future station-scale intensities/depths:

$$I_F^{(g)} = I_H^{(s)} \left[1 + \Delta_{F-H}{}^{(g)}(T,d)\right] \qquad \text{Eq. 4-3}$$

$$\Delta_{F-H}{}^{(g)}(T,d) = \frac{I_F^{(g)}(T,d) - I_H^{(g)}(T,d)}{I_H^{(g)}(T,d)} \qquad \text{Eq. 4-4}$$

$$\mathrm{I}_F^{(s)}(T,d) = I_H^{(s)}(T,d)\,\frac{I_F^{(g)}(T,d)}{I_H^{(g)}(T,d)} \qquad \text{Eq. 4-5}$$

Where, T and d denote return period and duration respectively, H and F denote historic and future, and s and g denote station and grid respectively.

Delta change factor was applied to all NARCCAP datasets to produce storm depths at station scale under future climate condition, and the results are presented in the Table 4-2.

Table 4-2: Design storm depths (in mm) calculated from observed data and NARCCAP future datasets

Return Period	Duration (h)	Observed			CrcmCcsm			CrcmCgcm			Hrm3Gfdl			Hrm3Hadcm3			Rcm3Cgcm3			Rcm3Gfdl		
		Case 1	Case2	Case3	Case 1	Case2	Case3	Case 1	Case2	Case3	Case 1	Case2	Case3	Case 1	Case2	Case3	Case 1	Case2	Case3	Case 1	Case2	Case3
2yr	3	30.4	30.4	29.9	32.8	32.9	33.6	33.1	33.8	32.5	33.3	35.1	34.7	26.6	26.4	26.5	42.7	40.8	42.5	36.0	34.9	37.0
	6	34.2	34.6	35.3	33.4	34.3	36.6	36.5	38.5	38.5	46.4	40.8	43.4	33.4	33.1	33.8	42.3	44.7	46.9	40.3	41.6	44.7
	12	37.9	38.3	40.1	38.4	38.9	40.7	42.2	42.1	44.1	46.2	48.7	53.6	38.3	38.9	40.8	48.4	47.4	51.2	46.3	47.0	50.0
	24	45.3	44.0	46.2	49.7	50.5	51.1	50.3	48.7	50.5	57.8	57.0	63.4	41.5	43.6	47.8	56.3	52.0	57.8	57.8	54.0	57.5
5yr	3	39.8	39.8	39.1	42.1	42.2	42.5	40.1	39.6	39.6	45.0	45.8	45.6	33.4	32.7	32.8	57.8	64.3	59.1	46.8	46.5	52.9
	6	46.9	47.6	49.0	45.6	46.1	50.2	48.7	50.4	51.9	64.8	58.1	63.3	43.3	44.5	44.3	64.9	71.2	72.5	58.0	58.4	65.0
	12	53.5	52.0	55.0	53.5	52.5	55.0	57.1	54.9	58.6	73.2	72.9	78.3	52.4	53.2	53.6	73.3	71.1	75.4	61.5	59.3	64.6
	24	58.7	57.5	61.8	64.8	63.4	67.1	66.2	65.2	67.4	81.6	79.5	92.8	58.4	60.7	64.3	75.1	72.8	80.2	71.6	69.8	76.7
10yr	3	45.4	45.4	45.2	49.2	48.9	49.0	43.9	43.2	44.2	53.2	52.3	52.9	37.5	37.0	37.0	67.6	77.6	70.0	57.3	57.4	63.8
	6	56.5	57.0	58.1	56.5	56.4	59.4	58.9	58.4	60.8	74.8	74.0	76.5	50.3	52.1	51.4	85.2	91.3	89.9	74.5	73.8	78.6
	12	65.0	63.1	64.9	64.5	46.7	64.4	67.5	65.4	67.9	97.1	93.5	94.9	63.1	62.4	62.1	91.9	91.1	91.7	73.6	70.3	73.9
	24	68.9	69.0	72.1	76.5	73.6	77.4	77.0	77.9	78.5	104.6	103.2	113.1	74.8	74.4	75.2	89.6	92.8	95.2	82.5	84.5	89.3
25yr	3	52.0	52.0	52.9	58.3	57.4	56.5	48.4	48.1	50.2	63.2	60.1	62.1	42.5	42.6	42.5	79.7	89.0	83.4	76.0	76.4	77.5
	6	70.4	69.9	69.6	75.3	73.0	70.7	74.5	69.7	72.0	87.0	100.1	93.6	60.0	61.6	60.2	119.6	119.1	111.8	102.5	99.6	96.1
	12	80.1	79.6	77.3	79.0	77.6	76.2	80.8	81.5	79.5	132.7	123.6	116.1	77.0	73.3	72.7	116.7	121.9	112.6	90.9	88.2	85.6
	24	83.7	86.6	85.2	93.0	91.6	87.6	91.1	95.8	92.7	145.2	147.2	138.8	101.0	93.5	89.0	111.5	126.2	114.2	100.1	109.0	105.3
50yr	3	56.5	56.5	58.6	65.6	64.3	62.5	51.2	52.0	54.3	70.0	65.5	68.9	45.9	46.6	46.6	88.6	93.4	93.5	94.1	95.5	87.5
	6	82.0	80.3	78.1	92.3	87.7	79.3	87.7	79.2	79.9	96.1	123.8	106.1	67.9	69.0	66.8	153.4	141.0	128.1	129.6	124.3	109.0
	12	91.4	94.0	86.6	89.8	89.4	85.1	90.4	95.3	88.0	162.1	149.5	132.1	87.4	81.7	80.7	135.5	149.6	128.3	105.2	104.9	94.2
	24	96.0	102.3	94.8	107.1	105.2	96.5	101.4	110.5	103.0	185.9	194.0	157.8	124.5	109.0	99.0	130.1	158.2	128.3	116.3	132.2	117.1
100yr	3	60.7	60.7	64.3	72.5	71.9	68.2	53.9	55.8	58.6	76.2	70.6	75.7	48.9	50.6	50.6	97.3	94.9	103.4	116.7	120.1	97.4
	6	94.8	91.2	86.5	114.8	106.8	88.0	102.9	88.8	87.9	105.6	151.0	118.5	76.3	76.1	73.3	195.6	163.6	144.3	163.2	154.1	121.8
	12	102.7	110.1	95.8	100.4	101.7	93.7	99.9	110.9	96.5	193.6	177.8	148.2	97.8	90.1	88.4	154.2	181.3	143.8	120.9	125.1	102.7
	24	109.6	120.5	104.4	122.4	116.3	109.9	111.9	126.2	113.5	238.7	256.8	176.8	151.7	125.6	109.1	151.2	197.6	142.3	135.8	160.9	128.9

Two traditionally derived storms have been traditionally adopted as representative storm, namely the SCS Type II and Chicago distribution [41]. Credit Valley Conservation uses 24hr Chicago storm distribution for hydrologic modeling for flood line delineation in the study area. The Chicago storm was developed by C.J. Keifer and H.H. Chu [28] on 25 years of rainfall record for the city of Chicago. The storm is generally applied to urban basins where peak runoff rates are largely influenced by peak rainfall intensities. Design storm depths to be used in the hydrologic model were discretized using Chicago distribution for a time step of 10 minutes. The peak intensity for the storm is computed using the following equation:

$$I_p = \frac{A}{(\Delta t + B)^C} \qquad \text{Eq. 4-6}$$

The 10-minute intensities are then distributed around the peak as rΔt before the peak and (1-r)Δt after the peak. MTO suggested using an r value of 0.38 for all MTO districts to provide a consistent application across the province. The IDF parameter values A, B and C were obtained from the IDF equation used by City of Mississauga [5]. The IDF parameters are presented in the Table 4-3. The intensities before and after the peak were calculated using the following equations:

Before the peak:

$$\int_{t_{b1}}^{t_{b2}} i_b \, dt_b = \left[\frac{At_b}{([t_b/r]+B)^c}\right]_{t_{b1}}^{t_{b2}} \qquad \text{Eq. 4-7}$$

After the peak:

$$\int_{t_{a1}}^{t_{a2}} i_a \, dt_a = \left[\frac{At_a}{([t_a/(1-r)]+B)^c}\right]_{t_{a1}}^{t_{a2}} \qquad \text{Eq. 4-8}$$

Where, i_a and i_b are intensities, t_b is the time before the peak intensity in minute, t_a is the time after the peak intensity in minute, A, B and C are IDF parameters. A sample calculation can be found in MTO Drainage Management Manual [41]

Discretized design storms for 24hr duration and 2, 5, 10, 25, 50 and 100 year return period were developed using Chicago distribution and IDF parameter listed in the Table 4-3. The temporal distribution of the six return period developed using theses IDF parameters were used for both observed and NARCCAP storm depths for the study area. A sample discretized storm for 24 hour and 100 year return period is shown in the following Figure 4-1.

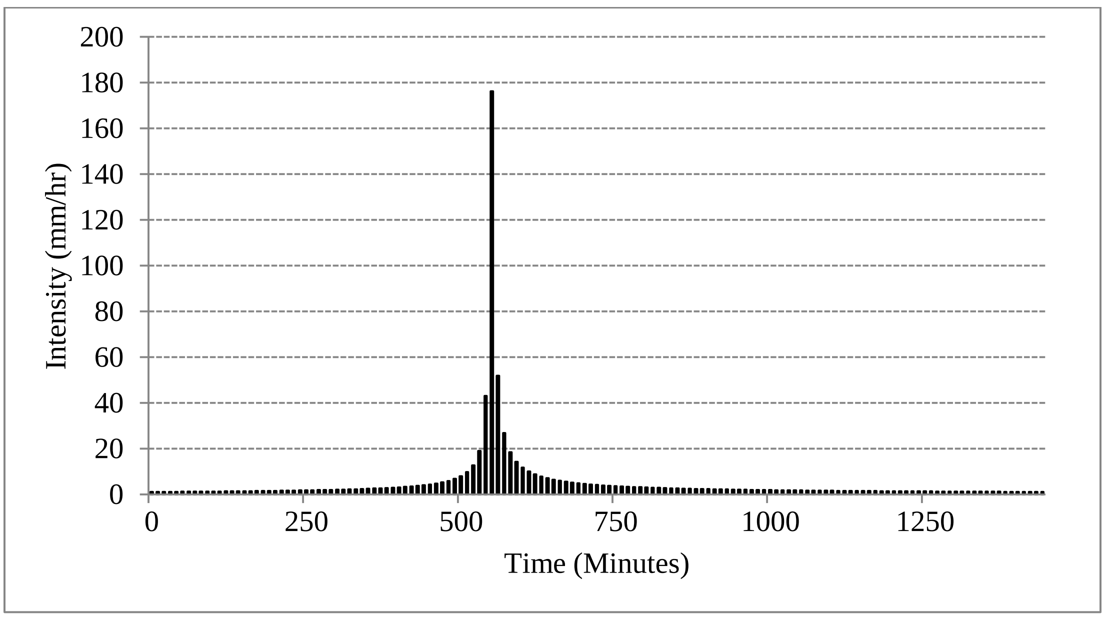

Figure 4-1: Chicago storm of 24 hr 100 year for city of Mississauga IDF parameters

Table 4-3: IDF Parameters of City of Mississauga IDF Curves

Parameter	Return Period					
	2	5	10	25	50	100
A	610	820	1010	1160	1300	1450
B	4.6	4.6	4.6	4.6	4.7	4.9
C	0.78	0.78	0.78	0.78	0.78	0.78

4.4.2 Hydrologic Modeling

The most widely used approach to simulate hydrological impact of climate change is done by inputting climate projections into a deterministic or conceptual hydrological model that contains physically based mathematical descriptions of hydrologic phenomena [11,18,22,29,33]. Precipitation data can be inputted into the hydrologic model in a form of continuous time series data or event-based data such as total rainfall depth. Considering the urban hydrological modeling capability, this study aimed to use Visual OTTHYMO v3.0 (VO3), the third version of the INTERHYMO – OTTHYMO hydrologic model simulation software package designed for Microsoft Windows OS [6]. It is a single event hydrologic model which simulates runoff from single storm events. The model is an appropriate design tool for use in projects such as watershed studies and stormwater management design [40]. The model includes four commands for four unit hydrograph options: STANDHYD - uses parallel standard instantaneous unit hydrographs for impervious and pervious areas of the catchment, and this method is recommended for modelling urban watersheds with greater than 20% impervious areas; NASHYD - uses the Nash instantaneous unit hydrograph method; WILHYD - uses the Williams and Hann (HYMO) unit hydrograph method; SCSHYD -

uses the Nash hydrograph method based on SCS parameters and with N being five reservoirs. The routing routines available to calculate the transformation of a streamflow hydrograph are based on the continuity equation and a storage discharge relation. The routines use variable storage coefficient method, Muskingum-Cunge and storage-indication method [7]. This study used an existing model of the study area developed for current landuse conditions using Visual OTTHYMO v3.0, and the model of the study area was obtained from the Credit Valley Conservation. The model contains 9 sub-catchment areas (shown in the Figure 4-2) with a total area of 478.66 ha, 6 sub-catchments were modeled using standard instantaneous unit hydrographs (the total impervious areas of which varies from 39% to 84%), and other 3 sub-catchments were modeled using Nash instantaneous unit hydrograph. The rainfall losses were computed by means of modified curve number procedures. The routing routine used for channel and pipe was variable storage coefficient method, and for the storage area was storage-indication method. The 24 hour duration storm depths of 2, 5, 10, 25, 50 and 100 year return for observed and future (six RCM+GCM pairs and average of six pairs) for case 1 were used as input in the hydrologic model for flow simulation. The design storm depths were discretized by using Chicago distribution as described in the previous section to input as design hyetographs in hydrological model. The 24 hour design storms used for flow simulation are listed in Table 4-4.

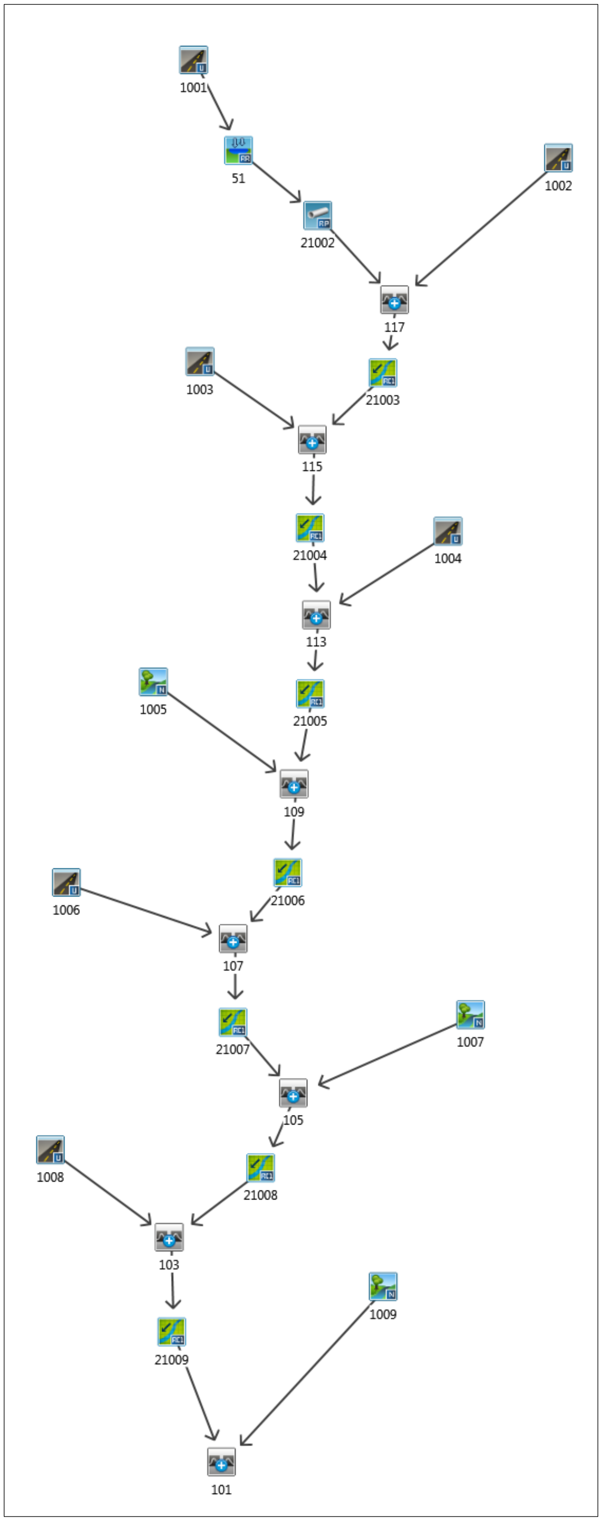

Figure 4-2: Hydrologic model schematic for Clearview Creek catchment

Table 4-4: Design storm depths (in mm) used for flow simulation

Return Period	Observed	CrcmCcsm	CrcmCgcm	Hrm3Gfdl	Hrm3Hadcm3	Rcm3Cgcm3	Rcm3Gfdl	Average
2	45.3	49.7	50.3	57.8	41.5	56.3	57.8	52.2
5	58.7	64.8	66.2	81.6	58.4	75.1	71.6	69.6
10	68.9	76.5	77.0	104.6	74.8	89.6	82.5	84.2
25	83.7	93.0	91.1	145.2	101.0	111.5	100.1	107.0
50	96.0	107.1	101.4	185.9	124.5	130.1	116.3	127.5
100	109.6	122.4	111.9	238.7	151.7	151.2	135.8	151.9

4.4.3 Hydraulic Modeling

The Hydrologic Engineer Center's River System Analysis System (HEC-RAS) software [24], that allows to perform one-dimensional steady and unsteady flow river hydraulics calculations, were used for flooding scenario analyses under future climate condition in the floodplain of Clearview Creek. The system includes a graphical user interface, separate hydraulic analyses components, data storage and management capabilities, graphic and reporting facilities. HEC-RAS is capable of modelling a full network of natural or constructed channels. HEC-RAS requires the input of geometric data to represent river network/reach, channel cross-section data, and hydraulic structure data such as bridge and culvert data.

The length of Creek modeled in this study is 2878m. The model includes 45 cross-sections and 4 culverts as shown in the Figure 4-3. The cross-section number started with 0 at the outlet of Creek on the shore of the Lake, and the river stations were numbered as the distance from the outlet. The cross-section data, high cord and low cord elevations for culverts were generated from a high resolution digital terrain model (DTM) by using HEC-GeoRAS [23]. HEC-GeoRAS, an extension for use with ArcGIS tools, specifically designed to process geospatial data for use with HEC-RAS. It enables the hydraulic engineers to create a HEC-RAS import file containing geometric data from a digital terrain model (DTM), process water surface profile data exported from HEC-RAS, and perform floodplain mapping. A 1m x 1 m resolution DTM was developed employing ArcGIS and using a 5m x 5m resolution DTM of the entire catchment area and recent survey data adjacent to the Creek obtained from Credit Valley Conservation. A 1m x 1 m resolution DTM was prepared using the survey data, existing 5m x 5m resolution DTM was resampled to 1m x 1 m resolution DTM, and finally mosaic 1m x 1 m resolution DTM was created using DTM from survey data as mosaic operator. Then, a RAS GIS file that contains cross-section elevations with bank station data, and high cord and low cord elevations for culverts was generated from the mosaic DTM using HEC-GeoRAS. The geometric data, hydraulic structure and flow data were completed in HEC-RAS. The Manning's roughness coefficient values, expansion and contraction coefficients for the cross-sections were completed following the Credit Valley Conservation's technical guideline [9] for hydrologic and hydraulic analyses. The detail survey data for the culverts (location, dimensions, length, height from obvert to top of road, photos etc.) were also obtained from the Credit Valley Conservation. Some buildings were set as obstructed area at cross-section of river stations 520, 2448, 2500 and 2545. As a mixed flow regime calculation was made, the boundary conditions were entered at both upstream and downstream ends of the Creek. For steady flow boundary condition, the known water surface elevation, mean annual water surface elevation (74.8m) for Lake Ontario at Mississauga [9] was entered at downstream end, and critical depth was selected as upstream boundary condition at river station 2878. The peak flows simulated for 24 hour storm depths listed in Table 4-4 were used as input in the HEC-RAS model.

The peak flows at the hydrologic elements 117, 115, 113, 109, 107, 105, 103 and 101 of the hydrologic model (shown in Figure 4-2) were entered at the river station 2878, 2672, 2297, 1779, 1556, 1001, 419 and 0. The peak flow values of observed/baseline, 6 RCM+GCM pairs and average of six pairs for steady flow simulation are listed in the Table 4-5.

Table 4-5: Peak flows (m^3/s) used for steady flow simulation in HEC-RAS

	RS	2yr	5yr	10yr	25yr	50yr	100yr		RS	2yr	5yr	10yr	25yr	50yr	100yr
Observed\baseline	2878	4.15	6.21	13.07	23.16	31.45	37.95	Future average	2878	5.19	13.61	23.52	36.61	49.79	64.33
	2672	5.14	7.23	13.26	23.28	31.45	38.53		2672	6.19	13.80	23.60	36.50	50.81	65.79
	2297	5.77	8.24	13.29	23.34	31.47	38.57		2297	7.02	13.84	23.66	36.84	50.88	66.03
	1779	4.43	6.64	10.82	17.77	23.72	29.07		1779	5.55	11.19	18.01	28.02	37.60	49.52
	1556	5.41	8.28	11.51	18.78	25.01	30.44		1556	6.94	11.91	19.03	29.33	39.19	51.03
	1001	5.25	7.91	12.22	19.51	25.64	31.20		1001	6.58	12.62	19.75	30.10	39.92	51.70
	419	6.27	9.34	12.79	20.22	26.54	32.27		419	7.93	13.21	20.47	31.11	41.11	53.01
	0	6.42	9.57	13.00	20.55	26.97	32.78		0	8.12	13.45	20.81	31.63	41.77	53.83
CrcmCcsm	2878	4.81	10.18	18.16	29.54	36.58	46.44	CrcmCgcm3	2878	4.91	11.20	18.47	28.24	35.07	39.33
	2672	5.77	10.47	18.27	29.58	36.47	47.21		2672	5.87	11.43	18.59	28.41	35.05	40.00
	2297	6.55	10.52	18.33	29.67	36.82	47.43		2297	6.65	11.48	18.66	28.50	35.24	40.09
	1779	5.14	8.90	14.33	22.28	28.01	35.08		1779	5.24	9.56	14.56	21.37	26.29	30.10
	1556	6.44	9.56	15.20	23.52	29.33	36.74		1556	6.55	10.23	15.43	22.56	27.61	31.53
	1001	6.08	10.26	15.91	24.18	30.11	37.34		1001	6.20	10.94	16.13	23.21	28.29	32.26
	419	7.36	10.79	16.49	25.05	31.13	38.57		419	7.50	11.67	16.73	24.09	29.21	33.37
	0	7.53	11.02	16.76	25.46	31.64	39.19		0	7.66	11.66	17.00	24.49	29.69	33.91
Hrm3Gfdl	2878	6.07	21.77	35.10	60.86	86.54	115.37	Hrm3Hadam3	2878	3.59	6.16	17.03	34.90	48.06	64.20
	2672	7.10	21.82	35.27	62.19	88.40	117.64		2672	4.55	7.18	17.17	34.87	48.83	65.66
	2297	8.07	21.87	35.43	62.35	89.05	118.25		2297	5.20	8.18	17.24	35.05	48.91	65.90
	1779	6.49	16.78	26.89	46.51	66.72	89.87		1779	3.82	6.59	13.56	26.15	36.19	49.42
	1556	8.10	17.76	28.20	48.01	68.60	92.61		1556	4.72	8.22	14.38	27.46	37.86	50.93
	1001	7.73	18.49	29.00	48.53	69.60	94.72		1001	4.60	7.85	15.09	28.14	38.50	51.60
	419	9.14	19.15	29.97	49.87	71.21	97.16		419	5.46	9.27	15.66	29.04	39.68	52.90
	0	9.36	19.47	30.47	50.66	72.29	98.68		0	5.59	9.50	15.91	29.53	40.31	53.73
Rcm3Cgcm3	2878	5.81	17.25	27.24	39.40	51.30	63.90	Rcm3Gfdl	2878	6.07	14.89	22.26	34.30	42.35	54.74
	2672	6.82	17.36	27.41	40.03	52.40	65.37		2672	7.10	15.05	22.42	34.28	42.82	55.83
	2297	7.76	17.43	27.50	40.11	52.41	65.59		2297	8.07	15.10	22.48	34.46	43.01	56.10
	1779	6.21	13.69	20.64	31.06	38.97	49.19		1779	6.49	12.09	17.20	25.72	32.21	41.63
	1556	7.77	14.52	21.79	31.47	40.46	50.70		1556	8.10	12.87	18.19	27.08	33.64	43.17
	1001	7.38	15.23	22.48	32.20	41.23	51.35		1001	7.73	13.57	18.92	27.77	34.33	43.81
	419	8.78	15.81	23.36	33.30	42.40	52.66		419	9.14	14.13	19.61	28.66	35.53	45.10
	0	8.99	16.06	23.73	33.83	43.08	53.48		0	9.36	14.39	19.93	29.14	36.11	45.80

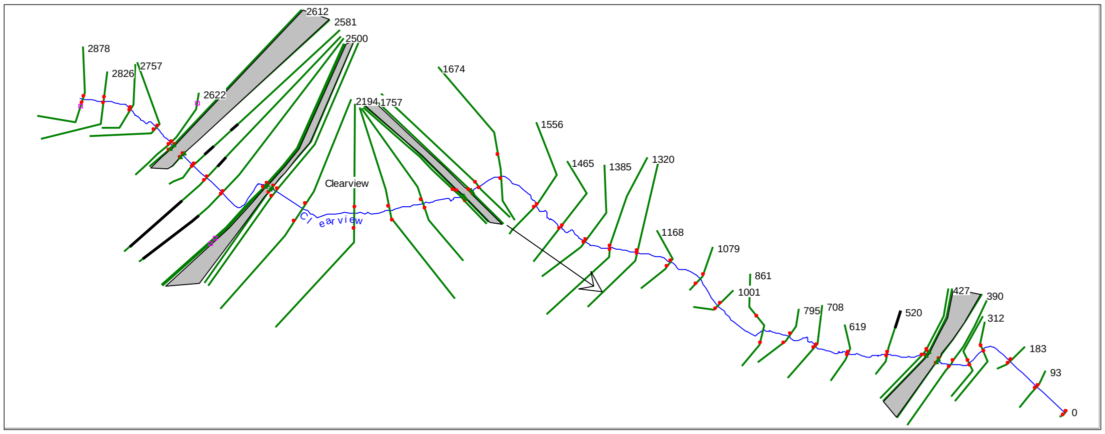

Figure 4-3: Geometric data schematic showing cross-section and culvert locations

4.5 Results and Discussion

4.5.1 Design Storm

Frequency analyses were performed on a total of 52 annual maximum time series including 4 observed, 24 NARCCAP current and 24 NARCCAP future dataset. The best fitted distribution among twenty seven distributions for annual maximum time series of four durations for NARCCAP current and future datasets are listed in the Table 4-1. Among the 96 selection for 48 NARCCAP datasets shown in the Table 4-1, L-Moment GEV Min was selected 15 times (the highest), that is 15.6% of the total selection and Gumbel EV1 Max was selected for 11 times that is 11.5% of the total selection. This reveals the importance of selection of appropriate distribution for calculation of storm depths considering climate change impact. The storm depths calculated from observed data and NARCCAP datasets are presented in Table 4-2. The delta change factor was applied to get the storm depths under future climate condition. The storm depths for all six RCM+GCM pairs show a significant increase in the future. All the data in the Table

4-2 are plotted as scatter plot on a graph (Figure 4-4) whose abscissa and ordinate are the values observed and NARCCAP future storm depths respectively. The abscissa and ordinate are plotted on the same scale and 45 degree line is drawn to facilitate interpretation of the scatter plot. The linear trendlines including the trendline equations and the dispersion of data (indicated by the R^2 values) above the 45-degree line reveal that the increase of storm depths under future climate is higher for higher values. The higher values of storm depths may either represent storm depths for higher return period or higher duration. The linear trendlines also show that the overall increase in storm depths is highest for case 1 (when the distributions were identified by Chi-square test), and lowest for case 3 (when frequency analyses was performed using Gumbel EV1 Max).

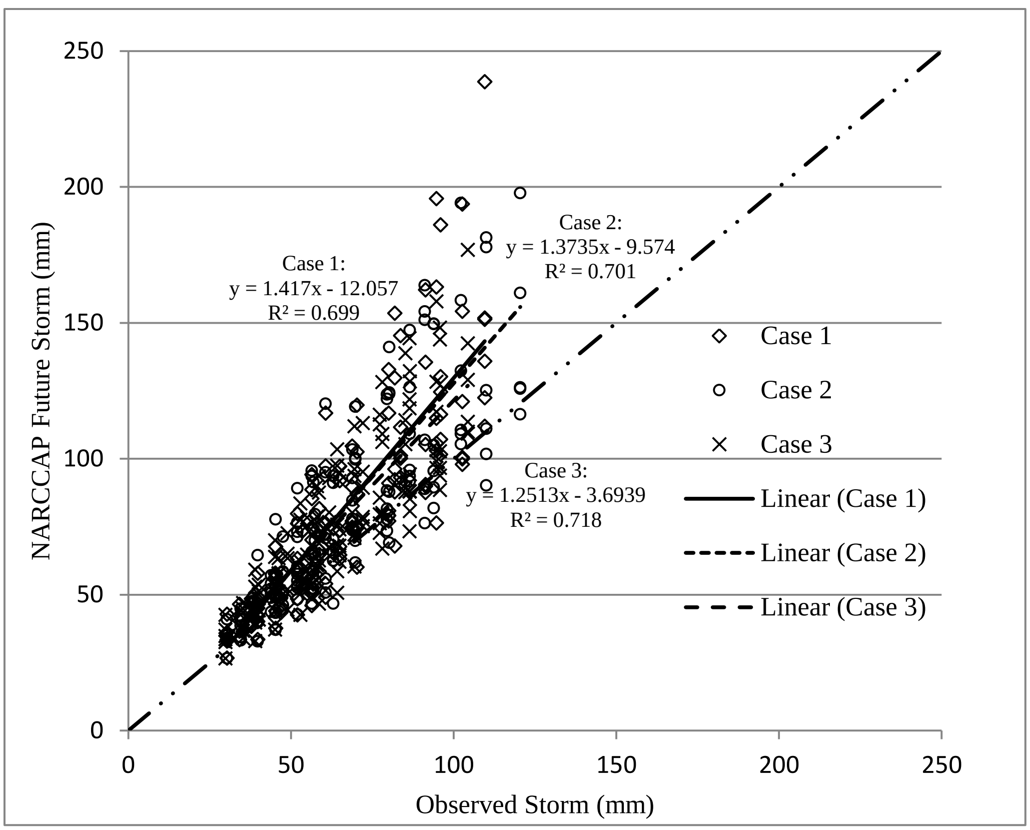

Figure 4-4: Scatterplot of design storm depths calculated from observed data and NARCCAP future datasets

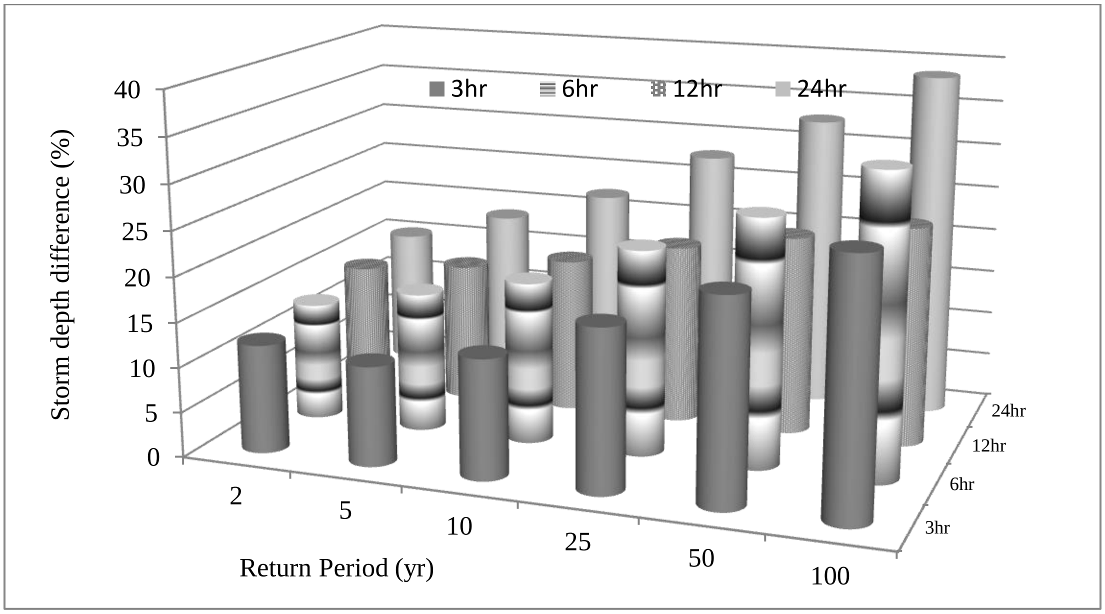

Figure 4-5: Difference between observed and NARCCAP future average storm depths for case 1

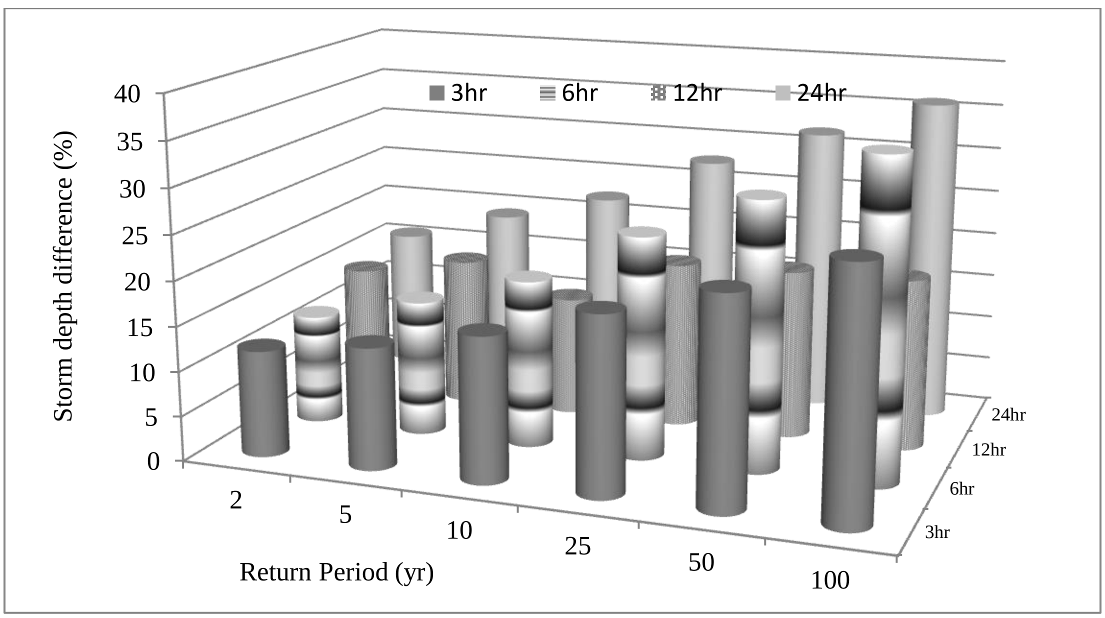

Figure 4-6: Difference between observed and NARCCAP future average storm depths for case 2

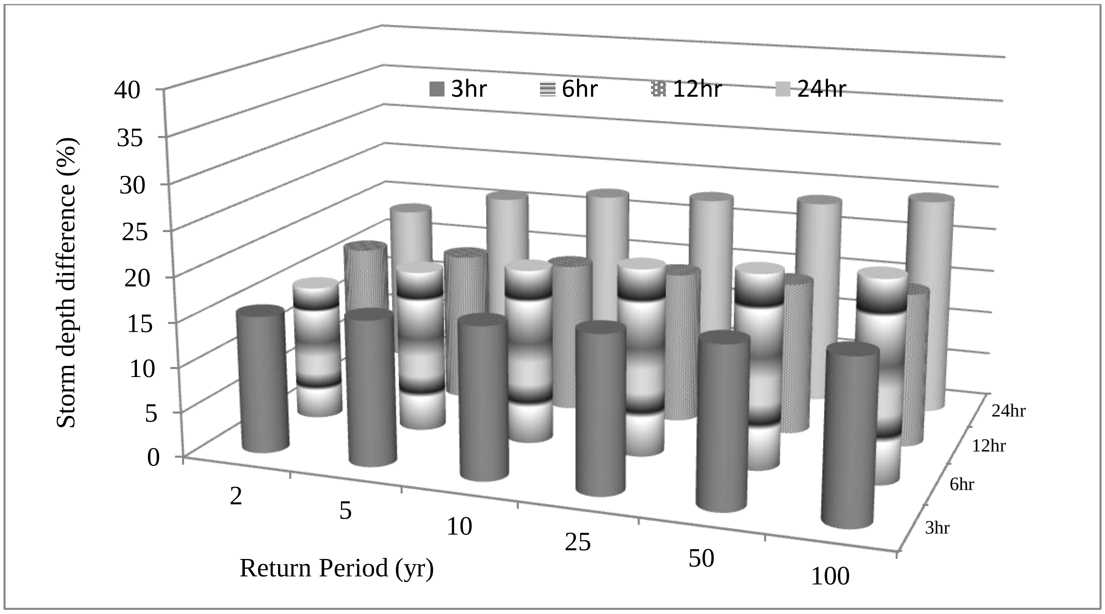

Figure 4-7: Difference between observed and NARCCAP future average storm depths for case 3

The percentage difference between storm depths calculated from observed data and NARCCAP future averages for four durations and six return periods are presented in the Figure 4-5, Figure 4-6 and Figure 4-7. These figures show significant increase of storm depths for all durations and return period; overall, the storm depths increase with the increase in return period. For example, storm depths of 24 hour duration for 2yr, 25yr and 100yr return period increased by 15.3%, 27.8% and 38.6% for case 1; 15.8%, 27.7% and 36% for case 2 and 18.4%, 22.8% and 24.6% for case 3. These figures also show that the storm depths increase with the increase in duration overall. For example, storm depths of 2yr return period for 3hr, 6hr, 12hr, 24hr duration increased by 12.1%, 13.2%, 14.3% and 15.3% for case 1; 11.9%, 12.2%, 14.5% and 15.8% for case 2 and 15.3%, 15.2%, 16.5% and 18.4% for case 3. The highest increase of 38.6% was observed for 24hour duration and 100 year return period storm depths for case 1. Therefore, the storm depths calculated in case 1 will be used as input in the hydrological model for flow simulation. The box plots in the Figure 4-8 shows the relative change (ratio of NARCCAP future storm depths of 6 RCM+GCM models and storm depths from observed data)) of storm depths for different durations and return period. It is revealed from the figure that the variability of relative change increase with an increase in return period and decrease with an increase in storm duration overall.

The overall uncertainty of the design storm for NARCCAP climate data was assessed using the co-efficient of variation (CV). For a given duration and return period, CV is calculated as the ratio between the standard deviation of NARCCAP storm depths to the corresponding mean values. CV was compared to assess the inter-model variability for different duration and return period for storm depths calculated from NARCCAP data sets under future climate conditions. The CV calculated for storm depths from 6 RCM+GCM pairs under future climate are presented in the Figure 4-9, Figure 4-10 and Figure 4-11. Overall the variability increases with an increase in return period and decrease with an increase in duration. For example, CV of 24 hour duration for 2yr, 25yr and 100yr return period are 11.2%, 17.1% and 27.2 % for case 1; 8%, 18.3% and 30.4% for case 2 and 9.7%, 17.2% and 18.4% for case 3. The CV of 2yr return period for 3hr, 6hr, 12hr, 24hr duration are 14%, 12.3%, 9.1% and 11.2% for case 1, 12.4%, 10.5%, 9.3% and 8.3% for case 2, and 13.9%, 11.5%, 10.9% and 9.7% for case 3.

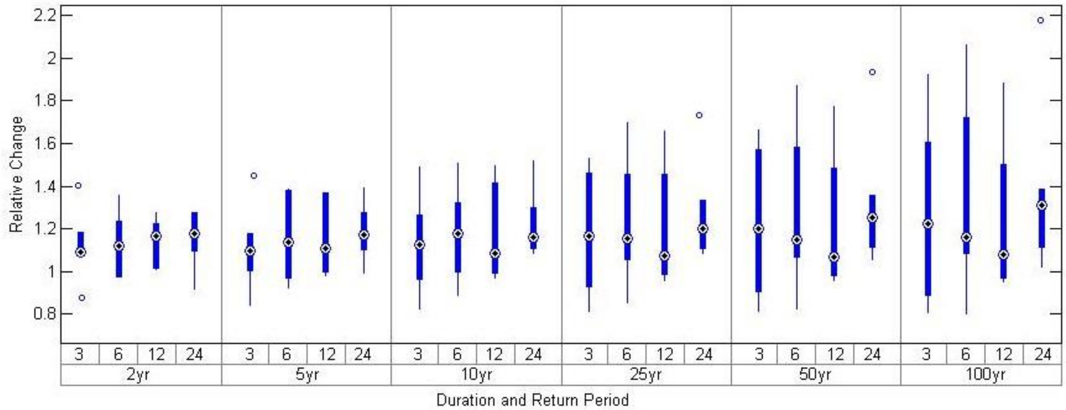

Figure 4-8: Box-plots of relative change calculated from observed and NARCCAP future storm depths

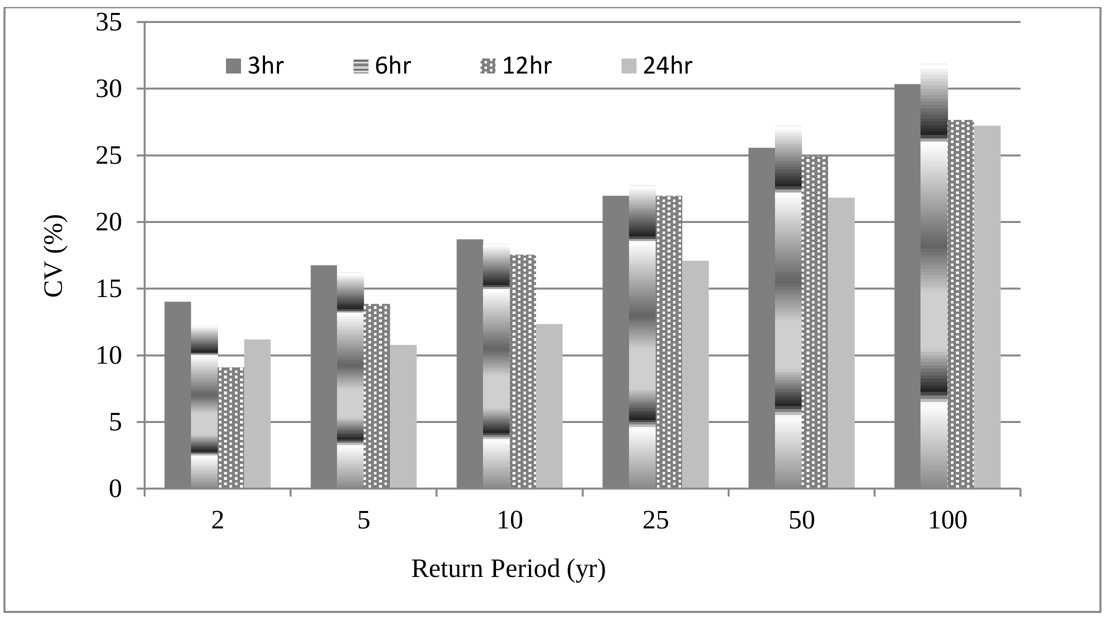

Figure 4-9: Comparison of CV of future storm depths for different return period and duration for case 1

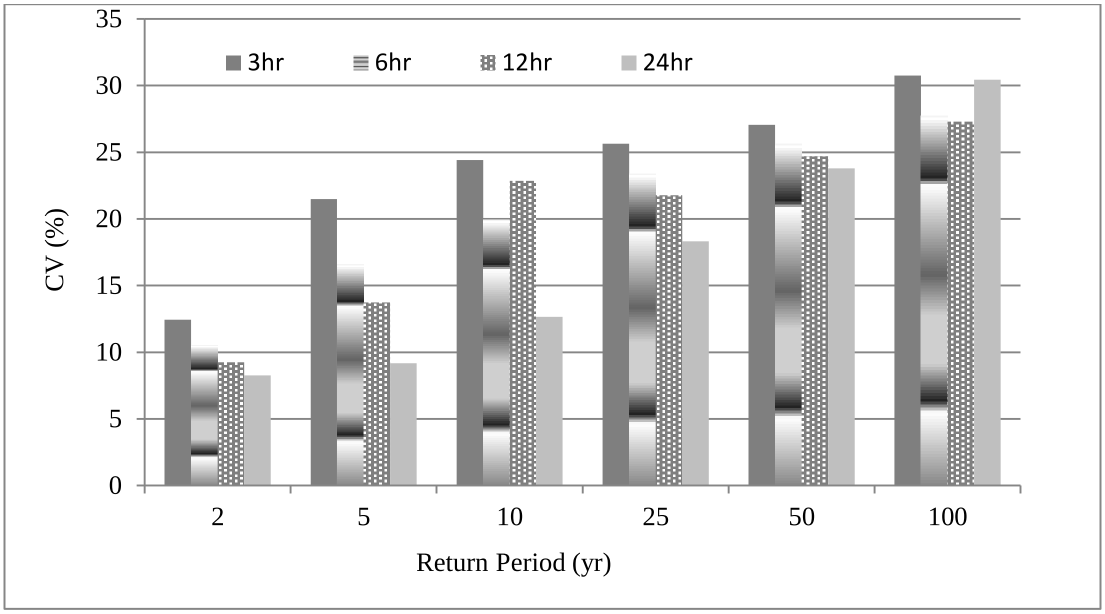

Figure 4-10: Comparison of CV of future storm depths for different return period and duration for case 2

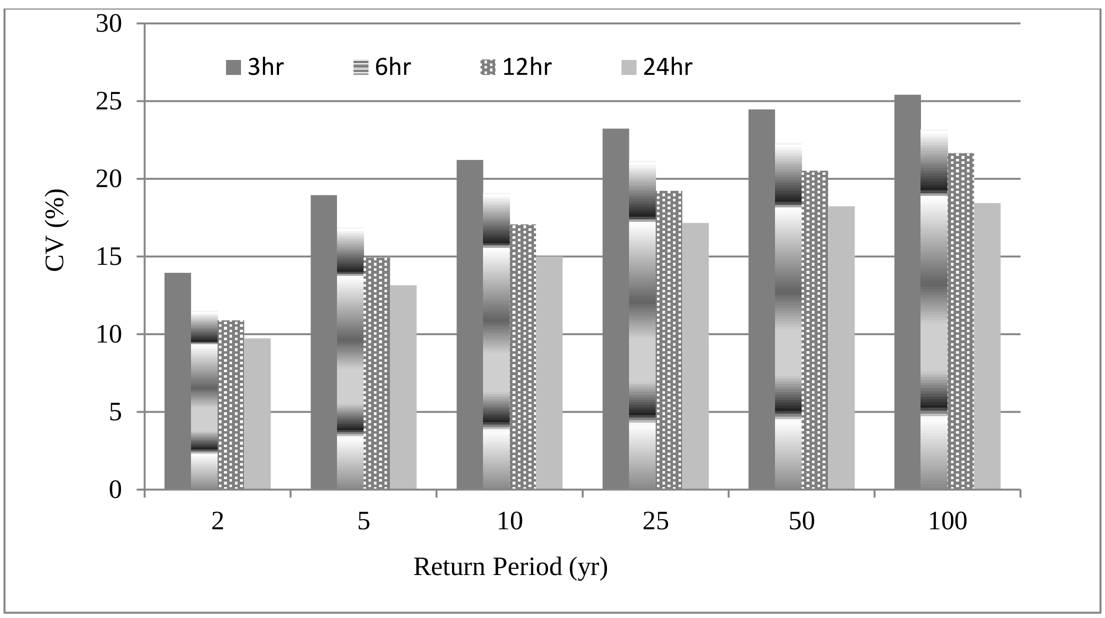

Figure 4-11: Comparison of CV of future storm depths for different return period and duration for case 3

4.5.2 Storm Flow

The increase in flows under future climate condition (difference between flows from observed and NARCCAP future average storms of 24 hour duration) at hydrologic element 101, 1003 and 1005 are presented in Figure 4-12. The hydrologic element 101 is the outlet of the catchment, and 1003 and 1005 are two sub-catchments with nearly same area of 23.26 and 25.82 ha. The sub-catchment 1003 was modeled as a highly urbanized area using standard instantaneous unit hydrographs as its total impervious area is about 84% , and the sub-catchment 1005 was modeled as a rural catchment using Nash instantaneous unit hydrograph. Analysis of flows at the outlet presents the hydrologic impact on the entire watershed, and the analysis of flows at two sub-catchments represent the response of climate impact in catchment with different landuse conditions. Flows from observed and NARCCAP future average storms at the outlet and two sub-catchments are presented in Figure 4-13, 4-14 and 4-15. Like increase in storm depths, percentage differences of the peak flow increase with an increase in return period overall. For example, increase of peak flows for 2yr, 25yr and 100 yr return period are 26.46%, 53.94% and 64.22% at the outlet, 21.69%, 32.93% and 51.61% for the sub-catchment area 1003, and 30.41%, 44% and 56.13% for the sub-catchment area 1005. The analyses of storm depths and peak flow results revealed that the percentage increase in peak flows are much higher than that of storm depths under future climate condition. The increase of storm depths of 24 hour duration and 2yr, 25yr and 100yr return period are 15.3%, 27.8% and 38.6%, those are 26.46%, 53.94% and 64.22% for peak flow at the outlet of the catchment. It is shown in Figure 4-14 and Figure 4-15 that the peak flows in the sub-catchment 1003 are much higher than the peak flows in the sub-catchment 1005. This is a common phenomenon that area with higher impervious area produces a higher peak flow. Figures 4-14 and 4-15 present that the peak flows for 2yr, 25yr and 100yr return period in sub-catchment 1003 are 2.72 m^3/s, 5.85 m^3/s and 7.87 m^3/s for baseline scenario and 3.31 m^3/s, 7.78 m^3/s and 11.93 m^3/s for future scenario; those are 0.22 m^3/s, 0.62 m^3/s and 0.93 m^3/s for baseline scenario and 0.28 m^3/s, 0.9 m^3/s and 1.45 m^3/s for future scenario in sub-catchment 1005. However, it is shown in Figure 4-12 that increase in peak flows under future climate condition in sub-catchment 1005 is higher than that in the sub-catchment 1003 - increase in storm depths of 24 hour duration and 2yr, 25yr and 100yr return period in the sub-catchment 1003 are 21.69%, 32.93% and 51.61 %, and the increases are 30.41%, 44% and 56.13 % in the sub-catchment 1005. The box plots in Figure 4-8 shows the relative change (NARCCAP future storm depths/observed storm depths) of storm depths for different durations and return periods. It is revealed from the figure that the variability of relative change increase with an increase in return period and decrease with an increase in storm duration overall. The box plots in Figure 4-16 shows the relative change (ratio of future peak flow from NARCCAP future storm depths of 6 RCM+GCM models and peak flow from observed storm depths) of storm depths for different return periods. It is revealed from the figure that the variability of relative change increases with an increase in return period overall if the outlier is also considered. Figure 4-8 and Figure 4-16 also show that the variability in relative change for peak flows is higher than the storm depths overall. The relative change of the 24 hour 100 year storm depths varies from 1.02 to 2.18 for six RCM+GCM data, and the relative change for flow of corresponding storms varies from 1.03 to 3.01.

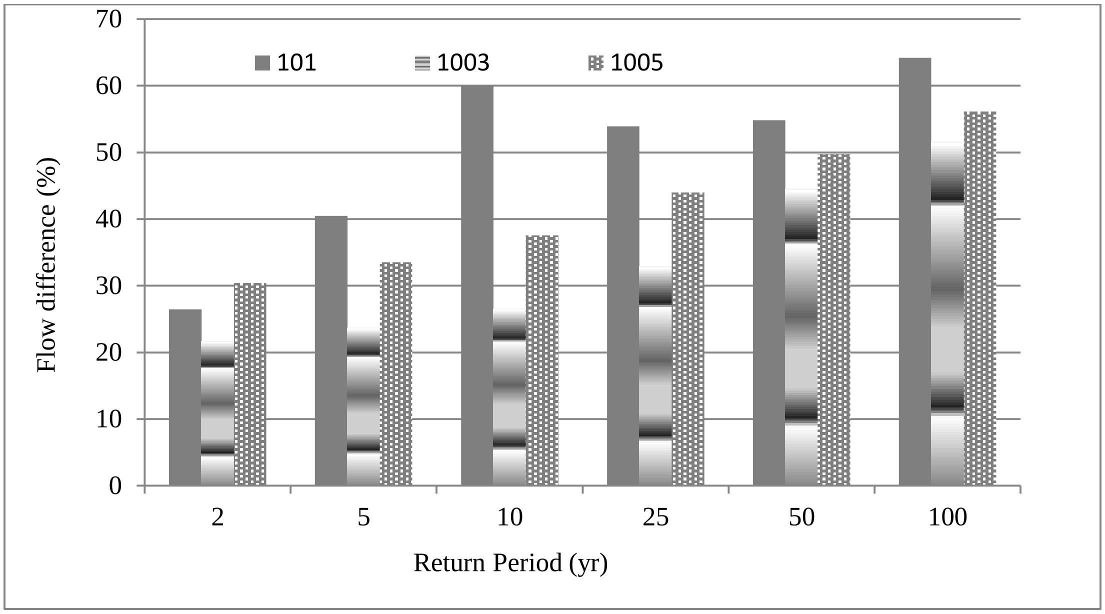

Figure 4-12: Flow difference for observed and NARCCAP future average storms

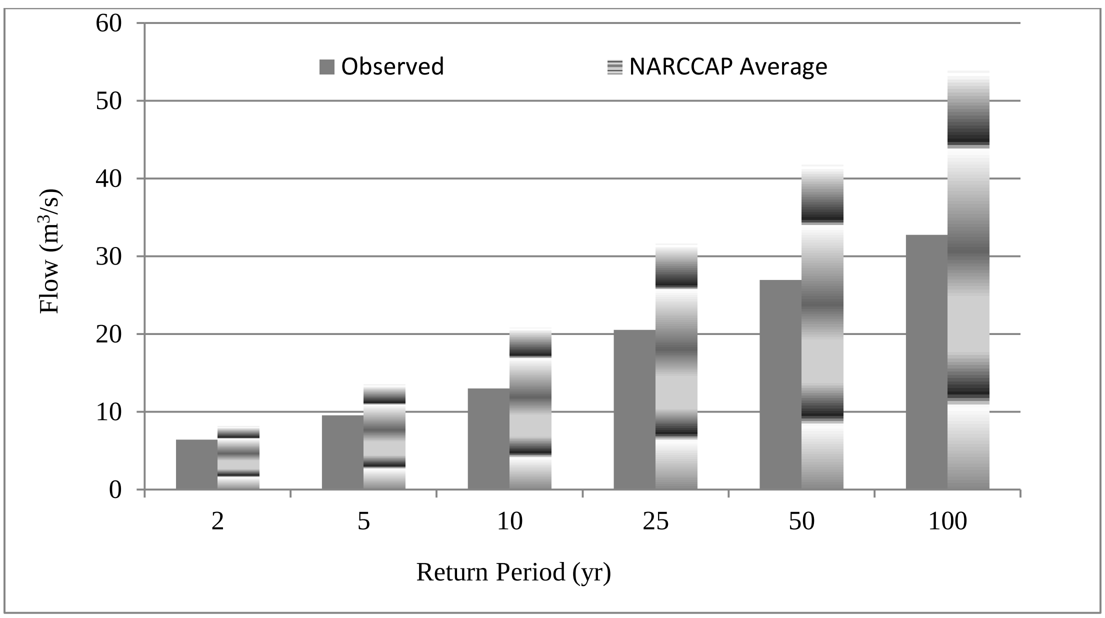

Figure 4-13: Flows from observed and NARCCAP future average storms at hydrologic element 101 (outlet of the catchment)

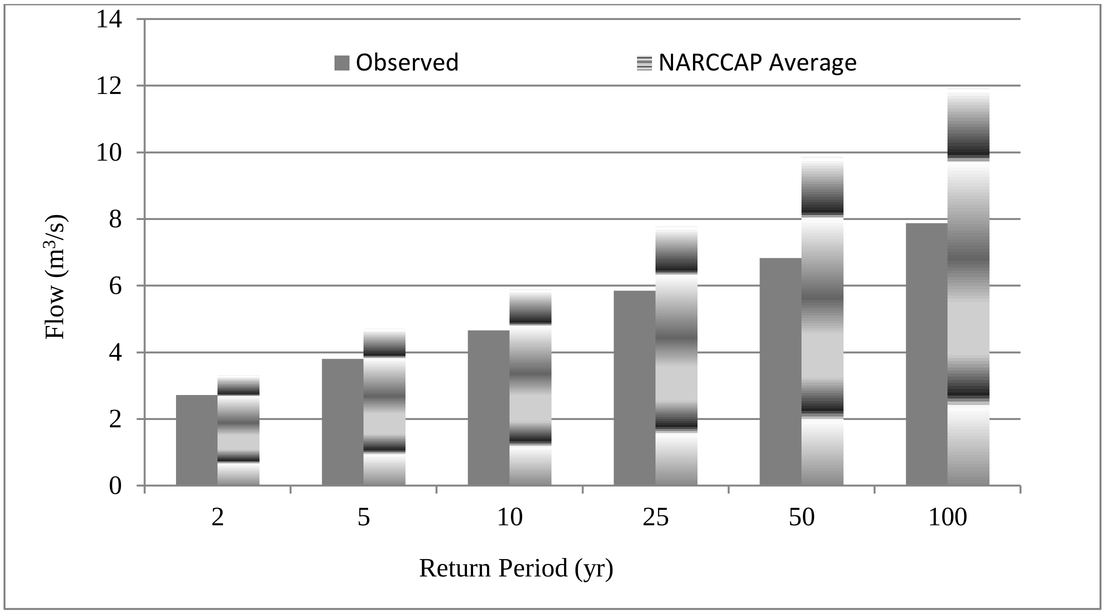

Figure 4-14: Flows from observed and NARCCAP future average storms at hydrologic element 1003

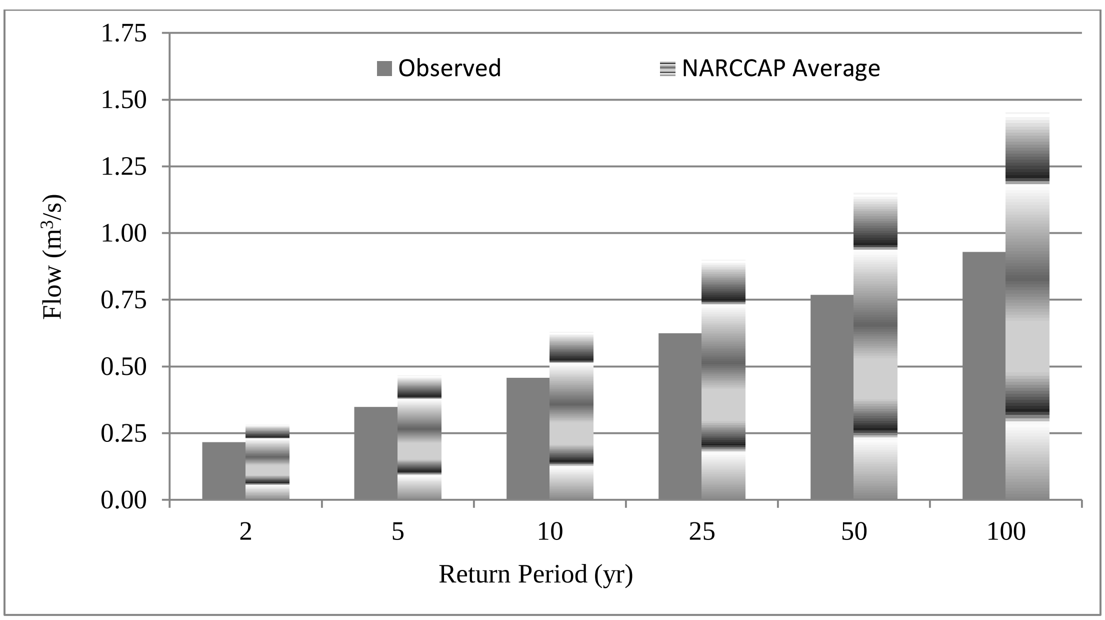

Figure 4-15: Flows from observed and NARCCAP future average storms at hydrologic element 1005

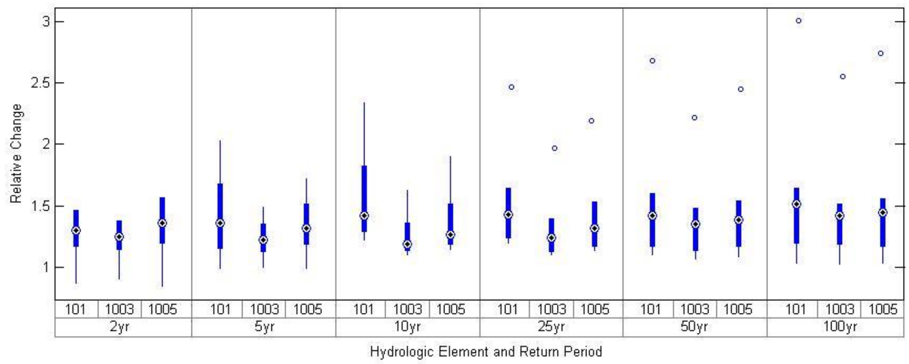

Figure 4-16: Box-plots of relative change of flows from observed and NARCCAP future storm depths

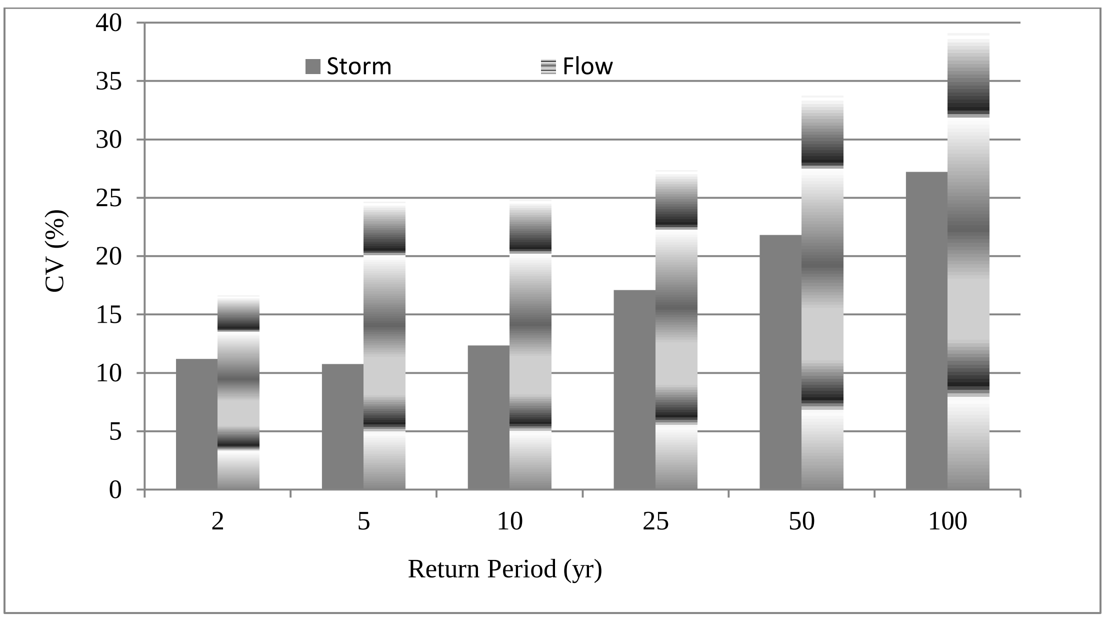

Figure 4-17: CV of future storm depths and flows for 24 hour storms at hydrologic element 101 (outlet of the catchment)

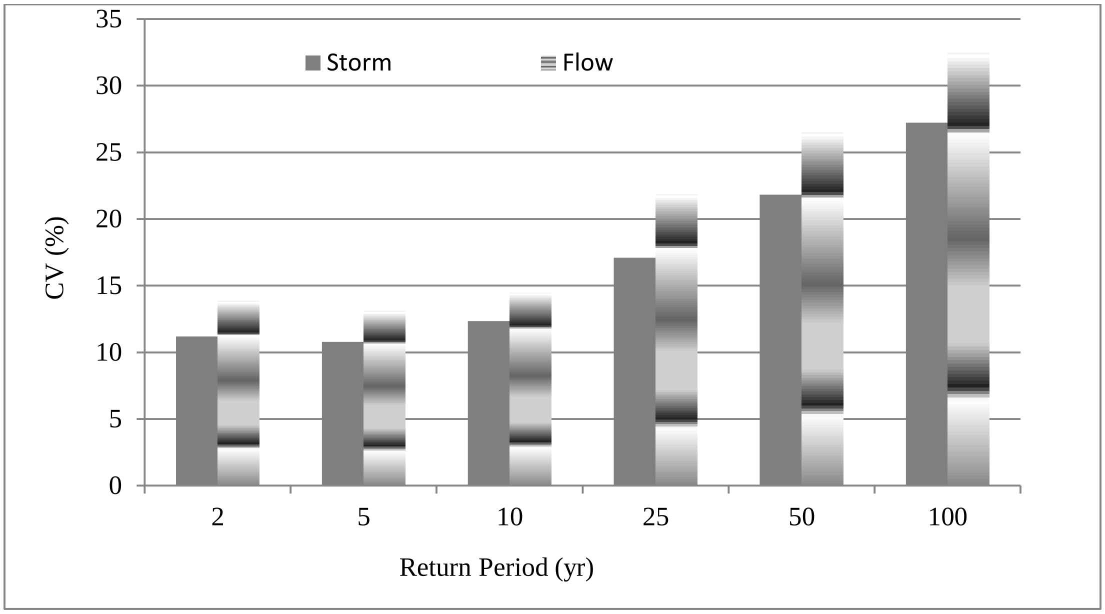

Figure 4-18: CV of future storm depths and flows for 24 hour storms at hydrologic element 1003

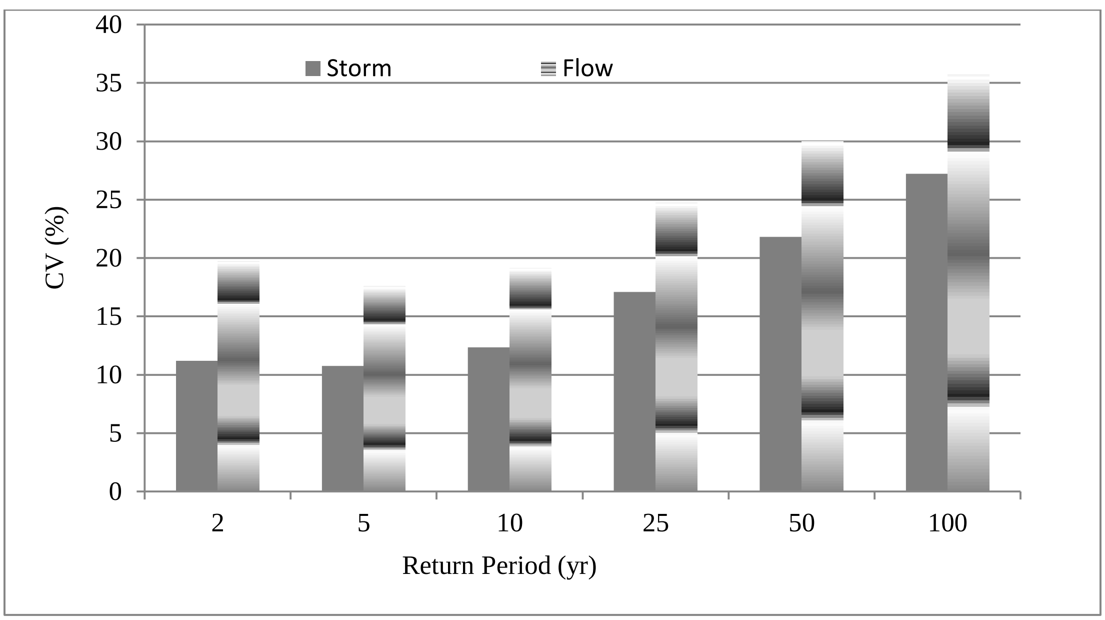

Figure 4-19: CV of future storm depths and flows for 24 hour storms at hydrologic element 1005

Similar to storm depths, the overall uncertainty of the peak flows for NARCCAP climate data was assessed using the co-efficient of variation (CV). CV was compared to assess the inter-model variability of the peak flows resulted from 24 hour storm depths of different return period calculated from six RCM+GCM pair data sets under future climate conditions. The CVs calculated for peak flows at the outlet (101), and sub-catchments 1003 and 1005 are presented in Figures 4-17, 4-18 and 4-19. The CVs for storm depths are also presented in the Figures.

Like the storm depths, the variability of the peak flow increases with an increase in return period. Figures 4-17, 4-18 and 4-19 show that the variability of peak flows are much higher than that of storm depths. The CV for peak flows of 100 year return period are 39.1%, 32.5% and 35.7% in the outlet, the sub-catchment 1003 and the sub-catchment 1005, respectively, and the CV for 24hour storm of 100 year return period is 27%. The figures also show that the variability is higher in case of the sub-catchment 1005 than in case of the sub-catchment 1003- the CV for 2 yr, 25yr and 100yr return period are 19.8%, 24.8% and 35.7% respectively in the sub-catchment 1005, those are 13.9%, 21.9% and 32.5% respectively in the sub-catchment 1003.

4.5.3 Hydraulic Analyses

The hydraulic metrics –water surface (W.S.) elevation, top width (top widths of the wetted cross section) and area (flow area of the entire cross-section including ineffective flow) were obtained from profile output table in HEC-RAS model and were used for the assessment of climate change impact on flooding. An increase in W.S. elevation and top widths represent an increase in flood inundation depth and extents under future climate condition. The increase of W.S. elevation and top widths are the differences of the values simulated for the flows resulted from the storm depths of observed data and averages of the six RCM+GCM pair climate data (listed in the Table 4-5). These metrics were analyzed for three stations – one near the most upstream of the Creek (river station 2674), one near the most downstream of the Creek (river station 357) and one in the middle of the Creek (river station 1665) and the results are shown in Figure 4-20. Increase in W.S. elevation and top widths were also calculated for all 45 cross-sections and averages (average of the increases at 45 cross-sections) are shown Figure 4-20. This figure shows that increase in W.S. elevation and top widths varies significantly among the cross sections. The increase in W.S. elevation for 2yr, 25 yr and 100 yr return period flow are 6cm, 13cm and 20 cm at river station 2674 ; 12cm, 45 cm and 67 cm at river station 357; and 7cm, 21cm and 28cm at river station 1465 respectively. The increase in top widths for 2yr, 25 yr and 100 yr return period flow are 8.2m, 21.9m and 39m at river station 2674;0.4m, 4.4 m and 124.7m at river station 357; and 5.5 m, 7.7m and 10.5m at river station 1465 respectively. The only reason of this variation is the shape of the cross-section. Average of increase in W.S. elevation and top widths of all cross sections show overall increase of inundation depths and extent along the Creek. The increase in W.S. elevation for 2yr, 25 yr and 100 yr return period flow are 6 cm, 22cm and 30cm respectively, and the increase in top widths are 4m, 23.7m and 37.1 m respectively. A map showing the flood line for 100 year return period flood for the current period and future period is presented in Figure 4-21. The blue and red line represents the flood line for the 100 year return period flow from observed data and average of six NARCCAP RCM+GCM pairs data sets respectively.

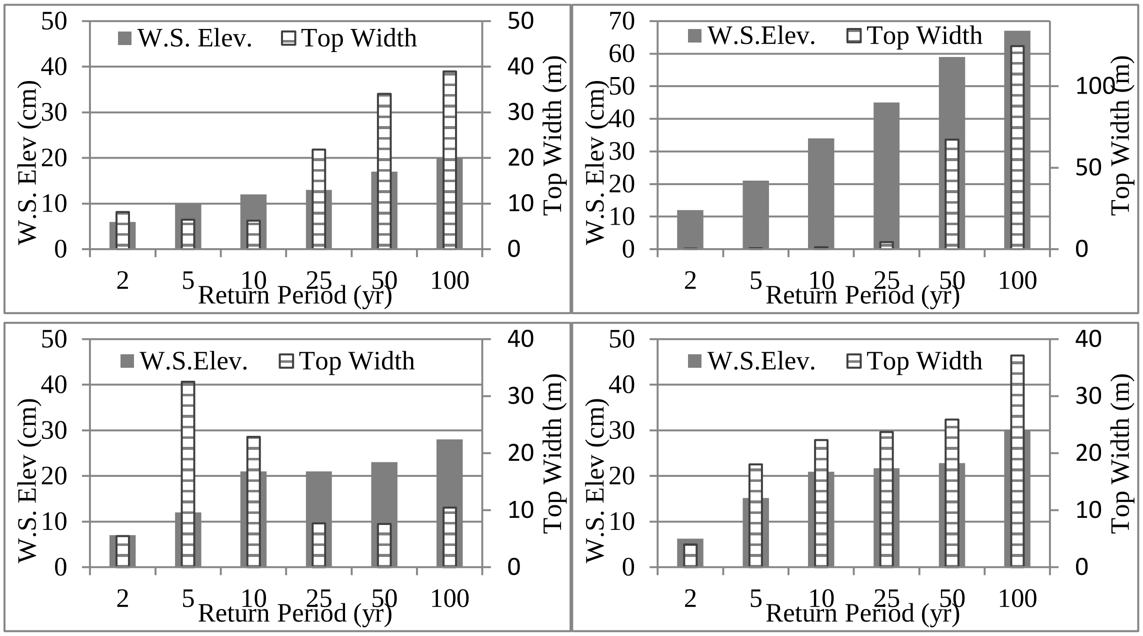

Figure 4-20: Increase of W.S. elevation and top width (top left, top right, bottom left and bottom right represent station 2674, 357, 1465 and average of 45 stations) along the Creek

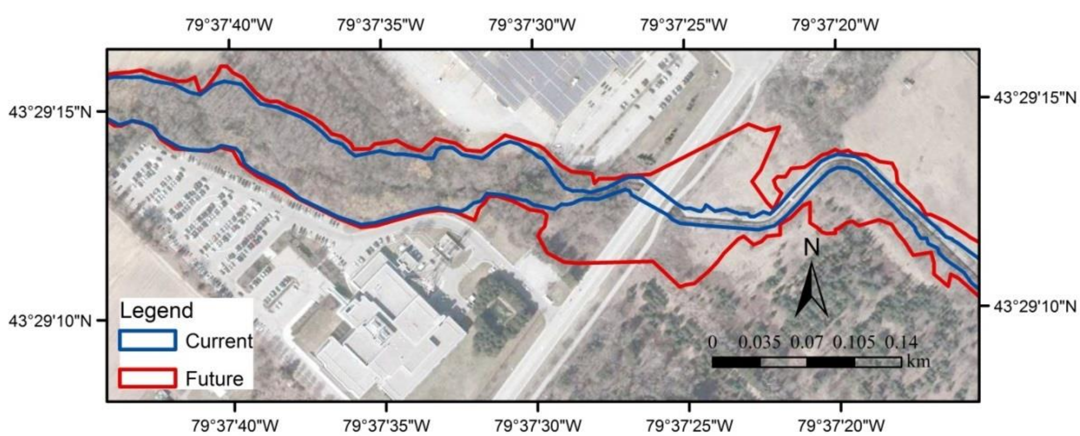

Figure 4-21: Flood line map for a section of Clearview Creek (orthophoto courtesy of the Credit Valley Conservation)

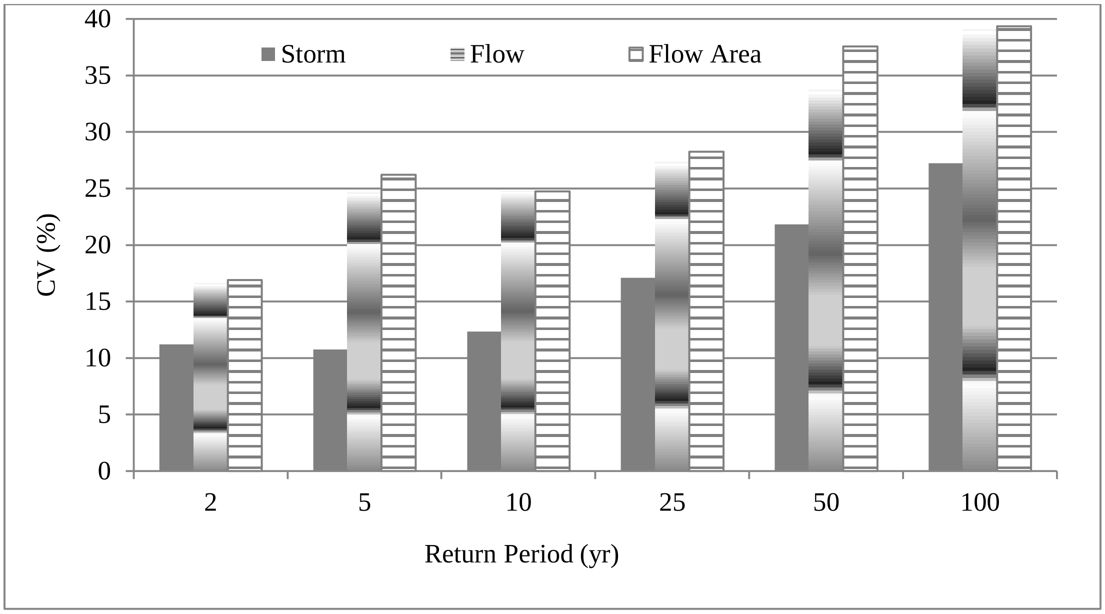

Figure 4-22: CV of storm depths, flows at outlet and average of flow areas at all cross-sections

The CVs of flow area for six RCM+GCM pair data under future climate were calculated for all 45 cross-sections and averages (average of the CVs at 45 cross-sections) and are shown Figure 4-22. The CVs for 24hr return period storms and corresponding flows at the outlet for different return period are also presented in Figure 4-21. The figure shows that the variability of flow area is much higher than the variability of storm depths, but the differences among variabilities in flow and in flow area are very small overall. For example, the CVs for 100 year return period storm depths, flows and flow area are 27.2%, 39.1% and 39.4 % respectively.

4.6 Conclusions

This study investigated the climate change impact on design storms, peak flows and flooding scenario using NARCCAP climate simulations based on A2 emission scenario described in the Special Report on Emissions Scenarios (SRES) for Clearview

Creek drainage area located in Southern Ontario, Canada. A statistical analysis software, Hydrognomon, hydrologic modeling tool Visual OTTHYMO and a river system analyses tool HEC-RAS were used for design storm depth calculation, simulation of flows and hydraulic metrics. The procedure followed and the findings of this study are concluded as follows:

Frequency analysis was performed on data from six RCM+GCM pairs by using the best fitted distribution among twenty seven distributions. Pearson chi-square test and Kolmogorov-Smirnov were used to test the goodness of fit of each distribution. L-Moment GEV Min was selected 15.6% of the total selections for NARCCAP data sets. The linear trendlines show that the overall increase of storm depths is highest when the distributions were identified by Chi-square test (case 1). The percentage increase (difference of average of storm depth from six model and observed data) for 24hr100yr storm depths is also highest for case 1. The storm depths of case 1 were used for flow simulation. A novel finding of this study is that there is a significant increase in storm depths for all durations and return period under future climate conditions, and the percentage increase in storm depth increases with an increase in return period and duration.

Peak flows using 24 hours storms of different return period were analysed, and the results show that the peak flow increase with a range of 26 % to 64% for 2yr and 100yr return period at the outlet of the Creek. Results also revealed that the peak flows from a catchment with higher impervious area are much higher than that for a catchment with a low impervious area, but the percentage increase in peak flows under future climate condition is less in a catchment with higher impervious area. The percentage increases of peak flows are much higher than that of storm depths under future climate condition.

Higher peak flows will result in increased flood inundation depths and extents in the Clearview Creek catchment area. Analysed hydraulic metrics simulated by HEC-RAS show an average increase in water surface elevation and extents (top widths of wetted cross sections) are 30 cm and 37.1 m for a 100 year return period flood overall. The spatial variability of the metrics along the Creek is very significant due to the shape of the cross sections. The increases in the metrics for other return period are also noteworthy.

The analysed CV values indicate that variability of flow simulated by Visual OTTHYMO and flow area simulated by HEC-RAS are much higher than the variability of the storm depths under future climate condition, and the difference between flow and flow area variability is insignificant overall. The box plot results indicate that the variability of relative change of storm depths increase with an increase in return period, and variability of relative change of storm depths decrease with the increase of duration. The box plot results also indicate that the variability in relative change for peak flows is higher than the storm depths overall.

The changes in urban stormwater runoff resulting from the effect of climate change will have important implication for selecting approaches for urban flood management measures. This study provides some information and knowledgebase that could be used for future development in the Clearview Creek catchment area as well as other Lake Ontario tributaries of similar characteristics.

Acknowledgement

We wish to thank the North American Regional Climate Change Assessment Program (NARCCAP) for providing the data used in this paper. The authors acknowledge the Credit Valley Conservation and Environment Canada for providing data and models for the study area. This study was supported by the Natural Science and Engineering Research Council of Canada (NSERC) discovery grant.

References

[1] Bates, B., Kundzewicz, Z.W., Wu, S., and Palutikof, J., "Climate change and water," Technical Paper of the Intergovermental Panel on Climate Change. Geneva: IPCC Technical Paper VI, 2008.

[2] Berggren,K., Olofsson, M.,Viklander, M., Svensson, G., and Gustafsson, A., "Hydraulic Impacts on Urban Drainage Systems due to Changes in Rainfall Caused by Climatic Change," J. Hydrol. Eng., 17 (1), 92-98, 2012.

[3] Brown, C., "The end of reliability." J. Water Resour. Plann. Manage., 136(2), 143-145, 2010.

[4] Chen, C., and Knutson, T., "On the verification and comparison of extreme rainfall indices from climate models." J. Clim., 21 (7), 1605-1621, 2008.

[5] City of Mississauga, Development requirement manual. City of Mississauga, Mississauga, Ontario, Canada, 2009.

[6] Civica Infrastructure, Visual OTTHYMO (VO) v3.0 User's Guide, Civica Infrastructure Inc., Vaughan, Ontario, Canada, 2013.

[7] Civica Infrastructure, Visual OTTHYMO (VO) v3.0 Reference Manual, Civica Infrastructure Inc., Vaughan, Ontario, Canada, 2012.

[8] Collins W.D., Bitz, C.M., Blackmon, M.L., Bonan, G.B., Bretherton, C.S., Carton, J.A., Chang, P., Doney, S.C., Hack, J.J., Henderson, T.B., Kiehl, J.T., Large, W.G., McKenna, D.S., Santer, B.D., and Smith, R.D., "The community climate system model version 3 (CCSM3)," J. Climate, 19: 2122-2143, 2006.

[9] Credit Valley Conservation (CVC), CVC standard parameters, 2011. Retrieved from http://www.creditvalleyca.ca/wp-content/uploads/2011/09/020-Standard-Parameters-Appendix-B.pdf (accessed 12 December 2015)

[10] Cunderlik, J.M., and Simonovic, S.P., "Inverse Flood Risk Modelling under Changing Climatic Condition," Hydrological Processes, 21(5), 563-577, 2007.

[11] Dibike, Y.B., & Coulibaly, P., "Validation of hydrological models for climate scenario simulation: the case of Saguenay watershed in Quebec," Hydrological Processes, 21(23), 3123-3135, 2007.

[12] Elguindi, N., Bi, X., Giorgi, F., Nagarajan, B., Pal, J., Solmon, F., Rauscher, S., and Zakey, A., RegCM Version 3.1 User's Guide, Trieste, Italy, 2007.

[13] Environment Canada, Canadian climate normal, 1981-2010 station data, 2015. Retrieved from http://climate.weather.gc.ca/climate_normals/results_1981_2010_e.html?stnID=5097&lang=e&StationName=Toronto&SearchType=Contains&stnNameSubmit=go&dCode=1 (accessed 11 October 2015)

[14] Eum, H., Sredojevic, D., and Simonovic, S.P., "Engineering procedure for the climate change flood risk assessment in the upper Thames River Basin," J. of Hydrol. Eng., 16, 608-612, 2011.

[15] Flato, G. M., "The Third Generation Coupled Global Climate Model (CGCM3)," 2005. Retrieved from http://www.ec.gc.ca/ccmac-cccma/default.asp?n=1299529F-1 (accessed 9 August 2015).

[16] Flood Damage Reduction Program (FDRP), 2015. Retrieved fromhttps://ec.gc.ca/eau-water/default.asp?lang=En&n= 0365F5C2-1 (accessed 9 August 2015)

[17] Forsee, W.J., and Ahmad, S., "Evaluating urban storm-water infrastructure design in response to projected climate change," J. Hydrol. Eng., 16 (11), 865-873, 2011.

[18] Gellens, D., and Roulin, E., "Streamflow response of Belgian catchments to IPCC climate change scenarios," J. Hydrol. 210, 242-258, 1998.

[19] GFDL GAMDT (The GFDL Global Model Development Team), "The new GFDL global atmospheric and land model AM2-LM2: Evaluation with prescribed SST simulations," J. Climate, 17, 4641-4673, 2004.

[20] Giorgi, F., Marinucci, M.R., and Bates, G.T., "Development of second generation regional climate model (RegCM2) I: boundary layer and radiative transfer processes," Mon. Weather Rev., 121, 2794-2813, 1993.

[21] Gordon, C., Cooper, C., Senior, C.A., Banks, H., Gregory, J.M., Johns, T.C., Mitchell, J.F.B., and Wood, R.A., "The simulation of SST, sea ice extents and ocean heat transports in a version of the Hadley Centre coupled model without flux adjustments," Climate Dynamics ,16, 147-168, 2000.

[22] Hamlet, A.F., and Lettenmaier, D.P., "Effects of climate change on hydrology and water resources in the Columbia River basin," J. Am. Water Resour. Assoc. 35 (6), 1597-1623, 1999.

[23] Hydrologic Engineering Center (HEC), HEC-GeoRAS GIS Tools for Support of HEC-RAS using ArcGIS User'sManual. U.S. Army Corps of Engineers, Davis, CA, USA, 2011.

[24] Hydrologic Engineering Center (HEC), HEC-RAS River Analysis System, Hydraulic Reference Manual. U.S. Army Corps of Engineers, Davis, CA, USA, 2010.

[25] IPCC, "Climate Change 2014: Synthesis Report," Contribution of Working Groups I, II and III to the Fifth Assessment Report of the Intergovernmental Panel on Climate Change, Core Writing Team, Pachauri, P.K. and Meyer, L.A. (eds.), IPCC, Geneva, Switzerland, 151 pp., 2014.

[26] Jones, R., Noguer, M., Hassell, D., Hudson, D., Wilson, S., Jenkins, G., and Mitchell, J., "Generating high resolution climate change scenarios using PRECIS," Met Office Hadley Center, Exter, p 40, 2004.

[27] Karla, A., and Ahmad, S., "Using Oceanic-atmospheric oscillations for long lead time streamflow forecasting," Water Resour. Res., 45, W03413, 2009.

[28] Keifer, D.J., and Chu, H.H., "Synthetic Storm Pattern for Drainage Design," ASCE Journal of the Hydraulics Division, Vol. 83 (HY4), pp: 1332.1-1332.25, 1957.

[29] Kite, G.W., Application of a land class hydrological model to climate change. Water Resour. Res. 29 (7), 2377-2384, 1993.

[30] Kozanis, S., Christofides, A., and Efstratiadis, A., "Scientific documentation of the hydrogram software version 4," Athens, pp173, 2010.

[31] Kundzewicz, Z.W., Mata L.J., Arnell, N.W., D¨oll, P., Kabat, P., Jimenez, B., Miller, K.A.,Oki, T., Sen, Z., and Shiklomanov. I.A., Fresh water resources and their management. In Climate Change2007. Impacts, Adaptation and Vulnerability. Contribution of Working Group II to the Fourth Assessment Report of the Intergovernmental Panel on Climate Change, Parry ML, Canziani OF, Palutikof JP, VanDerLinde PJ, Hanson CE(eds). Cambridge University Press: Cambridge, UK; 173-210, 2007.

[32] Lemmon, D.S. and Warren, F.J., Climate Change Impacts and Adaption: A Canadian Perspective. Ottawa, Ontario, Canada: Natural Resources Canada, 2004.

[33] Leung, R.L., and Wigmosta, M.S., "Potential climate change impacts on mountain watersheds in the Pacific Northwest," J. Am. Water Resour. Assoc. 35 (6), 1463-1471, 1999.

[34] Mailhot, A., Beauregard,I., Talbot, G., Caya, D., and Biner, S., "Future changes in intense precipitation over Canada assessed from multi-model NARCCAP ensemble simulations," Int. J. Climato., 32, 1151-1163, 2012.

[35] Mailhot, A., Duchesne, S., Caya, D., and Talbot, G., "Assessment of future change in intensity-duration-frequency (IDF) curves for Southern Quebec using the Canadian Regional Climate Model (CRCM)," J. Hydrol., 347, 197-210, 2007.

[36] Mearns, L.O., et al., 2007, updated 2012. The North American Regional Climate Change Assessment Program dataset, National Center for Atmospheric Research Earth System Grid data portal, Boulder, CO. Data downloaded 2015-07-07.

[37] Mearns, L. O., Gutowski, W.J., Jones, R., Leung, L.Y., McGinnis, S., Nunes, A.M.B. and Qian, Y., "A regional climate change assessment program for North America," EOS, 90 (36), 311-312, 2009.

[38] Milly, P.C.D., Betancourt, J., Falkenmark, M., Hirsch, R.M., Kundzewicz, Z.W., Lettenmaier, D.P., and Stouffer, R.J., "Climate change-stationary is dead: whither water management?" Science, 319 (5863), 573-574, 2008.

[39] Moglen, G.E., and Vidal,G.E.R., "Climate change impact and storm water infrastructure in the Mid-Atlantic region: design mismatch coming?" J. Hydrol. Eng., 19, 2014.

[40] MTO, Evaluation of Drainage Management Software, 2015. Retrieved from http://www.mto.gov.on.ca/english/publications/drainage/software/otthymo.shtml#WHATDOESITDO (accessed 12 December 2015).

[41] MTO, MTO Drainage management manual. Drainage and Hydrology Section, Ministry of Transportation, Ontario, Canada, 1997.

[42] Music, B., and Caya, D., "Evaluation of the hydrological cycle over the Mississippi River Basin as simulated by the Canadian regional climate model (CRCM)," J. Hydrometeor., 8, 969-988, 2007.

[43] Nakicenvoic, N., Davidson, O., Davis, G., Grübler, A., Kram, T., Rovere, E., Metz, M., Morita, T., Pepper, W., Pitcher, H., Sankovski, A., Shukla, P., Swart, R., Watson, R., and Dadi, Z., Special Report on Emissions Scenarios. A Special Report of Working Group III of the Intergovernmental Panel on Climate Change. Cambridge University Press Cambridge, 599, 2000.

[44] NARCCAP, North American Regional Climate Change Assessment Program, 2013. Retrieved from

http://www.narccap.ucar.edu/ (accessed 26 January 2013).

[45] Olsson, J., Berggren, K., Olofsson, M., and Viklander, M., "Apply-ing climate model precipitation scenarios for urban hydrological assessment: A case study in Kalmar City, Sweden,"Atmos.Res., 92(3), 364-375, 2009.

[46] Ontario Ministry of Natural Resources (OMNR), Technical Guide - River and Stream Systems: Flooding Hazard Limit. Ontario Ministry of Natural Resources, Ontario, Canada, 2002.

[47] Pope, V.D., Gallani, M.L., Rowntree, P.R., and Stratton, R.A., "The impact of new physical parameterizations in the Hadley Centre climate model—HadAM3," Climate Dynamics, 16, 123-146. 2000.

[48] Prudhomme, C., Reynard, N., and Crooks, S., "Downscaling of global climate models for flood frequency analysis: Where are we now?" Hydrol. Processes, 16(6), 1137-1150, 2002.

[49] Semadeni-Davies, A., Hernebring, C., Svensson, G., and Gustafsson, L., "The impacts of climate change and urbanisation on drainage in Helsingborg, Sweden: Combined sewer system," J. Hydrol., 350, 100-113, 2008.

[50] Valipour, M., "Optimization of neural networks for precipitation analysis in a humid region to detect drought and wet year alarms," Meteorological Application, 2015.

[51] Valipour M., "Long-term runoff study using SARIMA and ARIMA models in the United States," Meteorological Application, 22, 592-598, 2015.

[52] Valipour, M., "Use of surface water supply index to assessing of water resources management in Colorado and Oregon, US," Advances in Agriculture, Sciences and Engineering Research, 3(2):631-640, 2013.

[53] Valipour, M., "Estimation of Surface Water Supply Index Using Snow Water Equivalent," Advances in Agriculture, Sciences and Engineering Research, 3(1): 587-602, 2013.

[54] Zahmatkesh, Z., Karamouz, M., Goharian, E., and Burian, S.J., "Analyses of the effects of climate change on urban storm water runoff using statistically downscaled precipitation data and a change factor approach," J. Hydrologic Eng., 20(7), 05014022. 2015.

[55] Zhu, J., "Impact of climate change on extreme rainfall across the United States," J. Hydrol. Eng., 18(10), 1301-1309, 2013.

[56] Zhu, J., Stone, M.C., and Forsee, W., "Analysis of potential impact of climate change on intensity-duration-frequency (IDF) relationships for six regions in the United States," J. Water and Climate Change, 3(3), 185-196, 2012.

Chapter 5 : Conclusions and Recommendations

5.1 Conclusions

As our climate is changing, it is essential to investigate its impact on the hydrological processes and respective consequences on the flood management systems, for instance stormwater management infrastructures, and designation of flood risk area. This research work presented in this Ph.D. thesis aimed to investigate the impact of climate change on hydrological processes, and assess the potential impact of changed hydrological processes on urban drainage systems and flooding scenarios. The North American Regional Climate Change Assessment Program (NARCCAP) provided ensemble climate simulations for current (1971-2000) and future period (2041-2070) which were used in this study. The study area in this research encompasses Spencer creek watershed, West Central Mountain drainage area and Clearview Creek drainage area located in Southern Ontario, Canada. The overall procedure and findings of this research based on the above three study areas can be summarized as follows:

Spencer creek watershed

- NARCCAP provided eight RCM+GCM pair's precipitation and temperature time series for the current (1971-2000) and future (2041-2070) period were bias-corrected, and the RPSS and BSS results show an overall improvement for precipitation and temperature, higher improvement in the late spring and summer months in the case of precipitation and higher improvement in the summer months in case of temperature.
- A hydrologic model HBV was employed for continuous simulation by inputting bias-corrected precipitation and temperature time series.

- Averages of all RCM+GCM shows that precipitation will increase in the fall, winter and spring and decrease in the summer; the temperature will increase in all months, and evapotranspiration will increase in all months except July and August.
- The daily average flow will increase in the winter and decrease in the other seasons as shown by average of all RCM+GCM pair's data.
- Averages of all RCM+GCM pairs revealed an increase of annual average values for temperature, precipitation and evapotranspiration, and a small increase of annual average flow in future. The small increase in annual average flow could be contributed to the very high decrease in low flows although an increase of high flows.
- Flow duration analyses show an increase in high flows and decrease in low flows under future climate. An increase of high flow by 8.8% and a decrease of low flow by 12.9% were revealed by averages of five RCM+GCM pairs. The greatest increase in high flow by 13.2% and the highest decrease in low flow by 28.6% were projected by the WRFG+CGCM3 and WRFG+CCSM models.

West Central Mountain Drainage Area

- An extensive frequency analysis was performed on observed, NARCCAP six RCM+GCM pair's data set for design storm calculation by using the best fitted distribution among twenty seven distributions tested by Pearson chi-square test and Kolmogorov-Smirnov test. The delta change factor was applied to transpose design storm depth calculated from gridded NARCCAP projection to Hamilton Airport station.
- The L-moment Pareto distribution was selected the most often for data from six RCM+GCM pairs.

- Design storm depth will increase significantly for all duration and return period. The difference (increase) of design storm depths increases with the increase of return period overall. The increase of storm depth is higher for shorter duration with higher return period and also higher for longer duration with lower return period.
- Increase of design storm depth under future climate is higher for higher values as revealed by scatter plot, where the higher values may represent storm depths for higher return period or higher duration.
- Considering the urban hydrologic and hydraulic modeling capabilities, the PCSWMM modeling tools was used in this study.
- The deteriorated performance of three detention ponds were indicated by the performance ratio calculated from eight metrics as the increases were observed in 93% of all the metrics for all ponds, and visual inspection of time series plot of inflow, outflow, storage volume and depth.
- The storm sewer designed based on current climate condition will not be able to cope with the increased design storm depth under future climate condition as indicated by the increase of flooded and surcharged node, maximum water level, pipe flow ratio, conduits above full normal flow and for capacity limited.
- The worst performance of all detention ponds and storm sewer network were observed under RCM3+GFDL future scenario.

Clearview Creek drainage area

- In this research, the potential impact of climate change on design storms, peak flows and flooding scenarios was investigated using NARCCAP provided six RCM+GCM pair data sets.
- Design storm depths for different durations and return period were calculated by the same procedure applied in the previous study. Like the Hamilton Airport, the storm depths for all duration and return period will increase for Toronto Pearson International Airport, but indicates a comparatively higher increases for longer duration in case of higher return period. Overall the variability of storm depths as well as flow and flow area increase with the increase of return period, and variability of flow and flow area are much higher than the variability of the storm depths under future climate condition.
- The hydrologic and hydraulic simulations were performed by using single event hydrologic model simulation software Visual OTTHYMO and a hydraulic modeling tool - the Hydrologic Engineer Center's River System Analysis System (HEC-RAS).
- Averages of six RCM+GCM pairs revealed an the increase of peak flow with a range of 26% to 64% for 2yr and 100yr return period at the outlet of the Creek, and an average increase in water surface elevation and extents by 30cm and 37.1m, respectively, for a 100 year return period flood.

5.2 Recommendations

In traditional frequency analyses, it is generally assumed that the annual maximum time series for meteorological data at a given location are stationary (Rajagopalan, 2010; Ouarda, 2010). However, the meteorological observations and climate model simulations for current and future period may not be stationary due to climate change with continued emissions of greenhouse gases. In traditional frequency analyses, it is assumed that the probability distributions of extreme events do not change with time. But when data are non-stationary the distribution parameters change with time (Hounkpè 2015); therefore frequency analysis of non-stationary data requires a different approach. In this research the best fitted distribution was selected for each individual data set for frequency analysis, however the parameters of each fitted distribution were not considered to be time dependent. Non-stationary frequency analyses for design storm depth calculation are highly recommended for future research. For a more robust and accurate investigation of climate change impact at watershed scale, other recommendations identified for future research are: use of spatio-temporal higher resolution climate data aiming to reduction of the uncertainty in climate change impact; use of quantile bias-correction and other downscaling methods in the correction of bias in precipitation and temperature time series; detail investigation of sizing of stormwater management pond under future climate; use of high resolution Digital Terrain Model (DTM) for more accurate flood mapping (Very High Resolution Satellite Imagery, Lidar Scanners), and 2D hydraulic models in case of analysis of flooding scenario; and requirement of more detailed field studies for better verification of the results due to limited spatio-temporal field data of environmental parameters.

References

Hounkpè, J., Diekkrüger, B., Badou, D.F., Afouda, A.A. (2015). Non-Stationary flood frequency analysis in the Ouémé River Basin, Benin Republic. Hydrology, 2, 210-229.

Ouarda, T (2010). Bayesian nonstationarity frequency analysis of hydrological variables. Workshop on nonstationarity, hydrologic frequency analysis, and water management, Colorado Water Institute, Colorado State University, Information Series No. 109, 115-124.

Rajagopalan, B. (2010). Hydrologic frequency analysis in a changing climate. Workshop on nonstationarity, hydrologic frequency analysis, and water management, Colorado Water Institute, Colorado State University, Information Series No. 109, 107-114.